सत्यमेव जयते

Government of India
Bhabha Atomic Research Centre

JOURNAL PUBLICATIONS 2023

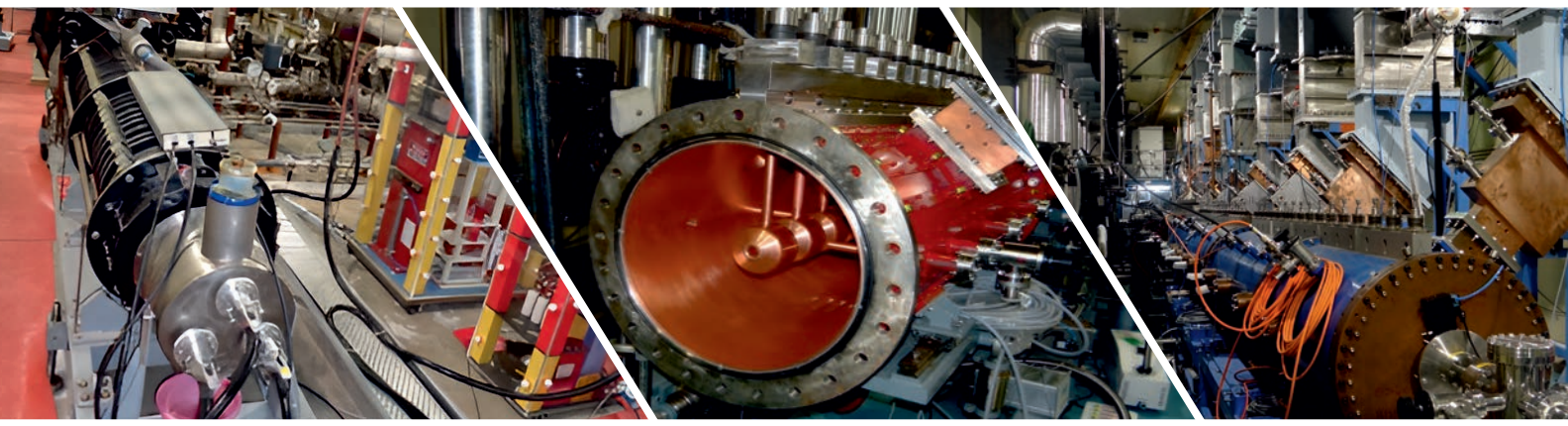

राष्ट्र की सेवा में परमाणु
भा प अ कें
BARC
ATOMS IN THE SERVICE OF THE NATION

BARC VISTA

Title:
BARC VISTA: Journal Publications 2023

Published by:
Scientific Information Resource Division
Bhabha Atomic Research Centre
Trombay, Mumbai
Maharashtra-400085, India
Email: headsird@barc.gov.in

Full report and Journal Publications are available at: https://barc.gov.in/barcvista

On the front cover: Important systems and sub-systems of LEHIPA Facility in BARC Trombay.
On the back cover: The state-of-art technologies developed in BARC with important applications in healthcare, industry and water purification.

JOURNAL PUBLICATIONS

1. Crystal structure of Synechococcus phycocyanin: implications of light-harvesting and antioxidant properties. Patel S.N., Sonani R.R., Chaubey M.G., et al. *3 Biotech*. Vol. 13(7), ArtNo. 247.
2. [99mTc]Tc-HYNIC-RM2: A potential SPECT probe targeting GRPR expression in prostate cancers. Vats K., Chakraborty A., Rakshit S., et al. *Nuclear Medicine and Biology*. Vol. 118-119, ArtNo. 108331.
3. 'Brine Management through brine mining of trace metals' for developing Secondary sources of nuclear fuel. Prasad T.L. *Nuclear Engineering and Technology*. Vol. 55(2), pg. 674-680.
4. "Exploring tin oxide based materials: A critical review on synthesis, characterizations and supercapacitive energy storage". Kedara Shivasharma T., Sahu R., Rath M.C., et al. *Chemical Engineering Journal*. Vol. 477, ArtNo. 147191.
5. 105Rh yield from the proton induced fission of uranium. Najumunnisa T., Musthafa M.M., Midhun C.V., et al. *Nuclear Physics A*. Vol. 1032, ArtNo. 122611.
6. 11-20 MeV Alvarez Drift Tube Linac for low energy proton accelerator. Teotia V., Malhotra S., Kumar P., et al. *Journal of Instrumentation*. Vol. 18(6), ArtNo. P06020.

7. 131I dose coefficients for a reference population using age-specific models. Singh P.K., Patni H.K., Roy R., et al. *Journal of Radiological Protection*. Vol. 43(4), ArtNo. 41508.

8. 14CO2 ACTIVITY IN AIR SAMPLES AND DILUTION FACTOR EVALUATION OF KAKRAPAR GUJARAT SITE, INDIA. Chandrakar A., Patra A.K., Joshi C.P., et al. *Radiocarbon*. Vol. 65(4), pg. 819-831.

9. 18F-FDG PET/CT Versus 68Ga-PSMA-11 PET/CT in Evaluation of Distant Metastatic Disease in Recurrent Renal Cell Carcinoma. Parghane R.V., Basu S. *Journal of Nuclear Medicine Technology*. Vol. 51(3), pg. 251-262.

10. 222Rn and progeny concentrations and equilibrium factor (F) in different types of dwellings typical of the west coast region of India. Vijith A.P., Mishra R., Sapra B.K., et al. *Nuclear and Particle Physics Proceedings*. Vol. 341 pg. 56-58.

11. 2D BN-biphenylene: structure stability and properties tenability from a DFT perspective. Singh M., Chakraborty B. *Physical Chemistry Chemical Physics*. Vol. 25(23), pg. 16018-16029.

12. 2-dimensional biphenylene monolayer as anode in Li ion secondary battery with high storage capacity: Acumen from density functional theory. Duhan N., Chakraborty B., Dhilip Kumar T.J. *Applied Surface Science*. Vol. 629, ArtNo. 157171.

13. 2D-IR Spectroscopy of Nitrosyl Stretch of Sodium Nitroprusside Reveals the Elusive Two Anomalous Regions in the DMSO-Water Mixture. Mora A.K., Singh P.K., Punna R., et al. *Journal of Physical Chemistry B*. Vol. 127(16), pg. 3701-3710.

14. 3D graphene-based materials and their potential application on wastewater management. Sahoo P.K., Nayak G., Gupta J., et al. *Environmental Quality Management*. Vol. 33(2), pg. 205-220.

15. 4-carboxyanilinium phosphite: A structural, vibrational, thermal and computational study. Panicker L. *Journal of Molecular Structure*. Vol. 1288, ArtNo. 135773.

16. 4d element induced improvement of structural disorder and development of weakly reentrant spin-glass behavior in NiRuMnSn. Gupta S., Chakraborty S., Bhasin V., et al. *Physical Review B*. Vol. 108(5), ArtNo. 54405.

17. 4E analysis and optimization of novel ejector-enhanced organic Rankine cycles by introducing new economic models. Srivastava M., Sarkar J., Sarkar A., et al. *Thermal Science and Engineering Progress*. Vol. 41, ArtNo. 101855.

18. 68Ga-Labeled Trastuzumab Fragments for ImmunoPET Imaging of Human Epidermal Growth Factor Receptor 2 Expression in Solid Cancers. Suman S.K., Mukherjee A., Pandey U., et al. *Cancer Biotherapy and Radiopharmaceuticals*. Vol. 38(1), pg. 38-50.

19. 68Ga-PSMA-11 PET/CT Imaging in Brain Gliomas and Its Correlation with Clinicopathological Prognostic Parameters. Verma P., Singh B.K., Sudhan M.D., et al. *Clinical Nuclear Medicine*. Vol. 48(12), pg. E559-E563.

20. A 2D Cu(ii) coordination polymer constructed with 2,5-pyridinedicarboxylic acid linker: synthesis, structural analysis and its selective transformation into Cu and CuO nanoparticles. Karmakar G., Tyagi A., Wadawale A.P., et al. *New Journal of Chemistry*. Vol. 47(30), pg. 14297-14305.

21. A Better Understanding of Solidification of Alloys Through Study of Glass/Crystal Composites. Vishwanadh B., Ghosh C., Dasgupta A., et al. *Transactions of the Indian Institute of Metals*.

22. A case study on seasonal and annual average indoor radon, thoron, and their progeny level in Kohima district, Nagaland, India. Jamir S., Sahoo B.K., Mishra R., et al. *Isotopes in Environmental and Health Studies*. Vol. 59(1), pg. 100-111.

23. A CFD-based approach to study the deposition and distribution behaviour of 212Pb in a calibration chamber. Agarwal T.K., Mishra R., Sapra B.K. *Environmental Science and Pollution Research*. Vol. 30(16), pg. 46950-46959.

24. A Clinical Conundrum with Diagnostic and Therapeutic Challenge: a Tale of Two Disorders in One Case. Gaikwad P., Bargir U.A., Shinde S., et al. *Journal of Clinical Immunology*. Vol. 43(8), pg. 1891-1902.

25. A combined powder x-ray and neutron diffraction studies on (1-x) NaNbO3-x Na0.50Bi0.50TiO3 solid solution. Jayakrishnan V.B., Mishra S.K., Shinde A.B., et al. *Journal of Solid State Chemistry*. Vol. 322, ArtNo. 123996.

26. A combined study on structural, magnetic and specific heat on double perovskite iridates Ln2CoIrO6 [Ln = Pr, Nd]. Datta R., Pradhan S.K., Saha R.A., et al. *Journal of Physics Condensed Matter*. Vol. 35(12), ArtNo. 125803.

27. A comparative photophysical study on the structurally related coumarin 102 and coumarin 153 dyes. Sayed M., Maity D.K., Pal H. *Journal of Photochemistry and Photobiology A: Chemistry*. Vol. 434, ArtNo. 114265.

28. A comparative study on pyrochlore phase formation in La2Zr2O7 in microscopic and macroscopic scale. Banerjee D., Parayil R.T., Gupta S.K., et al. *Journal of Radioanalytical and Nuclear Chemistry*.

29. A comparative study on the uptake of lanthanides from acidic feeds using extraction chromatography resins containing N,N,N',N'-tetra-n-alkyl diglycolamides with varying alkyl chain lengths in an ionic liquid. Yadav A.G., Gujar R.B., Valsala T.P., et al. *Journal of Chromatography A*. Vol. 1687, ArtNo. 463683.

30. A comprehensive investigation on CdO-SnO2 system: Structure, thermal expansion and energetics. Narang S., Aiswarya P.M., Dawar R., et al. *Journal of Alloys and Compounds*. Vol. 968, ArtNo. 171973.

31. A comprehensive review on unethical honey: Validation by emerging techniques. Brar D.S., Pant K., Krishnan R., et al. *Food Control*. Vol. 145, ArtNo. 109482.

32. A comprehensive study of radon in drinking waters of Hanumangarh district and the assessment of resulting dose to local population. Singla A.K., Kanse S., Kansal S., et al. *Environmental Geochemistry and Health*. Vol. 45(2), pg. 443-455.

33. A Computational Insight on the Effect of Encapsulation and Li Functionalization on Si12C12 Heterofullerene for H2 Adsorption: A Strategy for Effective Hydrogen Storage. Jaiswal A., Chakraborty B., Sahu S. *ACS Applied Energy Materials*. Vol. 6(6), pg. 3374-3389.

34. A Conceptual Catalytic Receiver Reactor for Solar Thermal Sulfuric Acid Decomposition. Tripathi V.M., Banerjee A.M., Nadar A., et al. *Energy Technology*. Vol. 11(6), ArtNo. 2201197.

35. A DFT study on the reaction pathway involved in the metal-ion-templated synthesis of benzo-21-crown-7(B21C7) from catechol and hexaethylene glycol ditosylate in the presence of base. Sisodiya D.S., Ali S.M., Chattopadhyay A. *Journal of Physical Organic Chemistry*. Vol. 36(3), ArtNo. e4471.

36. A donor strapped perylene bisimide macrocycle and its lemniscate dimer with extended charge separation. Veer S.D., Goswami T., Ravindranathan S., et al. *Organic Chemistry Frontiers*. Vol. 10(20), pg. 5099-5107.

37. A dual responsive ionic liquid-based polymeric hydrogel: a promising drug delivery vehicle for the treatment of breast cancer. Pansuriya R., Patel T., Mehra S., et al. *New Journal of Chemistry*. Vol. 47(30), pg. 14261-14272.

38. A high-density, 129-channel time-to-digital converter in FPGA for trigger-less data acquisition systems. Hari Prasad K., Chandratre V.B., Sukhwani M. *Nuclear Instruments and Methods in Physics Research, Section A: Accelerators, Spectrometers, Detectors and Associated Equipment*. Vol. 1056, ArtNo. 168657.

39. A Highly Porous and Flexible Carbon Nanotube Array Coated with Gold Nanoparticles: Application in Non-Enzymatic Ultrasensitive Detection and Monitoring of Blood/Saliva Glucose. Nechiyil D., Prakash J., Dey A., et al. *ChemistrySelect*. Vol. 8(17), ArtNo. e202300029.

40. A highly sensitive hemicyanine-based near-infrared fluorescence sensor for detecting toxic amyloid aggregates in human serum. Warerkar O.D., Mudliar N.H., Ahuja T., et al. *International Journal of Biological Macromolecules*. Vol. 247, ArtNo. 125621.

41. A highly sensitive method for uranium quantification in water samples at ultra-trace level by total reflection X-ray fluorescence, after its direct pre-concentration on the surface of amidoxime functionalized quartz sample supports. Sanyal K., Dhara S., Gumber N., et al. *Talanta*. Vol. 254, ArtNo. 124129.

42. A Hydrophobic Deep Eutectic Solvent for Nuclear Fuel Cycle: Extraction of Actinides and Dissolution of Uranium Oxide. Gamare J., Vats B.G. *European Journal of Inorganic Chemistry*. Vol. 26(35), ArtNo. e202300441.

43. A liposomal radionanoformulation for targeted drug delivery and real time monitoring by radionuclide imaging for HER2 overexpressing cancers. Suman S.K., Mukherjee A., Sharma R.K. *Drug Development Research*. Vol. 84(7), pg. 1553-1563.

44. A machine learning approach for correcting glow curve anomalies in CaSO4:Dy-based TLD dosimeters used in personnel monitoring. Pathan M.S., Pradhan S.M., Selvam T.P., et al. *Journal of Radiological Protection*. Vol. 43(3), ArtNo. 31503.

45. A Mega-Ampere Pulsed Current Generator Using Synchronization of Field Distortion Spark Gap Switches. Kanchi S., Shukla R., Sharma A. *IEEE Transactions on Plasma Science*. Vol. 51(7), pg. 1959-1965.

46. A method for in situ visualization of Protein-Nascent RNA interactions in single cell using Proximity Ligation Assay (IPNR-PLA) in mammalian cells. Das R., Dey A., Uppal S. *Transcription*. Vol. 14(45415), pg. 146-157.

47. A Multifunctional tannic acid-Fe3+-graphene oxide loaded alginate photothermal network: an interfacial water evaporator, a disinfector and a power generator. Amarnath M., Basu H., Basu R., et al. *Materials Advances*. Vol. 4(19), pg. 4537-4554.

48. A multivariate statistical and geospatial analysis of groundwater quality for drinking purposes in the Sagar district of Madhya Pradesh, India. Sharma A., Raidas H., Patel J.K., et al. *Groundwater for Sustainable Development*. Vol. 21, ArtNo. 100937.

49. A Nanocomposite of ZnO and N,P-Co-Doped Carbon Dots for the Photocatalytic Degradation of Various Dyes and their Kinetic Study. Bhavsar F.S., Mapari M.G., Tivalekar S.R., et al. *ChemistrySelect*. Vol. 8(43), ArtNo. e202301821.

50. A near infra-red emitting supramolecular dye-polymer assembly as promising platform for protamine sensing. Chakraborty G., Kant Chittela R., Nilaya Jonnalgadda P., et al. *Journal of Molecular Liquids*. Vol. 369, ArtNo. 120928.

51. A new compact micro-XRF spectrometer with polychromatic x-ray sample excitation. Wobrauschek P., Ingerle D., Prost J., et al. *X-Ray Spectrometry*.

52. A New Series of D1-A-D2-type ESIPT-TICT-AIE Active Orange-to-red Emissive Unsymmetrical Azines: Their All-throughout Mechanochemical Synthesis and Exploration of Photophysical Properties. Bhosle A.A., Banerjee M., Hiremath S.D., et al. *Chemistry - An Asian Journal*. Vol. 18(10), ArtNo. e202300048.

53. A phase-engineered nickel sulfide and phosphide (NiS-Ni2P) heterostructure for enhanced hydrogen evolution performance supported with DFT analysis. Das J.K., Sahu N., Mane P., et al. *Sustainable Energy and Fuels*. Vol. 7(17), pg. 4110-4119.

54. A Portable Technique for 226Ra Body Burden Estimation of Uranium Miners via Monitoring of 222Rn of Exhaled Breath. Patnaik R.L., Jha V.N., Singh M.K., et al. *Mapan - Journal of Metrology Society of India*.

55. A practical evaluation on integrated role of biochar and nanomaterials in soil remediation processes. Rajput V.D., Kumari A., Minkina T., et al. *Environmental Geochemistry and Health*. Vol. 45(12), pg. 9435-9449.

56. A proof of concept for the micellization of quercetin with anionic surfactants: Effect of counter ion. Vigneshwari R., Sivakumar K., Parinamachivayam G., et al. *Journal of Molecular Liquids*. Vol. 388, ArtNo. 122671.

57. A rationale for the rapid extraction of ultra-low-level uranyl ions in simulated bioassays regulated by Mn-dopants over magnetic nanoparticles. Mandal P., Sawant P.D., Bhattacharyya K. *RSC Advances*. Vol. 13(23), pg. 15783-15804.

58. A redox active organodiselenide as an efficacious catalyst for the synthesis of oxygen-containing heterocyclic compounds. Rahman N., Kushwah N., Priyadarsini K.I. *New Journal of Chemistry*. Vol. 47(33), pg. 15686-15693.

59. A review of electrochemical glucose sensing based on transition metal phosphides. Lakshmy S., Santhosh S., Kalarikkal N., et al. *Journal of Applied Physics*. Vol. 133(7), ArtNo. 70702.

60. A review of the synthesis, properties, and applications of 2D transition metal dichalcogenides and their heterostructures. Joseph S., Mohan J., Lakshmy S., et al. *Materials Chemistry and Physics*. Vol. 297, ArtNo. 127332.

61. A review on design aspects and behavioral studies of pile foundations in liquefiable soil. Pradhan M.K., Kumar P., Phanikanth V.S., et al. *Geomechanics and Geoengineering*. Vol. 18(5), pg. 347-379.

62. A robust lyophilized kit for convenient one-step formulation of [68Ga]Ga-DOTA-E−[c(RGDfK)]2 in hospital radiopharmacy for clinical PET imaging. Das S., Sahu S., Chakraborty A., et al. *Applied Radiation and Isotopes*. Vol. 196, ArtNo. 110725.

63. A search for decays of the Higgs boson to invisible particles in events with a top-antitop quark pair or a vector boson in proton-proton collisions at √s=13TeV. Tumasyan A., Adam W., Andrejkovic J.W., et al. *European Physical Journal C*. Vol. 83(10), ArtNo. 933.

64. A search for new physics in central exclusive production using the missing mass technique with the CMS detector and the CMS-TOTEM precision proton spectrometer. Tumasyan A., Adam W., Andrejkovic J.W., et al. *European Physical Journal C*. Vol. 83(9), ArtNo. 827.

65. A shear modified enhanced Gurson constitutive relation and implications for localization. Khan I.A., Benzerga A.A., Needleman A. *Journal of the Mechanics and Physics of Solids*. Vol. 171, ArtNo. 105153.

66. A Simplified and Affordable Arsenic Filter to Prevent Arsenic Poisoning: Lab-Scale Study and Pilot Experiment. Panda A.P., Jha U., Kumar S.A., et al. *ACS ES and T Water*. Vol. 3(12), pg. 4092-4102.

67. A simplified and cost-effective detection of cancer bio-markers using BODIPY and surfactant-templated fluorogenic self-assembly. Sarkar S., Gorai S., Potnis A., et al. New Journal of Chemistry. Vol. 47(46), pg. 21526-21532.

68. A simplified approach for determination of inflection points of flattening filter-free photon beam using in-house developed software and derivation of reference levels. Sharma S., Dixit D., Sharma S., et al. Journal of Medical Physics. Vol. 48(3), pg. 259-267.

69. A Simulated Annealing optimization technique to obtain uniform dose distribution in gamma irradiators. Chakrabarty S., Vishwakarma R.S., Selvam T.P. *Radiation Physics and Chemistry*. Vol. 209, ArtNo. 110959.

70. A Single Step Acid Assisted Microwave Digestion Method for the Complete Dissolution of Bauxite and Quantitation of its Composition (Al2O3, Fe2O3, SiO2, TiO2, Cr2O3, MgO, MnO and V2O5) by ICP-AES. Prasad A.D., Rastogi L., Thangavel S., et al. *Geostandards and Geoanalytical Research*. Vol. 47(2), pg. 403-413.

71. A SnO2/MXene hybrid nanocomposite as a negative electrode material for asymmetric supercapacitors. Padhy A., Lakshmy S., Chakraborty B., et al. *Sustainable Energy and Fuels*. Vol. 7(21), pg. 5271-5282.

72. A SNP-based linkage mapping revealed a mutant-origin major quantitative trait locus for seed size in A05 chromosome of groundnut (Arachis hypogaea L.). Bhad P.G., Mondal S., Badigannavar A.M. *Euphytica*. Vol. 219(8), ArtNo. 85.

73. A starch based sustainable bio-hybrid composite for surface assimilation of methylene blue: preparation, characterization, and adsorption study. Nambiar A.P., Pillai R., Sanyal M., et al. *Environmental Science: Advances*. Vol. 2(6), pg. 861-876.

74. A study on optimisation of vehicle allocation for evacuation during a site emergency at a nuclear power plant. Chandra A., Seshadri M., Chaudhury P. *International Journal of Operational Research*. Vol. 48(2), pg. 246-258.

75. A study on the evolution of carbide phases in Nb-1Zr-0.1C alloy under the influence of neutron and Ne ion irradiation. Goel L., Kumar N.N., Ali K., et al. *Journal of Alloys and Compounds*. Vol. 960, ArtNo. 170959.

76. A synoptic assessment of groundwater quality in high water-demand regions of coastal Andhra Pradesh, India. Kumari B., Keesari T., Pant D., et al. *Water Supply*. Vol. 23(9), pg. 3614-3634.

77. A treatise on occurrence, beneficiation and plant practices of tungsten-bearing ores. Das S.K., Nagesh C.H.R.V.S., Sreenivas T., et al. *Powder Technology*. Vol. 429, ArtNo. 118938.

78. A turn-on fluorescence sensor for detection of heparinase with heparin templated aggregation of tetracationic porphyrin derivative. Pandey S.P., Singh P.K., Jha P., et al. *International Journal of Biological Macromolecules*. Vol. 249, ArtNo. 125934.

79. A unified thermal-field emission theory for metallic nanotips. Ramachandran R., Biswas D. *Journal of Applied Physics*. Vol. 134(21), ArtNo. 214304.

80. Ab-initio study of C2/c, Cmca-12, Pbcn and P6122 phases of solid hydrogen. Gorai S., Modak P., Verma A.K. *Physica B: Condensed Matter*. Vol. 655, ArtNo. 414772.

81. Absence of magnetostriction and transition from rapid positive thermal expansion to negative thermal expansion at high temperatures in Sm0.5Y0.5Fe0.58Mn0.42O3 – A synchrotron X-ray diffraction study. Raut S., Mohanty H.S., Sharma R.K., et al. *Journal of Magnetism and Magnetic Materials*. Vol. 580, ArtNo. 170905.

82. AC Conductivity and Dielectric Constant of Fast Ion-Electronic Conductor AgI-C. Jayakrishnan V.B., Mishra S.K., Selvamani R., et al. *ECS Journal of Solid State Science and Technology*. Vol. 12(12), ArtNo. 123002.

83. Accessing copper selenide nanostructures through a 1D coordination polymer of copper(ii) with 4,4'-dipyridyldiselenide as a molecular precursor. Pal M.K., Karmakar G., Shah A.Y., et al. *New Journal of Chemistry*. Vol. 47(36), pg. 16954-16963.

84. Accurate Determination of the Bandgap Energy of the Rare-Earth Niobate Series. Garg A.B., Vie D., Rodriguez-Hernandez P., et al. *Journal of Physical Chemistry Letters*. Vol. 14(7), pg. 1762-1768.

85. Achieving perfect white light, color tunability and X-ray scintillation in nanocrystalline La2Hf2O7:Eu3+,Bi3+ by photon energy and doping engineering. Gupta S.K., Modak B., Mao Y. *Materials Today Chemistry*. Vol. 33, ArtNo. 101705.

86. Acid-Resistant Luminescent Si/UiO-66-Amidoxime (AO) Nanostructures for Rapid and Efficient Recovery of U(VI): Experimental and Theoretical Studies. Vaddanam V.S., Pamarthi A., Sengupta S., et al. *ACS Applied Nano Materials*. Vol. 6(10), pg. 8222-8237.

87. Activation cross section for the (n,2n) and (n,p) reactions on 103Rh, 48Ti and 52Cr from reaction threshold up to 25 MeV energy region. Singh R.K., Singh N.L., Mehta M., et al. *Applied Radiation and Isotopes*. Vol. 200, ArtNo. 110949.

88. Activation cross sections of radionuclides produced by alpha induced reactions on natCd up to 40 MeV for optimized production of 117mSn. Raja S.W., Acharya R. *European Physical Journal A*. Vol. 59(9), ArtNo. 214.

89. Acute and sub-acute oral toxicity assessment of 5-hydroxy-1,4-naphthoquinone in mice. Gohil D., Panigrahi G.C., Gupta S.K., et al. *Drug and Chemical Toxicology*. Vol. 46(4), pg. 795-808.

90. Additive energy functions have predictable landscape topologies. Story B., Sadhu B., Adams H., et al. *Journal of Chemical Physics*. Vol. 158(16), ArtNo. 164104.

91. Additive-Free Continuous, Weavable Carbon Nanotube Fibers as Wearable Multifunctional Gas Sensor. Rohilla R., Prakash J., Rao P., et al. *IEEE Sensors Journal*. Vol. 23(24), pg. 30102-30111.

92. Adsorption and dehydrogenation of ammonia on Ru55, Cu55 and Ru@Cu54 nanoclusters: role of single atom alloy catalyst. Chattaraj D., Majumder C. *Physical Chemistry Chemical Physics*. Vol. 26(1), pg. 524-532.

93. Adsorption of rare earth elements in carboxylated mesoporous carbon. Saha D., Bhasin V., Khalid S., et al. *Separation and Purification Technology*. Vol. 314, ArtNo. 123583.

94. Advances in the application of carbon nanotubes as catalyst support for hydrogenation reactions. Yadav M.D., Joshi H.M., Sawant S.V., et al. *Chemical Engineering Science*. Vol. 272, ArtNo. 118586.

95. Aerobic reduction of selenite and tellurite to elemental selenium and tellurium nanostructures by Alteromonas sp. under saline conditions. Kiran Kumar Reddy G., Pathak S., Nancharaiah Y.V. *International Biodeterioration and Biodegradation*. Vol. 179, ArtNo. 105571.

96. Age-dependent ingestion doses to the public of Rupnagar and Una regions of India due to intake of uranium. Mehta V., Kaur J., Shikha D., et al. *Journal of Radioanalytical and Nuclear Chemistry*. DOI:10.1007/s10967-023-09185-9

97. AI and CV based 2D-CNN algorithm: botanical authentication of Indian honey. Brar D.S., Aggarwal A.K., Nanda V., et al. *Sustainable Food Technology*. DOI:10.1039/D3FB00170A

98. AIE-Active 'Turn-On' Sensors for Highly Selective Detection of Bovine Serum Albumin**. Gawade V.K., Jadhav R.W., Singh P.K., et al. *ChemistrySelect*. Vol. 8(33), ArtNo. e202302474.

99. Al3+-Responsive Ratiometric Fluorescent Sensor for Creatinine Detection: Thioflavin-T and Sulfated-β-Cyclodextrin Synergy. Bais S., Singh P.K. *ACS Applied Bio Materials*. Vol. 6(10), pg. 4146-4157.

100. Al5BO9:Tb3+: Synthesis, structural characterization and thermoluminescence dosimetry studies for high intensity thermal neutron beams. Sen M., Shukla R., Pathak N., et al. *Ceramics International*. Vol. 49(20), pg. 33358-33368.

101. Alginate Encapsulation of Shoot Tips and Their Regeneration for Enhanced Mass Propagation and Germplasm Exchange of Genetically Stable Stevia rebaudiana Bert.. Subrahmanyeswari T., Laha S., Kamble S.N., et al. *Sugar Tech*. Vol. 25(3), pg. 542-551.

102. All-solid-state flexible supercapacitor based on a binary transition metal dichalcogenide grown on 2D/2D heterostructure materials. Patra A., Mane P., Pramoda K., et al. *Journal of Energy Storage*. Vol. 68, ArtNo. 107825.

103. Alpha-cadinol as a potential ACE-inhibitory volatile compound identified from Phaseolus vulgaris L. through in vitro and in silico analysis. Tripathi J., Gupta S., Gautam S. *Journal of Biomolecular Structure and Dynamics*. Vol. 41(9), pg. 3847-3861.

104. Alpha-induced production and robust radiochemical separation of 43Sc as an emerging radiometal for formulation of PET radiopharmaceuticals. Chakravarty R., Banerjee D., Chakraborty S. *Applied Radiation and Isotopes*. Vol. 199, ArtNo. 110921.

105. Alternative vehicular fuels for environmental decarbonization: A critical review of challenges in using electricity, hydrogen, and biofuels as a sustainable vehicular fuel. Sandaka B.P., Kumar J. *Chemical Engineering Journal Advances*. Vol. 14, ArtNo. 100442.

106. Americium doping induced self irradiation of SrBPO5: 241Am: Spectroscopic insight. Mohapatra M., Gupta S.K. *Materials Letters: X*. Vol. 17, ArtNo. 100185.

107. Amine-Functionalized Graphene-Rich NiFe Layered Double Hydroxide Nanostructure for Enhanced Electrocatalytic Water and Urea Oxidation. Tavar D., Ojha S.K., Zaidi Z., et al. *ACS Applied Nano Materials*. Vol. 6(24), pg. 22517-22531.

108. Amino acids induced modulations in linear PEO-PPO-PEO triblock copolymer microstructures and its exploration in prototypical drug solubilization. Chakrabarti C., Kakkad H., Desai S., et al. *Journal of Surfactants and Detergents*. Vol. 26(6), pg. 893-902.

109. Amphiphilic interaction-mediated ordering of nanoparticles in Pickering emulsion droplets. Sen D., Das A., Kumar A., et al. *Soft Matter*. Vol. 19(21), pg. 3953-3965.

110. Ample Lewis Acidic Sites in Mg2B2O5 Facilitate N2 Electroreduction through Bonding-Antibonding Interactions. Biswas A., Ghosh B., Sudarshan K., et al. *Inorganic Chemistry*. Vol. 62(34), pg. 14094-14102.

111. An ab initio study of catechol sensing in pristine and transition metal decorated γ-graphyne. Dewangan J., Mahamiya V., Shukla A., et al. *Nanotechnology*. Vol. 34(17), ArtNo. 170001.

112. An augmented QCD phase portrait: Mapping quark-hadron deconfinement for hot, dense, rotating matter under magnetic field. Mukherjee G., Dutta D., Mishra D.K. *Physics Letters, Section B: Nuclear, Elementary Particle and High-Energy Physics*. Vol. 846, ArtNo. 138228.

113. An evaluation of arsenic contamination status and its potential health risk assessment in villages of Nadia and North 24 Parganas, West Bengal, India. Singh S., Shukla A., Srivastava S., et al. *Environmental Science and Pollution Research*.

114. An experimental and numerical study: to investigate the switching characteristics of a field-distortion sparkgap switch in various SF6 admixtures. Kumar G.V., Verma R., Singh G., et al. *Engineering Research Express*. Vol. 5(4), ArtNo. 45079.

115. An experimental approach to delineate the reaction mechanism of Ti3AlC2 MAX-Phase formation. Yunus M., Maji B.C. *Journal of the European Ceramic Society*. Vol. 43(8), pg. 3131-3145.

116. An experimental investigation on rewetting of a 54 pins fuel bundle under steam environment by radial jet injection. Yadav S.K., Kumar M., Kumar R., et al. *Annals of Nuclear Energy*. Vol. 185, ArtNo. 109712.

117. An FPGA-based automated approach for identification and setting of the single electron response threshold voltage in portable TDCR systems. Sharma M.K., Agarwal S., Kulkarni M.S., et al. *Nuclear Instruments and Methods in Physics Research, Section A: Accelerators, Spectrometers, Detectors and Associated Equipment*. Vol. 1048, ArtNo. 167925.

118. An improved strain path dependent model under multiaxial cyclic loading for simulating material response of low C-Mn steel. Pandey V., Arora P., Gupta S.K., et al. *International Journal of Fatigue*. Vol. 167, ArtNo. 107322.

119. An Isothiazolanthrone-Based Self-Assembling Anticancer Color-Changing Dye for Concurrent Imaging and Monitoring of Cell Viability. Gour N., Kshtriya V., Khatun S., et al. *Chemistry - An Asian Journal*. Vol. 18(9), ArtNo. e202300044.

120. An outline of high-fidelity neutron transport simulations for advanced nuclear reactor concepts. Gupta A., Dwivedi D.K., Singh I., et al. *Nuclear and Particle Physics Proceedings*. Vol. 339-340 pg. 124-128.

121. An Overview of Vehicular Emission Standards. Singh S., Kulshrestha M.J., Rani N., et al. *Mapan - Journal of Metrology Society of India*. Vol. 38(1), pg. 241-263.

122. An ultrasensitive and selective method for visual detection of heparin in 100 % human plasma. Pandey S.P., Jha P., Singh P.K. *Talanta*. Vol. 253, ArtNo. 124040.

123. An ultrathin 2D NiCo-LDH nanosheet decorated NH2-UiO-66 MOF-nanocomposite with exceptional chemical stability for electrocatalytic water splitting. Sk S., Madhu R., Gavali D.S., et al. *Journal of Materials Chemistry A*.

124. An X-ray fluorescence and machine learning based methodology for the direct non-destructive compositional analysis of (Th1−xUx)O2 fuel pellets. Kanrar B., Sanyal K., Sarkar A., et al. *Journal of Analytical Atomic Spectrometry*. Vol. 38(9), pg. 1841-1850.

125. Analysis of Ductile-to-Brittle Transition Characteristics of Reactor Pressure Vessel Steels. Gupta C. *Nuclear Technology*. Vol. 209(4), pg. 560-581.

126. Analysis of dynamic responses of circulating fuel reactors using in-house 3D space-time kinetics code ARCH. Singh I., Gupta A., Kannan U. *Nuclear and Particle Physics Proceedings*. Vol. 339-340 pg. 66-69.

127. Analysis of Integral Experiment of the AHWR Critical Facility with Diffusion-Based Monte Carlo Method. Srivastava A., Bhandari D., Singh K.P., et al. *Nuclear Science and Engineering*. Vol. 197(4), pg. 703-710.

128. Analysis of Kobayashi benchmark with indigenous Monte Carlo neutron transport code PATMOC. Mallick A.K., Kannan U. *Physics Open*. Vol. 17, ArtNo. 100179.

129. Analysis of occupational radiation dose data and determination of suitable probability distribution. Patil S., Bakshi A. *Radiation Protection Dosimetry*. Vol. 199(11), pg. 1208-1222.

130. Analysis of PbBi eutectic after matrix separation by acid induced dispersive liquid-liquid microextraction followed by HR-CS-ETAAS determination. Madhavi K., Venkateswarlu G., Meeravali N.N., et al. Journal of Analytical Atomic Spectrometry. Vol. 38(11), pg. 2332-2341.

131. Analysis of residual cross sections from N 14 + Nb 93 reaction: Fusion dynamics of a non- α -cluster projectile. Sharma H., Maiti M., Nag T.N., et al. Physical Review C. Vol. 107(6), ArtNo. 64601.

132. Angiogenesis Imaging of Adrenocortical Carcinoma with Ga 68 NODAGA RGD Positron Emission Tomography: Opening New Horizons in Multimodality Imaging from Theranostic Perspective. Verma P., Chandak A., Shetye S.S., et al. Indian Journal of Nuclear Medicine. Vol. 38(2), pg. 183-184.

133. Anisotropic electrical properties of 200 MeV Ag+15 ion irradiated manganite films. Udeshi B., Hirpara B., Hans S., et al. Materials Chemistry and Physics. Vol. 301, ArtNo. 127688.

134. Anisotropy study of hydrogen diffusion along different directions of Zr-2.5%Nb alloy pressure tube using neutron imaging. Shukla S., Singh R.N., Kashyap Y.S., et al. Journal of Nuclear Materials. Vol. 580, ArtNo. 154414.

135. Anomalous Viscosity, Aggregation, and Non-Ergodic Phase of Laponite® RD in a Water–Methanol Binary Solvent. Tiwari P., Bohidar H.B., Das A., et al. *Clays and Clay Minerals*. Vol. 71(1), pg. 1-13.

136. Antioxidant and Anti-inflammatory Activities Mediate the Radioprotective Effect of Trianthema portulacastrum L. Extracts. Das U., Saha T., Sharma R.K., et al. *Natural Products Journal*. Vol. 13(5), ArtNo. e270622206422.

137. APMP/TCRI Key Comparison Report of Measurement of Air Kerma for Medium-Energy X-Rays (APMP.RI(I)-K3.2013). Chu C.H., Butler D.J., Tanaka T., et al. *Metrologia*. Vol. 60(0. 0416666666666667), ArtNo. 6009.

138. Application of conventional spray dryer to prepare nanosilica-alginate based rhodamine loaded microstructures and nanobeads. Mishra A., Melo J.S., Bhainsa K.C. *Journal of Materials Research*. Vol. 38(13), pg. 3362-3371.

139. Application of Drug Aggregation to Solubilize Antimicrobial Compound and Enhancing its Bioavailability. Mavani A., Ray D., Aswal V.K., et al. *Applied Biochemistry and Biotechnology*. Vol. 195(5), pg. 3206-3216.

140. Application of Machine Learning in Predicting Hepatic Metastasis or Primary Site in Gastroenteropancreatic Neuroendocrine Tumors. Padwal M.K., Basu S., Basu B. *Current Oncology*. Vol. 30(10), pg. 9244-9261.

141. Application of Multi Parameter Path Length Method for Resilience (MP-PLMR) to Engineering Systems. Prasad M., Gopika V., Andrews J. *ASCE-ASME Journal of Risk and Uncertainty in Engineering Systems, Part B: Mechanical Engineering*. Vol. 9(2), ArtNo. 21201.

142. Application of Thiourea Ameliorates Stress and Reduces Accumulation of Arsenic in Wheat (Triticum aestivum L.) Plants Grown in Contaminated Field. Shukla A., Pathak S.K., Singh S., et al. *Journal of Plant Growth Regulation*. Vol. 42(10), pg. 6171-6182.

143. Application of tracer technology in wastewater treatment processes: a review. Sarkar M., Sangal V.K., Pant H.J., et al. *Chemical Engineering Communications*. Vol. 210(1), pg. 16-33.

144. Application of ultrasound in heat exchanger handling supersaturated CaSO4 solution for reduction of scaling by induced precipitation and in-situ cleaning. Banakar V.V., Gogate P.R., Raha A., et al. *Chemical Engineering Science*. Vol. 276, ArtNo. 118814.

145. Applications of Energy Dispersive X-Ray Fluorescence Spectrometry and Direct Current Arc Atomic Emission Spectroscopy Methods for Grouping Study of Automobile Windshield Glasses for Glass Forensics. Sharma V., Sengupta A., Acharya R., et al. *ChemistrySelect*. Vol. 8(12), ArtNo. e202204901.

146. Appraisal of age-dependent radiological risk caused by ingestion of uranium in groundwater of Patiala district, Punjab. Mehta V., Kapil C., Shikha D., et al. *Journal of Radioanalytical and Nuclear Chemistry*.

147. Approach for C1 to C2 products commencing from carbon dioxide: A brief review. Dey G.R. *Petroleum*.

148. Arabinogalactan G1-4A isolated from Tinospora cordifolia induces PKC/mTOR mediated direct activation of natural killer cells and through dendritic cell cross-talk. Amin P.J., Shankar B.S. *Biochimica et Biophysica Acta - General Subjects*. Vol. 1867(4), ArtNo. 130312.

149. Are LMICs Achieving the Lancet Commission Global Benchmark for Surgical Volumes? A Systematic Review. Patil P., Nathani P., Bakker J.M., et al. *World Journal of Surgery*. Vol. 47(8), pg. 1930-1939.

150. Arsenic Contamination in Rice Agro-ecosystems: Mitigation Strategies for Safer Crop Production. Singh S., Rajput V.D., Upadhyay S.K., et al. *Journal of Plant Growth Regulation*. Vol. 42(10), pg. 6413-6424.

151. Ascorbic acid: a metabolite switch for designing stress-smart crops. Mishra S., Sharma A., Srivastava A.K. *Critical Reviews in Biotechnology*. Vol., ArtNo. .

152. Aspirin-Induced Ordering and Faster Dynamics of a Cationic Bilayer for Drug Encapsulation. Sahu S., Srinivasan H., Jadhav S.E., et al. *Langmuir*. Vol. 39(46), pg. 16432-16443.

153. Assaying of SNM using Simultaneous Detection of Fission Neutrons and Gammas by Employing a Novel Phoswich Detector. Sonu, Tyagi M., Kelkar A., et al. Nuclear Engineering and Technology. Vol. 55(7), pg. 2662-2669.

154. Assessing techno-economic uncertainties in nuclear power-to-X processes: The case of nuclear hydrogen production via water electrolysis. Bhattacharyya R., Singh K.K., Bhanja K., et al. International Journal of Hydrogen Energy. Vol. 48(38), pg. 14149-14169.

155. Assessing the efficiency of different solvents for detecting gliotoxin from soil, organic manures and crop plant. Jayalakshmi R., Mehetre S.T., Kannan R., et al. *International Journal of Environmental Analytical Chemistry*. Vol. 103(17), pg. 4953-4969.

156. Assessing the prospect of XAFS experiments of metalloproteins under in vivo conditions at Indus-2 synchrotron facility, India. Lahiri D., Agrawal R., Chandravanshi K., et al. *Journal of Synchrotron Radiation*. Vol. 30(Pt 2), pg. 449-456.

157. Assessment of a Novel Chemical Analysis Technique to Investigate Cesium in Glass by Developing Cesium Bismuth Iodide. Kumar B., Das B., Sinha P., et al. *Transactions of the Indian Ceramic Society*. Vol. 82(3), pg. 169-176.

158. Assessment of Biogrowth at Two Different Environments of Nuclear Power Plant Cooling Water System Located at Southern Coast of India. Ganesh S., Retna A.M., Wesley S.G., et al. *Asian Journal of Chemistry*. Vol. 35(1), pg. 69-78.

159. Assessment of Discharged 222Rn at Surface from Ventilation Shafts of Underground Uranium Mine at Narwapahar in India. Srivastava V.S., Jha S.K., Kulkarni M.S. *Mapan - Journal of Metrology Society of India*.

160. Assessment of Dose Rates to Non-human Biota of Terrestrial Environment around Kaiga Generating Station, Kaiga. Jain S., Joshi R.M., Ajith T.L., et al. *Mapan - Journal of Metrology Society of India*.

161. Assessment of Elements in Curcuma caesia Rhizome through Various Instrumentation Techniques. Atom R.S., Laitonjam W.S., Ningthoujam R.S. *Agricultural Science Digest*. Vol. 43(2), pg. 214-219.

162. Assessment of gamma radiation through agro-morphological characters in camellia sinensis L. (O.) kuntze. Singh S.K., Borthakur D., Tamuly A., et al. *International Journal of Radiation Biology*. Vol. 99(5), pg. 866-874.

163. Assessment of ionic site distributions in magnetic high entropy oxide of (Mn0·2Fe0·2Co0·2Ni0·2Zr0.2)3O4 and its catalytic behaviour. Shaw S.K., Kumari P., Sharma A., et al. *Physica B: Condensed Matter*. Vol. 652, ArtNo. 414653.

164. Assessment of Macronutrients and Physicochemical Parameters of Agricultural Soils in Nawanshahr-Hoshiarpur Districts of Punjab. Shikha D., Dadwal V., Kapil C., et al. *Indian Journal of Pure and Applied Physics*. Vol. 61(6), pg. 404-409.

165. Assessment of metallic membrane-based counter-current micro-contactor for non-dispersive solvent extraction: Experimental studies and modelling. Chaurasiya R.K., Singh K.K. *Chemical Engineering and Processing - Process Intensification*. Vol. 193, ArtNo. 109528.

166. Assessment of Radon (222Rn) and Thoron (220Rn) in Environmental Resources of a High-Background-Radiation Area, India. Prusty P., Sahu A., Jha S.K. *Mapan - Journal of Metrology Society of India*.

167. Assessment of radon, thoron, and their progeny concentrations in the dwellings of Shivalik hills of Jammu and Kashmir, India. Kaur M., Kumar A., Mehra R., et al. *Environmental Geochemistry and Health*. Vol. 45(8), pg. 5685-5701.

168. Association of Cutibacterium acnes with human thyroid cancer. Trivedi V., Noronha V., Sreekanthreddy P., et al. *Frontiers in Endocrinology*. Vol. 14, ArtNo. 1152514.

169. Astatine-211 for PSMA-targeted α-radiation therapy of micrometastatic prostate cancer: a sustainable approach towards precision oncology. Chakravarty R., Lan X., Chakraborty S., et al. *European Journal of Nuclear Medicine and Molecular Imaging*. Vol. 50(7), pg. 1844-1847.

170. Atomic site preference, electronic structures, and magnetic properties of γ-brass type pseudo-binary Mn2Zn11–Ni2Zn11 at high Mn-contents. Ghanta S., Mondal A., Das A., et al. *Journal of Alloys and Compounds*. Vol. 932, ArtNo. 167599.

171. Au ion beam engineered MXene incorporated TiO2 photoanodes for quantum dot sensitized solar cells. Singh I., Bhullar V., Devi D., et al. *Materials Science and Engineering: B*. Vol. 290, ArtNo. 116342.

172. Author Correction: A portrait of the Higgs boson by the CMS experiment ten years after the discovery (Nature, (2022), 607, 7917, (60-68), 10.1038/s41586-022-04892-x). Tumasyan A., Adam W., Andrejkovic J.W., et al. *Nature*. Vol. 623(7985).

173. Authors' Reply: Are LMICs Achieving the Lancet Commission Global Benchmark for Surgical Volumes? A Systematic Review. Patil P., Nathani P., Bakker J., et al. *World Journal of Surgery*. Vol. 47(12), pg. 3439-3440.

174. Auto-CREAM: Software application for evaluation of HEP with basic and extended CREAM for PSA studies. Garg V., Vinod G., Kant V. *Reliability Engineering and System Safety*. Vol. 236, ArtNo. 109318.

175. Azimuthal correlations in Z +jets events in proton–proton collisions at √s=13TeV. Tumasyan A., Adam W., Andrejkovic J.W., et al. *European Physical Journal C*. Vol. 83(8), ArtNo. 722.

176. Azimuthal Correlations within Exclusive Dijets with Large Momentum Transfer in Photon-Lead Collisions. Tumasyan A., Adam W., Bergauer T., et al. *Physical Review Letters*. Vol. 131(5), ArtNo. 51901.

177. Backstepping based model reference adaptive control for nuclear reactor with matched and unmatched uncertainties. Reddy P.M.S., Shimjith S.R., Tiwari A.P., et al. *Progress in Nuclear Energy*. Vol. 158, ArtNo. 104585.

178. Band gap and defect engineering of bismuth vanadate using La, Ce, Zr dopants to obtain a photoelectrochemical system for ultra-sensitive detection of glucose in blood serum. Prakash J., Nechiyil D., Ali K., et al. *Dalton Transactions*. Vol. 52(7), pg. 1989-2001.

179. Band-Gap Energy and Electronic d-d Transitions of NiWO4 Studied under High-Pressure Conditions. Errandonea D., Rodriguez F., Vilaplana R., et al. *Journal of Physical Chemistry C*. Vol. 127(31), pg. 15630-15640.

180. Battery-powered FPGA-based embedded system for ultrasonic pipe inspection and gauging systems. Kumar N.P., Patankar V.H. *Review of Scientific Instruments*. Vol. 94(3), ArtNo. 34712.

181. Benchmarking exercise of indigenous Monte Carlo neutron transport code PATMOC for hexagonal full core reactor geometry. Mallick A.K., Kannan U. *Nuclear and Particle Physics Proceedings*. Vol. 339-340 pg. 62-65.

182. Berberine and cyclodextrin based supramolecular assembly for the detection of a cancer biomarker in complex biomatrices via indicator displacement assay. Hasan F.F., Sarkar S., Chakraborty G. *Microchemical Journal*. Vol. 194, ArtNo. 109366.

183. Beta decay study of 126Sb and 126mSb. Mukherjee G., Nayak S.S., Datta J., et al. *Journal of Radioanalytical and Nuclear Chemistry*.

184. Bimetallic Zeolitic Imidazole Frameworks for Improved Stability and Performance of Intrusion-Extrusion Energy Applications. Amayuelas E., Sharma S.K., Utpalla P., et al. *Journal of Physical Chemistry C*. Vol. 127(37), pg. 18310-18315.

185. Binding of human serum albumin with uranyl ion at various pH: an all atom molecular dynamics study. Mishra V., Pathak A.K., Bandyopadhyay T. *Journal of Biomolecular Structure and Dynamics*. Vol. 41(15), pg. 7318-7328.

186. Bioactive compounds in Layacha brown rice (Oryza sativa L.) improve immune responses in mice via activation of transcription factor Nrf2. John S., Chauhan A., Thada A., et al. *Food Bioscience*. Vol. 53, ArtNo. 102785.

187. Bioactive fluorcanasite reinforced magnesium alloy-based porous bio-nanocomposite scaffolds with tunable mechanical properties. Garimella A., Ramya M., Ghosh S.B., et al. *Journal of Biomedical Materials Research - Part B Applied Biomaterials*. Vol. 111(2), pg. 463-477.

188. Biochemical characterization of clinically relevant mutations of human Translin. Pillai V., Gupta A., Rao A., et al. *Molecular and Cellular Biochemistry*. Vol. 478(4), pg. 821-834.

189. Biochemical Properties and Roles of DprA Protein in Bacterial Natural Transformation, Virulence, and Pilin Variation. Sharma D.K., Misra H.S., Bihani S.C., et al. *Journal of Bacteriology*. Vol. 205(2).

190. Biochemical separation of Cetuximab-Fab from papain-digested antibody fragments and radiolabeling with 64Cu for potential use in radioimmunotheranostics. Chakravarty R., Rohra N., Jadhav S., et al. *Applied Radiation and Isotopes*. Vol. 196, ArtNo. 110795.

191. Bio-conjugated carbon dots for the bimodal detection of prostate cancer biomarkers via sandwich fluorescence and electrochemical immunoassays. Korram J., Anbalagan A.C., Banerjee A., et al. *Journal of Materials Chemistry B*.

192. Biodegradable Methane Sulfonic Acid-Based Nonaqueous Dissolution, Estimation, and Recovery: Toward Development of a Simplified Scheme for Plutonium-Bearing Fuel Matrices. Kumar S.S., Srivastava A., Rao A. *Industrial and Engineering Chemistry Research*. Vol. 62(1), pg. 660-669.

193. Bio-functionalized magnetic nanoparticles for cost-effective adsorption of U(vi): experimental and theoretical investigation. Das C., Ghosh N.N., Pulhani V., et al. *RSC Advances*. Vol. 13(22), pg. 15015-15023.

194. Biogenic synthesis, characterization and application of silver nanoparticles as biostimulator for growth and rebaudioside-A production in genetically stable stevia (Stevia rebaudiana Bert.) under in vitro conditions. Laha S., Subrahmanyeswari T., Verma S.K., et al. *Industrial Crops and Products*. Vol. 197, ArtNo. 116520.

195. Biomass-Derived Carbon Dots as Nanoprobes for Smartphone-Paper-Based Assay of Iron and Bioimaging Application. Korram J., Koyande P., Mehetre S., et al. *ACS Omega*. Vol. 8(34), pg. 31410-31418.

196. Biophysical and molecular modeling evidences for the binding of sulfa molecules with hemoglobin. Mavani A., Ovung A., Luikham S., et al. *Journal of Biomolecular Structure and Dynamics*. Vol. 41(9), pg. 3779-3790.

197. Bismuth Vanadate and 3D Graphene Composite Photoanodes for Enhanced Photoelectrochemical Oxidation of Water. Sharma A., Manna S., Kumar S., et al. *ACS Omega*. Vol. 8(37), pg. 33452-33465.

198. Block Copolymer Encapsulation of Disarib, an Inhibitor of BCL2 for Improved Chemotherapeutic Potential. Joy R., Siddiqua H., Sharma S., et al. *ACS Omega*. Vol. 8(43), pg. 40729-40740.

199. Boesenbergia albomaculata (Zingiberaceae): a New Addition to the Flora of India. Dey S., Barbhuiya H.A. *Acta Phytotaxonomica et Geobotanica*. Vol. 74(2), pg. 135-138.

200. Bonding of isovalent homologous actinide and lanthanide pairs with chalcogenide donors: effect of metal f-orbital participation and donor softness. Chattaraj S., Bhattacharyya A. *Structural Chemistry*. Vol. 34(1), pg. 307-316.

201. Boron carbide thin film surface characterization after graphitic carbon removal using low-pressure oxygen gas RF plasma. Yadav P.K., Gupta R.K., Gupta S., et al. *Applied Optics*. Vol. 62(5), pg. 1399-1405.

202. Broken tooth: a biological foreign body—case report. Rao K., Bhandarkar P. *Egyptian Journal of Otolaryngology*. Vol. 39(1), ArtNo. 54.

203. Bubble formation at top-submerged nozzles immersed in a quiescent liquid. Sarkar S., Sen N., Singh K.K. *Progress in Nuclear Energy*. Vol. 161, ArtNo. 104709.

204. Bulk and monolayer thermoelectric and optical properties of anisotropic NbS2Cl2. Natarajan A.R., Gupta M.K., Mittal R., et al. *Materials Today Communications*. Vol. 34, ArtNo. 105309.

205. C24 Fullerene and its derivatives as a viable glucose sensor: DFT and TD-DFT studies. Tukadiya N.A., Jana S.K., Chakraborty B., et al. *Surfaces and Interfaces*. Vol. 41, ArtNo. 103220.

206. Calibration free laser ablation molecular isotopic spectrometry (CF-LAMIS) for boron isotopic composition determination. Mohan A., Banerjee A., Sarkar A. *Journal of Analytical Atomic Spectrometry*. Vol. 38(8), pg. 1579-1591.

207. Can fluid-solid contact area quantify wettability during flow? – A parametric study. Singh D., Roy S., Pant H.J., et al. *Chemical Engineering Science*. Vol. 280, ArtNo. 118992.

208. Capacitance-based absolute pressure gauge for beamline vacuum measurement applications. Teotia V., Kumar P., Sawant S., et al. *Journal of Instrumentation*. Vol. 18(9), ArtNo. P09031.

209. Capture of volatile I2 by dithioglycol functionalized HKUST-1 and its polymeric composite beads. Kolay S., Sahu A.K., Jha P., et al. *Journal of Solid State Chemistry*. Vol. 324, ArtNo. 124080.

210. Capture of Volatile Iodine Gas and Identification of Adsorption Sites in the Pore Network of Unsubstituted Imidazole Linker-Incorporated Zeolitic Imidazolate Framework-8. Nelliyil R.B., Mor J., Kolay S., et al. ACS Applied Materials and Interfaces. Vol. 15(42), pg. 49312-49320.

211. Carbon dioxide absorption in packed bed of lithium orthosilicate pebbles. Ghuge N.S., Mandal D., Jadeja M.C., et al. Separation Science and Technology (Philadelphia). Vol. 58(5), pg. 849-861.

212. Carbonate treated coffee powder (CTCP) for selective sorption of Pu4+ over Am3+, Np4+, NpO22+, and PuO22+ from aqueous acidic solution: Investigation on mechanism, kinetics, thermodynamics, stripping and radiolytic stability. Patil P., Sarathbabu M., Pathak S., et al. Applied Radiation and Isotopes. Vol. 194, ArtNo. 110695.

213. Carbon-Manganese Oxide Composite Derived from Wheat Flour: Kitchen-Inspired Green Synthesis and Applications in Energy Storage. Dutta Pathak D., Guleria A., Nuwad J., et al. *ACS Applied Electronic Materials*. Vol., ArtNo. .

214. Cation–Oxygen Bond Covalency: A Common Thread and a Major Influence toward Air/Water-Stability and Electrochemical Behavior of “Layered” Na–Transition-Metal-Oxide-Based Cathode Materials. Kumar B.S., Pradeep A., Srihari V., et al. *Advanced Energy Materials*. Vol. 13(19), ArtNo. 2204407.

215. Cd-induced cytosolic proteome changes in the cyanobacterium Anabaena sp. PCC7120 are mediated by LexA as one of the regulatory proteins. Srivastava A., Kumar A., Biswas S., et al. *Biochimica et Biophysica Acta - Proteins and Proteomics*. Vol. 1871(3), ArtNo. 140902.

216. CellUSorb: A high-performance, radiation functionalized cellulose based adsorbent for Uranium (VI) remediation in ground water. Misra N., Rawat S., Kumar Goel N., et al. *Separation and Purification Technology*. Vol. 322, ArtNo. 124215.

217. Cesium ion removal from low-level radioactive wastewater utilizing synthesized cobalt hexacyanoferrate-sand composite. Singh K.K., Rawat M., Rawat J., et al. *Radiochimica Acta*. Vol. 111(9), pg. 679-689.

218. CFD and machine learning based hybrid model for passive dilution of helium in a top ventilated compartment. Sharma P.K., Verma V., Chattopadhyay J. *Kerntechnik*. Vol. 88(6), pg. 697-709.

219. Characterization of BRCA2 R3052Q variant in mice supports its functional impact as a low-risk variant. Mishra A.P., Hartford S., Chittela R.K., et al. *Cell Death and Disease*. Vol. 14(11), ArtNo. 753.

220. Characterization of horse gram mutants for yield, nutrient, and anti-nutrient factors. Sudhagar R., Pushpayazhini V., Vanniarajan C., et al. *Journal of Environmental Biology*. Vol. 44(1), pg. 99-107.

221. Characterization of indigenous OSL phosphors LiCaAlF6:Eu,Y and α-Al2O3:C for space dosimetry. Singh A.K., Rawat N.S., Dhabekar B., et al. *Radiation Physics and Chemistry*. Vol. 211, ArtNo. 111041.

222. Characterization of instrumental PSF in neutron imaging experiments using logarithmic power spectral plot method. Kashyap Y., Shukla S., Shukla M., et al. *NDT and E International*. Vol. 139, ArtNo. 102922.

223. Characterization of terminal flowering cowpea (Vigna unguiculata (L.) Walp.) mutants obtained by induced mutagenesis digs out the loss-of-function of phosphatidylethanolamine-binding protein. Eswaramoorthy V., Kandasamy T., Thiyagarajan K., et al. *PLoS ONE*. Vol. 18(45638), ArtNo. e0295509.

224. Characterizing and demonstrating the role of Klebsiella SSN1 exopolysaccharide in osmotic stress tolerance using neutron radiography. Sharma S., Roy T., Kashyap Y., et al. *Scientific Reports*. Vol. 13(1), ArtNo. 10052.

225. Charge distribution of light mass fission products in the thermal neutron induced fission of 233U, 235U and 239Pu. Naik H., Singh R.J., Dange S.P. *Applied Radiation and Isotopes*. Vol. 197, ArtNo. 110804.

226. Charge distribution studies in the epi-cadmium neutron induced fission of 245Cm. Naik H., Singh R.J., Dange S.P., et al. *European Physical Journal A*. Vol. 59(10), ArtNo. 230.

227. Chemical and functional characteristics to detect sugar syrup adulteration in honey from different botanical origins. Brar D.S., Nayik G.A., Aggarwal A.K., et al. *International Journal of Food Properties*. Vol. 26(1), pg. 1390-1413.

228. Chemical characterization of automobile windshield glass samples by nuclear and radio-analytical techniques namely SEM-EDX, ED-XRF, PIXE, PIGE, and INAA and potential of external (in air) PIGE and INAA in conjunction with chemometrics for glass forensics. Sharma V., Acharya R., Sarkar A., et al. *Journal of Analytical Atomic Spectrometry*.

229. Chemical characterization of automobile windshield glass samples for major, minor, and trace elemental concentration determination by INAA and its comparison with ED-XRF and DC Arc AES in terms of analytical capabilities and possible applications for glas. Sharma V., Sengupta A., Acharya R., et al. *RSC Advances*. Vol. 13(8), pg. 5118-5133.

230. Chitosan based radiation crosslinked and grafted matrix: An environment friendly adsorbent for dye uptake. Kumar S., Tiwari A., Chaudhari C.V., et al. *Radiation Physics and Chemistry*. Vol. 208, ArtNo. 110876.

231. Chloroplast genome sequence of Nothapodytes nimmoniana (Icacinaceae), a vulnerable reservoir of camptothecin from Western Ghats. Darshetkar A.M., Godbole R.C., Pable A.A., et al. *Gene*. Vol. 883, ArtNo. 147674.

232. Cholesterol-Controlled Interaction of Ionic Liquids with Model Cellular Membranes. Hitaishi P., Raval M., Seth A., et al. *Langmuir*. Vol. 39(27), pg. 9396-9405.

233. Chromatography separation of minor actinides from Ln3+ rich high-level radioactive liquid waste (HLW) using bis-triazinyl-pyridine (BTP) resin. Anshul K., Selvakumar J., Srinivasan S., et al. *Separation Science and Technology (Philadelphia)*. Vol. 58(15-16), pg. 2631-2640.

234. Chromium hydroxide microsphere synthesis using droplet microfluidics. Sen N., Singh K.K., Gumber N., et al. *Journal of Dispersion Science and Technology*.

235. Citric acid-derived nanoporous molybdenum carbide electrocatalyst for HER: Effect of porosity on HER performance. Aich S., Banerjee A.M., Pai M.R., et al. *Journal of Materials Research*. Vol. 38(16), pg. 3861-3873.

236. Classification of the Fermi-LAT blazar candidates of uncertain type using extreme gradient boosting. Tolamatti A., Singh K.K., Yadav K.K. *Monthly Notices of the Royal Astronomical Society*. Vol. 523(4), pg. 5341-5352.

237. Climate action for the shipping industry: Some perspectives on the role of nuclear power in maritime decarbonization. Bhattacharyya R., El-Emam R.S., Khalid F. *e-Prime - Advances in Electrical Engineering, Electronics and Energy*. Vol. 4, ArtNo. 100132.

238. Cluster formation between an oxadiazole derivative with metal nanoclusters (Ag/Au/Cu), graphene quantum dot sheets, SERS studies, and solvent effects. S.Al-Otaibi J., Mary Y.S., Mary Y.S., et al. *Structural Chemistry*. Vol. 34(3), pg. 867-877.

239. Cluster spin-glass state with magnetocaloric effect in open framework structure of the Prussian blue analog molecular magnet Formula Presented. Bhatt P., Maiti N., Mukadam M.D., et al. *Physical Review B*. Vol. 108(1), ArtNo. 14412.

240. CMS pythia 8 colour reconnection tunes based on underlying-event data. Tumasyan A., Adam W., Andrejkovic J.W., et al. *European Physical Journal C*. Vol. 83(7), ArtNo. 587.

241. CO2 hydrogenation to formic acid on Pd-Cu nanoclusters: a DFT study. Chattaraj D., Majumder C. *Physical Chemistry Chemical Physics*. Vol. 25(3), pg. 2584-2594.

242. Coal waste-derived synthesis of yellow oxidized graphene quantum dots with highly specific superoxide dismutase activity: characterization, kinetics, and biological studies. Das T., Das S., Kumar P., et al. *Nanoscale*. Vol. 15(44), pg. 17861-17878.

243. Cobalt-Based Hydrotalcite: A Potential Non-Noble Metal-Based Heterogeneous Catalyst for Selective Hydrogenation of Aromatic Aldehydes. Neethu P.P., Venkatachalam G., Venkatesha N.J., et al. *Industrial and Engineering Chemistry Research*. Vol. 62(12), pg. 4976-4986.

244. Codoping of Yttria (Y2O3): Ho-Yb Nanoparticles with Li Increase Emitted Green Light Intensity for Security Ink and Bioimaging. Srivastava M., Sahu S.K., Singh A.R., et al. *ACS Applied Nano Materials*. Vol. 6(22), pg. 20887-20898.

245. Coexistence of a spin-valley-coupled Dirac semimetal and robust quantum spin Hall state with significant Rashba spin-splitting in a halogenated BiAs film. Dhori B.R., Jha P.K., Chakraborty B. *Journal of Materials Chemistry C*. Vol. 12(3), pg. 930-940.

246. Coexistence of superparamagnetism and superspin glass in non-stoichiometric Zn0.5Ca0.5Fe2O4 nanoferrite. Tiwari S., Lal G., Bhoi H., et al. *Journal of Magnetism and Magnetic Materials*. Vol. 570, ArtNo. 170466.

247. Cold atmospheric plasma: Its time-dependent effects on the elimination of bacterial colony on periodontal manual scalers. Viswanadh V., Gaikwad R.P., Kar R., et al. *Journal of Indian Society of Periodontology*. Vol. 27(5), pg. 503-507.

248. Collection efficiencies of ionization chambers in pulsed radiation beams: an exact solution of an ion recombination model including free electron effects. Fenwick J.D., Kumar S. *Physics in Medicine and Biology*. Vol. 68(1), ArtNo. 15016.

249. Collective enhancement of nuclear level density and its fade-out in Dy 161. Santhosh T., Rout P.C., Santra S., et al. *Physical Review C*. Vol. 108(4), ArtNo. 44317.

250. Combating fungal phytopathogens with human salivary antimicrobial peptide histatin 5 through a multi-target mechanism. Chadha S. *World Journal of Microbiology and Biotechnology*. Vol. 39(8), ArtNo. 215.

251. Combined effects of dry-wet irrigation, redox changes and microbial diversity on soil nutrient bioavailability in the rice field. Majumdar A., Dubey P.K., Giri B., et al. *Soil and Tillage Research*. Vol. 232, ArtNo. 105752.

252. Combined experimental and DFT investigation of temozolomide sensing properties of 2D−2D interface of rich oxygen vacancies of WO3−x and sulfur-doped g-C3N4 nanosheets hybrids composites. Rajkumar C., Veerakumar P., Mane P., et al. *Journal of Environmental Chemical Engineering*. Vol. 11(2), ArtNo. 109459.

253. Combined Experimental and Theoretical Insights on Selectivity of Rare Earth Elements with Tetra-2-ethylhexyl Diglycolamide. Mondal S., Singh D.K., Sharma J.N., et al. *ChemistrySelect*. Vol. 8(33), ArtNo. e202301842.

254. Combined experiments and atomistic simulations for understanding the effect of ZnO on the sodium silicate and sodium borosilicate glass network. Sahu P., Musharaf Ali S., Shenoy K.T., et al. *Journal of Non-Crystalline Solids*. Vol. 618, ArtNo. 122550.

255. Combined Thermodynamic, Theoretical, and Biological Study for Investigating N-(2-Acetamido)iminodiacetic Acid as a Potential Thorium Decorporation Agent. Sharma S., Ali M., Kumar A., et al. *Inorganic Chemistry*. Vol. 62(46), pg. 18887-18900.

256. Co-micellization conduct and structural dynamics of block copolymers in water and salt solution environment for drug solubilization enhancement. Patel D., Gawali S.L., Kuperkar K., et al. *Colloid and Polymer Science*. Vol. 301(8), pg. 919-931.

257. CoMnCrGa: a novel ferromagnetic material with high spin-polarization for room temperature spintronics. Gupta S., Chakraborty S., Bhasin V., et al. *Journal of Materials Chemistry C*. Vol. 11(44), pg. 15489-15499.

258. Compaction of Calf Thymus DNA by a Potential One-Head-Two-Tail Surfactant: Properties of Nanomaterials and Biological Testing for Gene Delivery. Dyagala S., Paul M., Aswal V.K., et al. *ACS Applied Bio Materials*. Vol. 6(9), pg. 3848-3862.

259. COMPARATIVE ANALYSIS OF MORPHOLOGICAL AND STRUCTURAL CHANGES IN GAMMA AND ELECTRON BEAM IRRADIATED SUGARCANE BAGASSE. Kapoor K., Tyagi A.K., Das M., et al. *Cellulose Chemistry and Technology*. Vol. 57(45323), pg. 61-70.

260. Comparative Effect of Physiological Salts upon Micellization of T1304 and T1307. Rudani B.A., Sarolia J., Rai R., et al. *Langmuir*. Vol. 39(26), pg. 9060-9068.

261. Comparative Investigations on Detuning Estimator for Experimental RF Cavity. Keshwani R.T., Mukhopadhyay S., Gudi R.D., et al. *IEEE Transactions on Instrumentation and Measurement*. Vol. 72, ArtNo. 2526309.

262. Comparative Metabolomic Profiling of Horse Gram (Macrotyloma uniflorum (Lam.) Verdc.) Genotypes for Horse Gram Yellow Mosaic Virus Resistance. Rajaprakasam S., Shanmugavel P., Chockalingam V., et al. *Metabolites*. Vol. 13(2), ArtNo. 165.

263. Comparative Phenotypic, Genomic, and Transcriptomic Analyses of Two Contrasting Strains of the Plant Beneficial Fungus Trichoderma virens. Pachauri S., Zaid R., Sherkhane P.D., et al. *Microbiology Spectrum*. Vol. 11(2).

264. Comparative sensitivity and relative biological effectiveness of gamma-rays, X-rays and electron beams in aromatic Joha rice derived from different locations in Assam state. Bordoloi D., Sarma D., Das B.K. *Cereal Research Communications*.

265. Comparative Studies on Mutagenic Effectiveness and Efficiency in Horsegram [Macrotyloma uniflorum (Lam) Verdc.]. Priyanka S., Sudhagar R., Vanniarajan C., et al. *Legume Research*. Vol. 46(8), pg. 959-966.

266. Comparative study of hydroxyapatite synthesized using Schiff base and wet chemical precipitation methods. Anandan D., Kumar A., Jaiswal A.K. *Journal of the Mechanical Behavior of Biomedical Materials*. Vol. 148, ArtNo. 106200.

267. Comparative transcriptomics of stem rust resistance in wheat NILs mediated by Sr24 rust resistance gene. Vishwakarma G., Saini A., Bhardwaj S.C., et al. *PLoS ONE*. Vol. 18(45638), ArtNo. e0295202.

268. Comparing fatigue life prediction capability of critical plane models using multiaxial test database on 17 materials. Arora P., Gupta S.K., Samal M.K., et al. *Fatigue and Fracture of Engineering Materials and Structures*. Vol. 46(4), pg. 1330-1356.

269. Comparison of 99mTc-methylenediphosphonate and 68Ga-BPAMD PET/computed tomography imaging in bone metastasis. Vatsa R., Kaur D., Shekhar S.S., et al. *Nuclear Medicine Communications*. Vol. 44(6), pg. 463-470.

270. Comparison of effectiveness and efficiency of electron beam over gamma rays to induce novel mutations in mungbean (Vigna radiata L. Wilczek). Dhole V.J., Souframanien J., Reddy K.S., et al. *Applied Radiation and Isotopes*. Vol. 194, ArtNo. 110719.

271. Comparison of long-term and short-term trends of annual rainfall in India: a case study. Gangarde A., Dauji S., Londhe S. *ISH Journal of Hydraulic Engineering*. Vol. 29(3), pg. 411-424.

272. Comparison of NDT Data Fusion for Concrete Strength using Decision Tree and Artificial Neural Network. Dauji S. *Journal of Scientific and Industrial Research*. Vol. 82(8), pg. 831-840.

273. Comparison of the performance of solvent wash reagents used for the primary cleanup of degraded PUREX solvent. Mishra S., Mukhopadhyaya C., Patra C., et al. *Radiochimica Acta*. Vol. 111(1), pg. 53-62.

274. Compatible and energy conserving multi-material arbitrary Lagrangian Eulerian scheme for multi-group radiation hydrodynamics simulations. Sijoy C.D. *Computer Physics Communications*. Vol. 287, ArtNo. 108695.

275. Competition between fusion and quasifission in the angular momentum dependent dynamics of heavy element synthesis reactions. Tanaka T., Hinde D.J., Dasgupta M., et al. *Physical Review C*. Vol. 107(5), ArtNo. 54601.

276. Competitive effects of salt and surfactant on the structure of nanoparticles in a binary system of nanoparticle and protein. Saha D., Kumar S., Mata J.P., et al. *Physical Chemistry Chemical Physics*. Vol. 25(33), pg. 22130-22144.

277. Composite of α-FeOOH and Mesoporous Carbon Derived from Indian Blackberry Seeds as Low-Cost and Recyclable Photocatalyst for Degradation of Ciprofloxacin. Dutta D.P., Abraham S. *Catalysts*. Vol. 13(1), ArtNo. 191.

278. Composite Vanadium-Iron Metal Membrane for Hydrogen Recovery in Ammonia Production Unit. Parashar R., Nailwal B.C., Goswami N., et al. *Journal of Membrane Science and Research*. Vol. 9(1), ArtNo. 549300.

279. Compositional variation in Gd2Zr2-xHfxO7:Eu3+ pyrochlore by modulating Zr/Hf ratio and their immediate impact on luminescence properties. Jafar M., Gupta S.K., Sudarshan K., et al. *Journal of Molecular Structure*. Vol. 1272, ArtNo. 134198.

280. Composition-dependent photoluminescence in nanocrystalline La2Hf2−xZrxO7:Eu phosphor: role of chemical twin Zr/Hf environments around a luminescent center. Gupta S.K., Nigam S., Mao Y. *Physical Chemistry Chemical Physics*. Vol. 26(3), pg. 1749-1761.

281. Composition-independent Curie point (Tc) in ferroelectric (1 − x)PbTiO3–xBi(Li1/2Nb1/2)O3 solid solution. Kumar N., Kumari E., Krishna P.S.R., et al. *Journal of the American Ceramic Society*. Vol. 106(1), pg. 430-437.

282. Comprehensive in situ and ex situ β-glucosidase-assisted assessment reveals Indian mangoes as reservoirs of glycosidic aroma precursors. Godse R., Bawane H., Rajkhowa R., et al. *Food Research International*. Vol. 173, ArtNo. 113355.

283. Comprehensive oxidative process for the removal of antimony from the surfaces of nuclear reactor coolant systems. Bhaskarapillai A., Nishad P.A., Rufus A.L. *Chemosphere*. Vol. 312, ArtNo. 137166.

284. Comprehensive review on sampling, characterization and distribution of microplastics in beach sand and sediments. Tiwari M., Sahu S.K., Rathod T., et al. *Trends in Environmental Analytical Chemistry*. Vol. 40, ArtNo. e00221.

285. Comprehensive study on the origin of orthorhombic phase stabilization in Gd-doped HfO2 and DFT calculations. Banerjee D., Dey C.C., Kumar R., et al. *Physical Chemistry Chemical Physics*. Vol. 25(32), pg. 21479-21491.

286. Concept of accident tolerant fuel in nuclear reactors. Yadav K.K., Pal U., R. K. *Nuclear and Particle Physics Proceedings*. Vol. 341 pg. 62-66.

287. Concerns and coping mechanisms of breast cancer survivor women from Asia: a scoping review. Sarang B., Bhandarkar P., Parsekar S.S., et al. *Supportive Care in Cancer*. Vol. 31(9), ArtNo. 528.

288. Concurrent influence of geological parameters on the integrated nano-pore structure and discretized pore families of the petroliferous Cambay shale assessed through multivariate dependence measure. Bal A., Misra S., Mukherjee M., et al. *Frontiers in Earth Science*. Vol. 11, ArtNo. 1157122.

289. Confining charge-transfer complex in a metal-organic framework for photocatalytic CO2 reduction in water. Karmakar S., Barman S., Rahimi F.A., et al. *Nature Communications*. Vol. 14(1), ArtNo. 4508.

290. Conformational effects in the vibrational and electronic spectra of propionaldehyde: Experimental and theoretical studies. Sharma N., Shastri A., Das A.K., et al. *Journal of Chemical Physics*. Vol. 159(14), ArtNo. 144301.

291. Conformational, Reactivity Analysis, Wavefunction-Based Properties, Molecular Docking and Simulations of a Benzamide Derivative with Potential Antitumor Activity-DFT and MD Simulations. Al-Otaibi J.S., Mary Y.S., Mary Y.S., et al. *Polycyclic Aromatic Compounds*. Vol. 43(3), pg. 2015-2031.

292. Constraints on anomalous Higgs boson couplings to vector bosons and fermions from the production of Higgs bosons using the ττ final state. Tumasyan A., Adam W., Andrejkovic J.W., et al. *Physical Review D*. Vol. 108(3), ArtNo. 32013.

293. Continuous monitoring of COVID-19 pandemic trend for policy making: improvised application of Sen's innovative method. Dauji S. *International Journal of Healthcare Technology and Management*. Vol. 20(3), pg. 197-231.

294. Continuous–discrete filtering techniques for estimating states of nonlinear differential–algebraic equations (DAEs) systems. Bhase S., Bhushan M., Kadu S., et al. *International Journal of Dynamics and Control*. Vol. 11(1), pg. 162-182.

295. Contrasting complexation behaviour of zwitterionic amyloid probe, SYPRO orange with β-cyclodextrin and captisol. Mora A.K., Hundani P.Z., Nath S. *Journal of Photochemistry and Photobiology A: Chemistry*. Vol. 441, ArtNo. 114712.

296. Controlled synthesis of photoresponsive bismuthinite (Bi2S3) nanostructures mediated through a new 1D bismuth-pyrimidylthiolate coordination polymer as a molecular precursor. Kulkarni A.Y., Karmakar G., Shah A.Y., et al. *Dalton Transactions*. Vol. 52(44), pg. 16224-16234.

297. Convenient synthesis of 6-Amino-2-naphthol by Copper-catalyzed Ullmann reaction. Jagushte K.U., Ketkar R.N., Thakkar C., et al. *Tetrahedron Letters*. Vol. 128, ArtNo. 154693.

298. Conventional and new-breeding technologies for improving disease resistance in lentil (Lens culinaris Medik). Roy A., Sahu P.K., Das C., et al. *Frontiers in Plant Science*. Vol. 13, ArtNo. 1001682.

299. Cooper Basin REM gas shales after CO2 storage or acid reactions: Metal mobilisation and methane accessible pore changes. Pearce J.K., Blach T., Dawson G.K.W., et al. *International Journal of Coal Geology*. Vol. 273, ArtNo. 104271.

300. Cooperative interaction of a highly hydrophilic pluronic with bile salts of different hydrophobicity. Wagh S.S., Sarolia J., Patil Y.K., et al. *Colloids and Surfaces A: Physicochemical and Engineering Aspects*. Vol. 672, ArtNo. 131709.

301. Copper decorated graphyne as a promising nanocarrier for cisplatin anti-cancer drug: A DFT study. Deb J., Kundu A., Garg N., et al. *Applied Surface Science*. Vol. 622, ArtNo. 156885.

302. Copper metal insertion in porphyrin core compromises the photocytotoxicity of free base porphyrin: Revelation during synthesis of natCu/[64Cu]Cu-porphyrin complex. Kumar N., Guleria M., Shelar S., et al. *Journal of Photochemistry and Photobiology A: Chemistry*. Vol. 441, ArtNo. 114754.

303. Copper oxide modified biphasic titania for enhanced hydrogen production through photocatalytic water splitting. Nikhila M.P., Anjali C., Nidhisha V., et al. *Results in Engineering*. Vol. 20, ArtNo. 101474.

304. Co-precipitation synthesis of pseudocapacitive λ-MnO2 for 2D MXene (Ti3C2Tx) based asymmetric flexible supercapacitor. Thanigai Vetrikarasan B., Nair A.R., Karthick T., et al. *Journal of Energy Storage*. Vol. 72, ArtNo. 108403.

305. Correction to: Continuous–discrete filtering techniques for estimating states of nonlinear differential–algebraic equations (DAEs) systems (International Journal of Dynamics and Control, (2023), 11, 1, (162-182), 10.1007/s40435-022-00955-z). Bhase S., Bhushan M., Kadu S., et al. *International Journal of Dynamics and Control*. Vol. 11(2).

306. Correlation of micro-structure with the opto-electronic properties of the sol-gel derived powder Sn1-xCdxO2 nanoparticles. Ali S.I., Dutta D., Mandal A.C. *Materials Chemistry and Physics*. Vol. 301, ArtNo. 127627.

307. Corrigendum to “Effect of phase interfaces to dimple pattern” [Mater. Lett. 337 (2023) 133954] (Materials Letters (2023) 337, (S0167577X23001398), (10.1016/j.matlet.2023.133954)). Das A. *Materials Letters*. Vol. 344, ArtNo. 134407.

308. Corrigendum to “MOF (M=Zr, Zn, Co)@COFs hybrid composite as a potential adsorbent for UO22+ and Methylene blue (MB) from solutions” [Mater. Today Commun. 34 (2023) 105336] (Materials Today Communications (2023) 34, (S2352492823000260), (10.1016/j.mtcomm.2. Koppula S., Jagasia P., Manabolu Surya S.B. *Materials Today Communications*. Vol. 36, ArtNo. 106854.

309. Corrigendum to “Role of Nb content in tailoring the microstructure and magnetic anisotropy of soft magnetic W/CoFeB alloy thin films prepared with varying the substrate temperature” [J. Alloy. Compd. 910 (2022) 164930] (Journal of Alloys and Compounds (20. Gupta N., Kumar D., Gupta M., et al. *Journal of Alloys and Compounds*. Vol. 967, ArtNo. 171792.

310. Corrigendum to “Structural, dielectric, electric and magnetic properties of magnesium substituted lithium nanoferrites” [Ceram. Int. 49 (2023) 31114–31123, (S0272884223019818), (10.1016/j.ceramint.2023.07.056)]. Hashim M., Nayak D.R., Ahmed A., et al. *Ceramics International*. Vol. 49(22), pg. 35700-35701.

311. Corrigendum: “Measurement of 73Ge(n,γ) cross sections and implications for stellar nucleosynthesis” [Phys. Lett. B 790 (2019) 458–465, (S037026931930070X), (10.1016/j.physletb.2019.01.045)]. Lederer-Woods C., Battino U., Ferreira P., et al. *Physics Letters, Section B: Nuclear, Elementary Particle and High-Energy Physics*. Vol. 840, ArtNo. 137835.

312. Corrosion behaviour of oxide film formed on carbon steel in high temperature alkaline water in the presence of zinc and magnesium ions. Suresh S., Bera S., Palogi C., et al. *Corrosion Engineering Science and Technology*. Vol. 58(5), pg. 492-507.

313. Cost effective red emitting Eu3+ doped natural sodium feldspar (NaAlSi3O8) powder and photophysical changes on transition to glassy state. Saha P., Shukla R., Parayil R.T., et al. *Results in Optics*. Vol. 13, ArtNo. 100566.

314. Countrywide monitoring of absorbed dose rate in air due to outdoor natural gamma radiation in India. Mitra P., Mishra M.K., Reddy G.P., et al. *Radiation Protection Dosimetry*. Vol. 199(12), pg. 1336-1350.

315. Coupled Ion-Conduction Mechanism for Enhanced Ionic Conductivity in Mg2B2O5 Nanowires Enabled Poly(ethylene oxide)-Based Quasi Solid State Electrolytes. Sharma S.K., Mor J. *Journal of Physical Chemistry C*. Vol. 127(25), pg. 11854-11863.

316. Coupled neutronics–thermal-hydraulics analyses of unprotected transients in LBE-cooled Compact High-Temperature Reactor. Dwivedi D.K., Gupta A., Kannan U. *Life Cycle Reliability and Safety Engineering*. Vol. 12(3), pg. 259-268.

317. Coupling of topological interface states in 1D photonic crystal. Sharma R., Jena S., Udupa D.V. *Optical Materials*. Vol. 137, ArtNo. 113508.

318. Coupling Single-Ni-Atom with Ni-Co Alloy Nanoparticle for Synergistically Enhanced Oxygen Reduction Reaction. Saifi S., Dey G., Karthikeyan J., et al. *Inorganic Chemistry*. Vol. 62(21), pg. 8200-8209.

319. Creep Fracture Complexions. Das A. *Journal of Materials in Civil Engineering*. Vol. 35(5), ArtNo. 4023057.

320. CRISPR-Cas12a assisted specific detection of mpox virus. Singh M., Misra C.S., Bindal G., et al. *Journal of Medical Virology*. Vol. 95(8), ArtNo. e28974.

321. Cross-species amplification and genetic variation among blackgram genotypes using SSR markers developed from mungbean DNA sequence scaffolds harbouring putative resistance genes. Raizada A., Jegadeesan S. *Electronic Journal of Plant Breeding*. Vol. 14(1), pg. 21-30.

322. Crystal Growth, Physicochemical Investigation, and Raman Spectroscopy: Exploration of Intramolecular Charge Transfer in NLO Chromophore DAST. Sivakumar T., Logeswari A., William Carry M., et al. *Crystal Growth and Design*.

323. Crystal structure analysis of phycoerythrin from marine cyanobacterium Halomicronema. Patel S.N., Sonani R.R., Gupta G.D., et al. *Journal of Biomolecular Structure and Dynamics*. Vol. 41(9), pg. 3752-3761.

324. Crystal structure of phosphate bound Acyl phosphatase mini-enzyme from Deinococcus radiodurans at 1Å resolution. Khakerwala Z., Kumar A., Makde R.D. *Biochemical and Biophysical Research Communications*. Vol. 671 pg. 153-159.

325. Crystal structures of PirA and PirB toxins from Photorhabdus akhurstii subsp. akhurstii K-1. Prashar A., Kinkar O.U., Kumar A., et al. *Insect Biochemistry and Molecular Biology*. Vol. 162, ArtNo. 104014.

326. Crystallization kinetics and structural studies of Li1.25Al0.5Ge1.5P2.75Mo0.25O12 (LAGPM) glass/glass-ceramics based solid state electrolyte. Das A., Goswami M., Nayak C., et al. *Materials Chemistry and Physics*. Vol. 296, ArtNo. 127291.

327. Crystallographic structural variations in nano-crystalline Sc2O3 under pressure. Yadav D., Bura N., Bhoriya A., et al. *Physica Scripta*. Vol. 98(4), ArtNo. 45707.

328. CTAB induced growth and shrinkage of Pluronics® P103 micelles: Experimental and theoretical rationale. Patel D., Tripathi N., Ray D., et al. *Journal of Molecular Liquids*. Vol. 391, ArtNo. 123315.

329. Cu interfaced Fe/Pt multilayer with improved (001) texture, enhanced L10 transformation kinetics and high magnetic anisotropy. Kumar S., Srihari V., Sharma G., et al. *Journal of Magnetism and Magnetic Materials*. Vol. 567, ArtNo. 170327.

330. Cucurbit[7/8]uril assisted modulations in the photophysical properties of 4',6-diamidino-2-phenylindole dye. Sayed M., Maity D.K., Pal H. *Journal of Photochemistry and Photobiology A: Chemistry*. Vol. 445, ArtNo. 115088.

331. Culinary spices and herbs in managing early and long-COVID-19 complications: A comprehensive review. Maurya D.K., Sharma D. *Phytotherapy Research*. Vol. 37(11), pg. 4908-4931.

332. Curious Behavior of Fe3+-As3+ Chemical Interactions and Nucleation of Clusters in Aqueous Medium. Das S., Mishra G., Halder D., et al. *Inorganic Chemistry*. Vol. 62(30), pg. 11966-11975.

333. Current Density Dependence of Transport Selectivity of Metal Ions in the Electrodriven Process across the Cation Exchange Membrane. Mani A.M., Chaudhury S., Meena G. *Journal of Physical Chemistry B*. Vol. 127(41), pg. 8879-8887.

334. Curvature modulated structural and magnetic properties of CoO/Co thin films deposited onto 2-D nanosphere array. Tripathi J., Kumar Y., Kumar D., et al. *Journal of Magnetism and Magnetic Materials*. Vol. 565, ArtNo. 170179.

335. Damage-Coupled Cyclic Plasticity Model for Prediction of Ratcheting–Fatigue Behavior under Strain and Stress Controlled Ratcheting for Two Different Nuclear Piping Steels. Das P., Khutia N., Dey P.P., et al. *Journal of Materials Engineering and Performance*.

336. De novo granulation of sewage-borne microorganisms: A proof of concept on cultivating aerobic granular sludge without activated sludge and effective enhanced biological phosphorus removal. Sarvajith M., Nancharaiah Y.V. *Environmental Research*. Vol. 224, ArtNo. 115500.

337. Decay-Associated Fluorescence for Boron Determination in Uranium-Based Nuclear Fuels. Verma P. *ACS Omega*. Vol. 8(49), pg. 47271-47276.

338. Deciphering structural changes in LiNixMnyCozO2 cathodes of Li ion batteries during cycling: Experimental and theoretical investigations. Abharana N., Halankar K.K., Srihari V., et al. *Solid State Ionics*. Vol. 398, ArtNo. 116270.

339. Decoding transport selectivity of ions in polymer membranes by In-situ impedance spectroscopy. Mani A.M., Kumar A., Chaudhury S. *Separation Science and Technology (Philadelphia)*. Vol. 58(14), pg. 2411-2421.

340. Decomposition kinetics of sodium amalgam in fixed bed of WC-coated tubular SS-304 packing: Modelling and validation. Manivannan S., Mandal D., Dabhade P.A., et al. *Asia-Pacific Journal of Chemical Engineering*. Vol. 18(3), ArtNo. e2893.

341. Deep Eutectic Solvent-Based Highly Sensitive Turn-On Fluorescent Probe for D2O. Patil S.M., Gupta S.K., Goswami D., et al. *ACS Omega*. Vol. 8(36), pg. 32444-32449.

342. Deep neural network-based pulse shape discrimination of neutrons and γ -rays in organic scintillation detectors. Karmakar A., Pal A., Anil Kumar G., et al. *Pramana - Journal of Physics*. Vol. 97(4), ArtNo. 157.

343. Defect assisted magneto-tunable photoresponse in ZnO-rGO/La0.7Sr0.3MnO3/ITO heterojunctions. Deb D., Choudhary R.J., Yusuf S.M., et al. *Materials Science and Engineering: B*. Vol. 290, ArtNo. 116353.

344. Defect induced tunable light emitting diodes of compositionally modulated zinc gallium germanium oxides. Gupta S.K., Modak B., Abraham M., et al. *Chemical Engineering Journal*. Vol. 474, ArtNo. 145595.

345. Defect properties and solution energies of dopants in NASICON-type LiGe2(PO4)3 solid electrolyte: a first-principles study. Das A., Goswami M., Ghosh P.S. *Physical Chemistry Chemical Physics*. Vol. 25(45), pg. 31230-31237.

346. Defect-Engineered 3D Nanostructured MoS2 for Detection of Ammonia Gas at Room Temperature. Rajbhar M.K., De S., Sanyal G., et al. *ACS Applied Nano Materials*. Vol. 6(7), pg. 5284-5297.

347. Defect-engineered MnO2 nanoparticles by low-energy ion beam irradiation for enhanced electrochemical energy storage applications. Maharana B., Rajbhar M.K., Sanyal G., et al. *Electrochimica Acta*. Vol. 464, ArtNo. 142868.

348. Defect-Engineering of 2D Dichalcogenide VSe2 to Enhance Ammonia Sensing: Acumens from DFT Calculations. Sanyal G., Kaur S.P., Rout C.S., et al. *Biosensors*. Vol. 13(2), ArtNo. 257.

349. Defect-Induced Adsorption Switching (p- to n- Type) in Conducting Bare Carbon Nanotube Film for the Development of Highly Sensitive and Flexible Chemiresistive-Based Methanol and NO2 Sensor. Prakash J., Rao P.T., Rohilla R., et al. *ACS Omega*. Vol. 8(7), pg. 6708-6719.

350. Defects and doping engineered two-dimensional o-B2N2 for hydrogen evolution reaction catalyst: Insights from DFT simulation. Chodvadiya D., Dalsaniya M.H., Som N.N., et al. *International Journal of Hydrogen Energy*. Vol. 48(13), pg. 5138-5151.

351. Degradation assessment of corroded RC frames using in-structure response spectra from shake table tests and numerical simulation. Nagender T., Parulekar Y.M., Shinde P., et al. *Bulletin of Earthquake Engineering*. Vol. 21(12), pg. 5683-5715.

352. Dehydration induced selective ion trapping by topology constrained atomically thin graphene-crown membranes. Sahu P., Ali S.M. *Molecular Systems Design and Engineering*. Vol. 8(12), pg. 1540-1558.

353. Deinococcus lineage and Rad52 family-related protein DR0041 is involved in DNA protection and compaction. Ujaoney A.K., Anaganti N., Padwal M.K., et al. *International Journal of Biological Macromolecules*. Vol. 248, ArtNo. 125885.

354. Delineating the role of defect and compositions in luminescent ZnO-ZnGa2-xAlxO4:Cr3+ micro composites towards efficient photon utilization. Gupta S.K., Sudarshan K., Rawat N.S., et al. *Journal of Luminescence*. Vol. 257, ArtNo. 119730.

355. Density functional theoretical assessment of titanium metal for adsorption of hydrogen, deuterium and tritium isotopes. Boda A., Chandorkar N., Ali S.M. *Theoretical Chemistry Accounts*. Vol. 142(5), ArtNo. 46.

356. Density, Viscosity, Speed of Sound, and Refractive Index of Nitric Acid-Water System. Rajesh M., Sen N., Singh K.K. *Journal of Chemical and Engineering Data*. Vol., ArtNo. .

357. Deoxyglucose-conjugated persistent luminescent nanoparticles for theragnostic application in fibrosarcoma tumor model. Sharma K.S., Melwani P.K., Yadav H.D., et al. *RSC Advances*. Vol. 13(19), pg. 13240-13251.

358. Depth distribution analysis of alloying and impurity elements in Ni-Ti alloy thin films using secondary ion mass spectrometer. Karki V., Das A., Sanyal K., et al. *Thin Solid Films*. Vol. 773, ArtNo. 139836.

359. Depth profile analysis of 100 keV Ni ions in Si 〈100〉 substrate. Alam M.A., Tiwari M.K., Devi D., et al. *Spectrochimica Acta - Part B Atomic Spectroscopy*. Vol. 206, ArtNo. 106707.

360. Descriptor sliding mode observer based fault tolerant control for nuclear power plant with actuator and sensor faults. Surjagade P.V., Deng J., Shimjith S.R., et al. *Progress in Nuclear Energy*. Vol. 162, ArtNo. 104774.

361. Design and development of Fabry–Perot etalon based color filter using ebeam GLAD technique: Simulation and experiment. Haque S.M., De R., Misal J.S., et al. *Optics Communications*. Vol. 541, ArtNo. 129551.

362. Design and development of half impulse radiating antenna based ultra wide band system. Singh S.K., Mitra S., Chandra R., et al. *Frequenz*. Vol. 77(45574), pg. 443-449.

363. Design and development of induction heating based pulsed spray dryer for alkali metal chloride salts: interrogation through CFD approach. Nimbalkar U.D., Gaval V., Mandal D., et al. *Brazilian Journal of Chemical Engineering*.

364. Design and development of low density, high strength ZrNbAlVTi high entropy alloy for high temperature applications. Chakraborty P., Sarkar A., Ali K., et al. *International Journal of Refractory Metals and Hard Materials*. Vol. 113, ArtNo. 106222.

365. Design and Synthesis of BODIPY-Hetero[5]helicenes as Heavy-Atom-Free Triplet Photosensitizers for Photodynamic Therapy of Cancer. Koli M., Gupta S., Chakraborty S., et al. *Chemistry - A European Journal*. Vol. 29(57), ArtNo. e202301605.

366. Design, characterization and evaluation of a new 99mTc-labeled folate derivative with affinity towards folate receptor. Das S., Sakhare N., Kumar D., et al. *Bioorganic and Medicinal Chemistry Letters*. Vol. 86, ArtNo. 129240.

367. Design, fabrication, and characterization of a drift tube linac type double gap re-buncher cavity. Mathew J.V., Priyadarshini P., Sista V.L.S. *Review of Scientific Instruments*. Vol. 94(12), ArtNo. 123302.

368. Design, synthesis and development of a dual inhibitor of Topoisomerase 1 and poly (ADP-ribose) polymerase 1 for efficient killing of cancer cells. Guha Majumdar A., Shree S., Das A., et al. *European Journal of Medicinal Chemistry*. Vol. 258, ArtNo. 115598.

369. Design, synthesis and evaluation of 177Lu-labeled inverso and retro-inverso A9 peptide variants targeting HER2-overexpression. Kumar Sharma A., Sharma R., Dev Sarma H., et al. *Bioorganic Chemistry*. Vol. 140, ArtNo. 106761.

370. Designing a large area field emitter for uniform electron emission. Rudra R., Biswas D. *Physics of Plasmas*. Vol. 30(9), ArtNo. 93106.

371. Designing Climate-Resilient Crops for Sustainable Agriculture: A Silent Approach. Ghag S.B., Alok A., Rajam M.V., et al. *Journal of Plant Growth Regulation*. Vol. 42(10), pg. 6503-6522.

372. Detection of fatigue crack initiation pre-cursor in meta-stable SS 304LN using Rayleigh surface wave harmonic generation. Metya A.K., Pramanick A.K., Bar H.N., et al. *Materials Characterization*. Vol. 201, ArtNo. 112959.

373. Detection of gamma radiation processed onion during storage using propidium iodide based fluorescence microscopy. Sharma T., Kavita, Mishra B.B., et al. *Food Chemistry*. Vol. 398, ArtNo. 133928.

374. Detection of high-frequency quasi-periodic oscillation during the reflare of MAXI J1348-630. Kumar R., Bhatt N., Bhattacharyya S. *Monthly Notices of the Royal Astronomical Society: Letters*. Vol. 524(1), pg. L55-L60.

375. Detection of polycyclic aromatic hydrocarbons on a sample of comets. Venkataraman V., Roy A., Ramachandran R., et al. *Journal of Astrophysics and Astronomy*. Vol. 44(2), ArtNo. 89.

376. Determination of concentrations of some elements in marine consumables from Thane creek area (Mumbai, India) using ED-XRF technique; and risk assessment. Tiwari M., Rathod T.D., Sahu S.K., et al. *International Journal of Environmental Analytical Chemistry*. Vol. 103(20), pg. 8986-9001.

377. Determination of Curcumin on Functionalized Carbon Nano Tube Modified Electrode and Probing its Interaction with DNA and Copper Ion. Sahoo S., Satpati A.K. *Journal of Analysis and Testing*. Vol. 7(2), pg. 136-146.

378. Determination of thallium in vegetative plant leaves near industrial areas by high-resolution continuum source electrothermal atomic absorption spectrometry after salt induced cloud point extraction. Meeravali N.N., Madhavi K., Sahayam A.C. *Spectrochimica Acta - Part B Atomic Spectroscopy*. Vol. 200, ArtNo. 106613.

379. Determination of thermochemical properties of lead vanadates. Aiswarya P.M., Dawar R., Narang S., et al. *Journal of Thermal Analysis and Calorimetry*. Vol. 148(12), pg. 5557-5571.

380. Developing N,N,N',N'-tetra (2-ethylhexyl) diglycolamide encapsulated polymeric beads as promising rare earth extracting agents. Choudhury D., Yadav K.K., Singh D.K., et al. *Separation Science and Technology (Philadelphia)*. Vol. 58(15-16), pg. 2665-2676.

381. Developing post-modified Ce-MOF as a photocatalyst: a detail mechanistic insight into CO2 reduction toward selective C2 product formation. Karmakar S., Barman S., Rahimi F.A., et al. *Energy and Environmental Science*.

382. Development and characterization of gamma ray and EMS induced mutants for powdery mildew resistance in blackgram. Tamilzharasi M., Kumaresan D., Thiruvengadam V., et al. *International Journal of Radiation Biology*. Vol. 99(8), pg. 1267-1284.

383. Development and validation of diffusion based CFD model for modelling of hydrogen and carbon monoxide recombination in passive autocatalytic recombiner. Gera B., Verma V., Chattopadhyay J. *Nuclear Engineering and Technology*. Vol. 55(9), pg. 3194-3201.

384. Development and validation of operational reactor physics code "ORPAC" for research reactors at Trombay. Kumar J., Singh T., Pandey P., et al. *Radiation Physics and Chemistry*. Vol. 202, ArtNo. 110552.

385. Development of a BODIPY-based ratiometric fluorescence off-on dosimeter for gamma radiation. Choudhary M.K., Mula S. *New Journal of Chemistry*. Vol. 47(19), pg. 9045-9049.

386. Development of a coupled neutronics-CFD system for 540 MWE Indian Pressurized heavy water reactors (IPHWRs) and verification with slow online refuelling transient. Jha A., Gupta A. *Nuclear Engineering and Design*. Vol. 409, ArtNo. 112323.

387. Development of a highly efficient gadolinium(III) potentiometric sensor using two aza-crown ether-based multiple diglycolamides (DGAs). Sharma D.B., Mahanty B., Mohapatra P.K., et al. *Microchemical Journal*. Vol. 194, ArtNo. 109323.

388. Development of a high-rate-capable O3-structured 'layered' Na transition metal oxide by tuning the cation-oxygen bond covalency. Biswas I., Kumar B.S., Pradeep A., et al. *Chemical Communications*. Vol. 59(29), pg. 4332-4335.

389. Development of a New Ground Motion Model for a Peninsular Indian Rock Site. Akella R.K., Agrawal M.K., Chattopadhyay J. *Proceedings of Engineering and Technology Innovation*. Vol. 23 pg. 36-47.

390. Development of a new Monte-Carlo neutron transport code for radiation shielding. Das A., Singh T. *Nuclear and Particle Physics Proceedings*. Vol. 339-340 pg. 156-159.

391. Development of a new thermo-mechanical processing route for Nb-5Mo-1Zr-0.1C (wt%) alloy. Vishwanadh B., Kumar N.N., Samyuktha G., et al. *Journal of Alloys and Compounds*. Vol. 942, ArtNo. 168860.

392. Development of a portable pulsed fast ⩾106 neutron generator based on a flexible miniature plasma focus tube. Niranjan R., Srivastava R., Joycee J., et al. Plasma Physics and Controlled Fusion. Vol. 65(7), ArtNo. 75010.

393. Development of a rapid and ultra-sensitive RNA:DNA hybrid immunocapture based biosensor for visual detection of SARS-CoV-2 RNA. Dey A., Prakash J., Das R., et al. PNAS Nexus. Vol. 2(3), ArtNo. pgad031.

394. Development of a Simple Electroless Method for Depositing Metallic Pt-Pd Nanoparticles over Wire Gauge Support for Removal of Hydrogen in a Nuclear Reactor. Sanap K.K., Mali S.S., Tyagi D., et al. *Materials*. Vol. 16(19), ArtNo. 6541.

395. Development of a single sphere neutron spectrometer using α-Al2O3:C based optically stimulated luminescence detectors. Tripathy S.P., Kulkarni M.S., Paul S., et al. *Radiation Measurements*. Vol. 160, ArtNo. 106892.

396. Development of Am-241 Activity Standards. Sharma R., Kulkarni D.B., Anuradha R., et al. *Mapan - Journal of Metrology Society of India*. Vol., ArtNo. .

397. Development of an external PIGE method using nitrogen from atmospheric air as external beam current normalizer and its application to nondestructive quantification of total boron mass fraction in boron containing neutron absorbers. Raja S.W., Acharya R. *Analytica Chimica Acta*. Vol. 1266, ArtNo. 341353.

398. Development of an indigenous multi-collector inductively coupled plasma mass spectrometer. Kumar Y., Bhatia R.K., Ravisankar E., et al. *Indian Journal of Physics*. Vol., ArtNo. .

399. Development of DNA Bio-chip for Detection of Mutations of rpoB, embB and inhA Genes in Drug-Resistant Mycobacterium Tuberculosis. Jain B., Kulkarni S. *Indian Journal of Clinical Biochemistry*. Vol. 38(2), pg. 242-250.

400. Development of FPGA-based standalone, portable TDCR system. Sharma M.K., Agarwal S., Kulkarni M.S., et al. *Journal of Instrumentation*. Vol. 18(5), ArtNo. P05016.

401. Development of large size fast timing and radiation resistant PVT-based plastic scintillator detector. Alex L., Paulraj R., Sonu, et al. *Journal of Materials Science: Materials in Electronics*. Vol. 34(2), ArtNo. 127.

402. Development of process for purification of strontium nitrate rich solution to qualify for 90Sr–90Y generator. Pareek P., Singh S.K., Mukhopadhyay S., et al. *Journal of Radioanalytical and Nuclear Chemistry*. Vol. 332(9), pg. 3579-3585.

403. Development of site-specific time distribution pattern of rainfall for Tarapur, India. Harshanth R., Dauji S., Srivastava P.K. *Journal of Earth System Science*. Vol. 132(2), ArtNo. 77.

404. DFT and MD investigations of the biomolecules of phenothiazine derivatives: interactions with gold and water molecules and investigations in search of effective drug for SARS-CoV-2. Al-Otaibi J.S., Mary Y.S., Mary S., et al. *Journal of Biomolecular Structure and Dynamics*. Vol. 41(10), pg. 4522-4533.

405. DFT stimulation and experimental insights of chiral Cu(ii)-salen scaffold within the pocket of MWW-zeolite and its catalytic study. Lakhani P., Chodvadiya D., Jha P.K., et al. *Physical Chemistry Chemical Physics*. Vol. 25(20), pg. 14374-14386.

406. DGA-functionalized super-magnetic acid-stable sorbent for treatment of acidic rich nuclear effluent. Khan P.N., Pahan S., Sengupta A., et al. *New Journal of Chemistry*. Vol. 47(33), pg. 15455-15459.

407. Diagnostic potential of serum HSP90 beta for HNSCC and its therapeutic prognosis after local hyperthermia therapy. Shetake N.G., Kumar A., Huilgol N., et al. *PLoS ONE*. Vol. 18(45607), ArtNo. e0281919.

408. Diagnostics of Inductively Coupled Plasma Under the Influence of Immersed RF Self-Biased Substrate Electrode. Karar P., Kumar G., Kar R., et al. *IEEE Transactions on Plasma Science*. Vol. pg. 1-8.

409. DICOM CT-based Monte Carlo dose calculations for prostate permanent implant using 125I seed sources. Mishra S., Deshpande S., S. Pathan M., et al. *Radiation Physics and Chemistry*. Vol. 210, ArtNo. 111021.

410. Dielectric spectroscopy and magnetoelectric coupling in dilute Fe substituted quasi-one-dimensional spin chain calcium cobalt manganite films. Thankachen N., Pathak B.Y., Pandya R.J., et al. *Journal of Vacuum Science and Technology A: Vacuum, Surfaces and Films*. Vol. 41(1), ArtNo. 13403.

411. Differentiation of Discordant Lesions on Dual-Tracer PET/CT (68Ga-PSMA-11 and 18F-FDG) in Prostate Carcinoma: Diagnosis of Second Primary Malignancies. Chalikandy A., Yadav S., Basu S. *Journal of Nuclear Medicine Technology*. Vol. 51(3), pg. 1-4.

412. Diffusion of Cs+ in compacted Na+/K+–saturated smectite-rich natural clay: role of clay microstructure. Kumar S., Chandane A., Sengupta A., et al. *Journal of Radioanalytical and Nuclear Chemistry*. Vol. 332(1), pg. 203-210.

413. Diffusion of radioisotopes in Fe-montmorillonite relevant to geological disposal of HLW. Chikkamath S., Patel M.A., Kar A.S., et al. *Physics and Chemistry of the Earth*. Vol. 131, ArtNo. 103429.

414. Diglycolamic acid for the mutual separation of lanthanides and actinides from dilute nitric acid solution: solvent extraction, dynamic light scattering, and spectroscopic investigations. Dhawa A., Ravi J., Puspalata R., et al. *New Journal of Chemistry*. Vol. 48(1), pg. 281-299.

415. Diglycolamides as highly efficient carrier ligands for actinide transport in supported liquid membranes. Ansari S.A., Mohapatra P.K. *Desalination and Water Treatment*. Vol. 285 pg. 47-66.

416. Dimensionality reduction and sensitivity improvement for TACTIC Cherenkov data using t-SNE machine learning algorithm. Das M.P., Dhar V.K., Verma S., et al. *Nuclear Instruments and Methods in Physics Research, Section A: Accelerators, Spectrometers, Detectors and Associated Equipment*. Vol. 1057, ArtNo. 168683.

417. Dimethylpiperazine on Air-Water Interface: Vibrational Sum frequency Generation study of a cyclic tertiary amine. SENGUPTA S., SAHA A., VIRMANI A., et al. *Journal of Molecular Liquids*. Vol. 391, ArtNo. 123248.

418. Dinitro Derivative of Naphthalimide as a Fluorescent Probe for Tumor Hypoxia Imaging. Kumari R., R V., Sunil D., et al. *Polycyclic Aromatic Compounds*. Vol. 43(1), pg. 54-63.

419. Direct assessment of the variations in the intensity ratios of M and L X-ray lines of U in various compounds by total reflection X-ray fluorescence spectrometry. Dhara S. *Spectrochimica Acta - Part B Atomic Spectroscopy*. Vol. 201, ArtNo. 106625.

420. Direct configuration mode microwave sintering of natural uranium dioxide pellets. Singh G., Mohod S., Varma P.V.S., et al. *Ceramics International*. Vol. 49(11), pg. 18969-18976.

421. Discovery of high-pressure post-perovskite phase in HoCrO3. Mall A.K., Garg N., Verma A.K., et al. *Journal of Physics and Chemistry of Solids*. Vol. 172, ArtNo. 111078.

422. Discrimination of binary mixture of toxic gases using ZnO nanowires-based E-nose. Sinju K.R., Bhangare B.K., Debnath A.K., et al. *Journal of Materials Science: Materials in Electronics*. Vol. 34(20), ArtNo. 1562.

423. Discrimination of Fast and Thermal Neutrons Using a Novel Phoswich Detector of LaCl3and LiI:Eu Single Crystal Scintillators. Sonu, Tyagi M., Patel T., et al. *IEEE Transactions on Nuclear Science*. Vol. 70(7), pg. 1325-1330.

424. Distinct anharmonic characteristics of phonon-driven lattice thermal conductivity and thermal expansion in bulk MoSe2 and WSe2. Gupta M.K., Kumar S., Mittal R., et al. *Journal of Materials Chemistry A*. Vol. 11(40), pg. 21864-21873.

425. Distinction between low-barrier hydrogen bond and ordinary hydrogen bond: a case study of varying nature of charge assisted hydrogen bonds of diglycine perchlorate crystal. Choudhury R.R., Chitra R., Panicker L. *Materials Research Express*. Vol. 10(7), ArtNo. 75102.

426. Diverse mechanisms in proton knockout reactions from the Borromean nucleus 17Ne. Wamers F., Lehr C., Marganiec-Gałązka J., et al. *European Physical Journal A*. Vol. 59(7), ArtNo. 154.

427. DivIVA Phosphorylation Affects Its Dynamics and Cell Cycle in Radioresistant Deinococcus radiodurans. Chaudhary R., Kota S., Misra H.S. *Microbiology Spectrum*. Vol. 11(2) .

428. Does women empowerment associate with reduced risks of intimate partner violence in India? evidence from National Family Health Survey-5. Ghoshal R., Patil P., Gadgil A., et al. *PLoS ONE*. Vol. 18(45607), ArtNo. e0293448.

429. Does women's empowerment and their socioeconomic condition affect the uptake of breast cancer screening? Findings from NFHS-5, India. Patil P., Sarang B., Bhandarkar P., et al. *BMC Women's Health*. Vol. 23(1), ArtNo. 7.

430. Dopant-activated magnetism and local structure properties of cubic shape Co, Mn:In2O3. Dhamodaran M., Yadav R.K., Karuppannan R., et al. *Materials Science in Semiconductor Processing*. Vol. 168, ArtNo. 107818.

431. Dose measurement using a leuco crystal violet film system with high sensitivity for food irradiation applications. Kaarunya Dhevi G.G., Sanyal B., Prakasan V., et al. *Radiation Physics and Chemistry*. Vol. 213, ArtNo. 111206.

432. Dosimetric characterization of LiCaAlF6:Eu,Y for its application in mix thermal n-γ fields. Singh A.K., Dhabekar B., Sen M., et al. *Radiation Physics and Chemistry*. Vol. 210, ArtNo. 111015.

433. Dual Excited State Proton Transfer Pathways in the Bifunctional Photoacid 6-Amino-2-naphtol. Jagushte K.U., Sadhukhan N., Upadhyaya H.P., et al. *Journal of Physical Chemistry B*. Vol. 127(45), pg. 9788-9801.

434. Dual Single-Atomic Co-Mn Sites in Metal-Organic-Framework-Derived N-Doped Nanoporous Carbon for Electrochemical Oxygen Reduction. Dey G., Jana R., Saifi S., et al. *ACS Nano*. Vol. 17(19), pg. 19155-19167.

435. Dubyaea atropurpurea (Asteraceae): an addition to the flora of India. Dey S., Barbhuiya H.A., Moaakum. *Rheedea*. Vol. 33(2), pg. 92-96.

436. Dynamic phase transformation driven microstructure and texture development during deformation of Zr-2.5wt.%Nb in α+β phase field. Bharat Reddy G., Kapoor R., Sarkar A. *Acta Materialia*. Vol. 261, ArtNo. 119354.

437. Dynamic Response of Single Crystal Al, Cu & Ni Upon Impact : MD and Ab-Initio Calculations. Madhavan S., Mishra V., Lakshmi Narayana P.V., et al. *Journal of Dynamic Behavior of Materials*. Vol. 9(1), pg. 24-35.

438. Dynamics of hydrogen bond reorganization in the S1(ππ*) state of 9-Anthracenecarboxaldehyde. Ghosh R., Datta S., Mora A.K., et al. *Journal of Photochemistry and Photobiology A: Chemistry*. Vol. 436, ArtNo. 114379.

439. Dynamics of spatially confined ns laser induced atmospheric air plasma and shock waves: visualization vis-à-vis validation. Guthikonda N., Kameswari D.P.S.L., Manikanta E., et al. *Journal of Physics D: Applied Physics*. Vol. 56(30), ArtNo. 305501.

440. Dynamics of the interaction of tetracycline with a monolayer of model cell membrane using VSFG spectroscopy. Virmani A., Saha A., Sengupta S., et al. *Indian Journal of Physics*. Vol. 97(6), pg. 1697-1706.

441. Dysprosium site occupancy in SrZnO2 nanophosphors probed through XANES. Manju N., Rajput P., Vij A., et al. *Physical Chemistry Chemical Physics*. Vol. 25(41), pg. 28473-28478.

442. Editorial: Abiotic stress signaling in plants: functional genomic intervention, volume II. Srivastava A.K., Pandey A., Böhmer M., et al. *Frontiers in Plant Science*. Vol. 14, ArtNo. 1334467.

443. Editorial: Anti-cancer drug delivery: lipid-based nanoparticles. Alkilany A.M., Elhissi A., Alshaer W., et al. *Frontiers in Oncology*. Vol. 13, ArtNo. 1248272.

444. Editorial: Plants for future climate: responses and adaptations to combined, multifactorial, and sequential stresses. Kumar V., Srivastava A.K., Sytar O., et al. *Frontiers in Plant Science*. Vol. 14, ArtNo. 1290649.

445. Editorial: Reviews in radiation oncology. Lee D.Y., Sudhandiran G., Sharma S.D. *Frontiers in Oncology*. Vol. 13, ArtNo. 1283431.

446. Editorial: TGF-β signalling pathways and their enigmatic role as a friend and foe in human health and diseases. Betapudi V., Patro B.S., Saika S., et al. *Frontiers in Molecular Biosciences*. Vol. 10, ArtNo. 1232454.

447. Editorial: Trends of microbial technologies in rehabilitation of contaminated environments. Deka Boruah H.P., Chauhan P.S., Acharya C. *Frontiers in Microbiology*. Vol. 14, ArtNo. 1268002.

448. Editorial: Women in chemistry 2022. Fahim I.S., André V., Mohanty J., et al. *Frontiers in Chemistry*. Vol. 11, ArtNo. 1230005.

449. Effect of Ageing Treatment on the Stress Corrosion Cracking Susceptibility of Precipitation Hardenable 17–4 PH Stainless Steel. Bhambroo R., Roychowdhury S., Kain V., et al. *Transactions of the Indian Institute of Metals*. Vol. 76(8), pg. 2193-2200.

450. Effect of ajwain (Trachyspermum ammi) extract and gamma irradiation on the shelf-life extension of rohu (Labeo rohita) and seer (Scomberomorus guttatus) fish steaks during chilled storage. Mishra P.K., Kakatkar A.S., Kamal Gautam R., et al. *Food Research International*. Vol. 163, ArtNo. 112149.

451. Effect of annealing environment on the luminescence and structural properties of pure CePO4 and Tb: CePO4 nanowires. Tripathi S., Kumar Y., Nand M., et al. *Journal of Luminescence*. Vol. 257, ArtNo. 119666.

452. Effect of C deuteration in forming isotopic polymorph of glycine silver nitrate. Chitra R., Choudhury R.R., Capet F., et al. *Structural Chemistry*.

453. Effect of Co doping on structural and magnetic properties of kagome like La based cuprate francisite Cu3La(SeO3)2O2Cl. Manna P., Kanthal S., Ahmed M.A., et al. *Journal of Applied Physics*. Vol. 133(19), ArtNo. 193902.

454. Effect of curvature on bilayer thickness of liposome suspensions in water. Pal A., Khakhar D., Ray D., et al. *Physica Scripta*. Vol. 98(11), ArtNo. 115018.

455. Effect of dopant oxidation states on enhanced low ppm CO sensing by copper doped zinc oxide. Rudra P., Chakraborty N., Srihari V., et al. *Materials Chemistry and Physics*. Vol. 295, ArtNo. 127047.

456. Effect of Dy3+ ions substitution on structural, electrical, and dielectric properties of SrDyxFe12-xO19 hexaferrite prepared by sol-gel combustion method. Mahapatro J., Meena S.S., Agrawal S. *Journal of Electroceramics*. Vol. 51(2), pg. 104-121.

457. Effect of electron beam radiation on the mechanical, electrical, heat shrinkable and morphological properties of linear low-density polyethylene/polyolefin elastomer blends. Agarwal R., Singh M., Ray Chowdhury S., et al. *Progress in Rubber, Plastics and Recycling Technology*.

458. Effect of fluorescent dyes on the scintillation efficiency, improved light yield and radiation hardness of polystyrene-based plastic scintillator: a comparative study. Alex L., Paulraj R., Tyagi M. *Radiation Effects and Defects in Solids*. Vol. 178(45448), pg. 589-606.

459. Effect of gamma irradiation on shape memory, thermal and mechanical properties of polycaprolactone. Prajapati S., Gogoi R., Tyagi V.K., et al. *Radiation Physics and Chemistry*. Vol. 204, ArtNo. 110671.

460. Effect of Heat Input on the Weld Thermal Cycle, Microstructure, Tensile Damage and Fracture Behavior of Pulsed Laser-Welded Dual-Phase Steel. Gandhi A.D., Kundu A., Kumar R., et al. *Journal of Materials Engineering and Performance*.

461. Effect of hydration of a room temperature ionic liquid on the cation-cation interaction of UO22+ and NpO2+ ions. Verma P.K., Bhattacharyya A., Mohapatra P.K. *New Journal of Chemistry*. Vol. 47(15), pg. 7391-7398.

462. Effect of Laser Energy Density on Phase Evolution in Laser Surface Melted As-Cast Zr–Cu Alloy. Singh V., Vishwanadh B., Mishra S.C., et al. *Transactions of the Indian Institute of Metals*.

463. Effect of magnetic phase coexistence on spin-phonon coupling and magnetoelectric effect in polycrystalline Sm0.5Y0.5Fe0.58Mn0.42O3. Raut S., Chakravarty S., Mohanty H.S., et al. *Physica B: Condensed Matter*. Vol. 651, ArtNo. 414593.

464. Effect of monetite reinforced into the chitosan-based lyophilized 3D scaffolds on physicochemical, mechanical, and osteogenic properties. Singh Y.P., Bhaskar R., Agrawal A.K., et al. *International Journal of Polymeric Materials and Polymeric Biomaterials*. Vol. 72(15), pg. 1161-1178.

465. Effect of morphological properties on the particle size distribution measurements and modelling of porous and nonspherical aerosol behaviour. Pujala U., Subramanian V., Anand S., et al. *Progress in Nuclear Energy*. Vol. 163, ArtNo. 104811.

466. Effect of non-Planckian spectrum on shock velocities and subsonic to transonic transition in mid-Z witness plate elements. Ghosh K., Mishra G. *Physics of Plasmas*. Vol. 30(9), ArtNo. 92703.

467. Effect of Oxygen Ion Irradiation on Nb-1Zr-0.1C Alloy Characterized Using X-Ray Diffraction Line Profile Analysis. Dutta A., Sarkar A., Bysakh S., et al. *Nuclear Science and Engineering*. Vol. 197(12), pg. 3160-3174.

468. Effect of particle and pore morphology on optical transmission of yttria based laser host ceramics: A small-angle scattering investigation. Selvamani R., Kumar S., Singh G., et al. *Nuclear Instruments and Methods in Physics Research, Section B: Beam Interactions with Materials and Atoms*. Vol. 537 pg. 104-110.

469. Effect of phase interfaces to dimple pattern. Das A. *Materials Letters*. Vol. 337, ArtNo. 133954.

470. Effect of picosecond-laser induced microstructuring of Ti6Al4V bio-alloy on its tribological and corrosion properties. Kedia S., Nilaya J.P. *Applied Physics A: Materials Science and Processing*. Vol. 129(10), ArtNo. 710.

471. Effect of Postdeposition Heat Treatment on the Nanoplasmonic Behavior of Glancing Angle-Deposited Silver Nanostructures. De R., Goud B.K., Kar C., et al. *Physica Status Solidi (A) Applications and Materials Science*. Vol. 220(19), ArtNo. 2300427.

472. Effect of pulverisation on sulfide and tin antimonide anodes for sodium-ion batteries. Priyanka P., Nalini B., Soundarya G.G., et al. *Frontiers in Energy Research*. Vol. 11, ArtNo. 1266653.

473. Effect of quantum plasma on 2p photoionization cross section of Al + 3 ion embedded in shock compressed aluminium. Das M. *European Physical Journal D*. Vol. 77(1), ArtNo. 7.

474. Effect of strontium loading on the structural and thermodynamic properties of Ca10-xSrx(PO4)6F2(x= 2, 4, 6, 8) solid solutions for radioactive waste immobilization. Das P., Govind Vats B., Mohapatra M., et al. *Journal of Solid State Chemistry*. Vol. 324, ArtNo. 124101.

475. Effect of thermal annealing on an emissive layer containing a blend of a small molecule and polymer as host for application in OLEDs. Meer B.B., Sharma D., Tak S., et al. *RSC Advances*. Vol. 13(48), pg. 33668-33674.

476. Effect of Thermal Cycling on Fracture Toughness of Hydrided Zr–2.5Nb PT Material. Narayana Murty T., Kumar S., Bind A.K., et al. *Transactions of the Indian Institute of Metals*. Vol. 76(1), pg. 31-37.

477. Effect of titanium swift heavy ion irradiation on ferroelectric triglycine sulphate (TGS) 〈011〉 oriented single crystals. Sabarish V.C.B., Durairajan A., Graça M.P.F., et al. *Journal of Materials Science: Materials in Electronics*. Vol. 34(21), ArtNo. 1566.

478. Effect of Zn2+-Zr4+ co-substitution on structural, magnetic and dielectric properties of Ba0.5Ca0.5ZnxZrxFe12−2xO19 hexaferrite. Godara S.K., Meena S.S., Jasrotia R., et al. *Journal of Materials Science: Materials in Electronics*. Vol. 34(15), ArtNo. 1195.

479. Effect of ZnO morphologies on its sensor response and corresponding E-nose performance. Sinju K.R., Bhangare B.B., Prakash J., et al. *Materials Science and Engineering: B*. Vol. 298, ArtNo. 116870.

480. Effect on structure, stability, and H+ irradiation on Nd3+/Ru4+-loaded iron phosphate glass for nuclear applications. Joshi A.C., Roy M., Dutta D.P., et al. *Journal of the American Ceramic Society*. Vol. 106(4), pg. 2271-2287.

481. Effective dose estimation of radon, thoron and their progeny concentrations in the environs of Himalayan belt, India. Semwal P., Agarwal T.K., Joshi M., et al. *International Journal of Environmental Science and Technology*. Vol. 20(4), pg. 4127-4138.

482. Effective gene silencing using type I–E CRISPR system in the multiploid, radiation-resistant bacterium Deinococcus radiodurans. Misra C.S., Pandey N., Appukuttan D., et al. *Microbiology Spectrum*. Vol. 11(5).

483. Effective proliferation control of MCF7 breast cancer using microsecond duration electrical pulse. Kumar G., Sarathi R., Sharma A. *Journal of Cancer Research and Therapeutics*. Vol. 19(7), pg. 1725-1730.

484. Effects of Air/Water-Stability, “Aqueous” Processing and Binder-Type on the Chemical-Mechanical-Electrochemical Stability of Na-Titanate Based Anodes for Na-Ion Batteries. Pradeep A., Kumar B.S., Abharana N., et al. *Journal of the Electrochemical Society*. Vol. 11(1), ArtNo. 110531.

485. Effects of elevated temperature steam oxidation and subsequent quenching on light water reactor clad. Singh A.R., Puranik B., Gokhale O., et al. *Progress in Nuclear Energy*. Vol. 155, ArtNo. 104510.

486. Effects of hydrogen bonding on intramolecular/intermolecular proton-coupled electron transfer using a Ruthenium-anthraquinone dyad in ultrafast time domain. Dey A., Ghorai N., Das A., et al. *Journal of Photochemistry and Photobiology A: Chemistry*. Vol. 441, ArtNo. 114709.

487. Effects of intrinsic and extrinsic multi-phased lattice structure and chemical heterogeneity on the control of ferrimagnetic properties in Co rich spinel ferrite. Bhowmik R.N., Kishor G., Sherin D., et al. *Journal of Magnetism and Magnetic Materials*. Vol. 588, ArtNo. 171412.

488. Effects of ionic liquids on biomembranes: A review on recent biophysical studies. Mitra S., Sharma V.K., Ghosh S.K. *Chemistry and Physics of Lipids*. Vol. 256, ArtNo. 105336.

489. Effects of microstructure on radiolytic degradation of nuclear grade cationic resins: Gel versus macro-porous. Mal D., Puspalata R., Amirthapandian S., et al. *Radiation Physics and Chemistry*. Vol. 211, ArtNo. 111081.

490. Efficient Charge Transfer in the Perovskite Quantum Dot-Hemin Biocomposite: Is This Effective for Optoelectronic Applications?. Sayyad U.S., Burai S., Bhatt H., et al. *Journal of Physical Chemistry Letters*. Vol. 14(23), pg. 5397-5402.

491. Efficient oxygen reduction reaction of rare earth perovskite SmMnO3. Mahalik R.R., Hota I., Soren S., et al. *Inorganic Chemistry Communications*. Vol. 154, ArtNo. 110924.

492. Efficient Plutonium Extraction and Electrochemical Insights in a Hydrophobic Deep Eutectic Solvent for Radioactive Waste Management. Patil S.M., Jayachandran K., Sahu M., et al. *Journal of the Electrochemical Society*. Vol. 11(1), ArtNo. 113503.

493. Efficient Removal of Uranyl Ions Using PAMAM Dendrimer: Simulation and Experiment. Maity T., Aggarwal A., Dasgupta S., et al. *Langmuir*. Vol. 39(19), pg. 6794-6802.

494. Ekavimsati patrani (21 leaves) used during Vinayaka Chaviti festival in India: medicinal, environmental and cultural importance. Kora A.J. *Advances in Traditional Medicine*. Vol. 23(2), pg. 393-405.

495. Electric-Field Emission Mechanism in Q-Carbon Field Emitters. Haque A., Karmakar S., Trivedi R.K., et al. *ACS Omega*. Vol. 8(10), pg. 9307-9318.

496. Electrochemical and spectroscopic evaluation of 6-MP and its interaction with carbon dots and dsDNA. Ipte P.R., Manna S., Satpati A.K. *Microchemical Journal*. Vol. 184, ArtNo. 108159.

497. Electrochemical capacitance and cubic-rhombohedral phase transition of sodium intercalated ferrimagnetic manganese hexacyanoferrate based open framework material. Bhatt P., Sharma M.K., Mukadam M.D., et al. *Sustainable Materials and Technologies*. Vol. 35, ArtNo. e00532.

498. Electrochemical performance of K+ -intercalated MnO2 nano-cauliflowers and their Na-ion-based pseudocapacitors. Chowdhury A., Shukla R., Bhattacharyya K., et al. *Materials Science and Engineering: B*. Vol. 295, ArtNo. 116581.

499. Electrochemical separation and purification of no-carrier-added 177Lu for radiopharmaceutical preparation: Translation from bench to bed. Patra S., Chakravarty R., Singh K., et al. *Chemical Engineering Journal Advances*. Vol. 14, ArtNo. 100444.

500. Electron beam assisted recycling of polyurethane (PU) sponge: Turning it into a superabsorbent for wastewater treatment. Jha A., Shaik K.A., Bhardwaj Y.K., et al. *Journal of Applied Polymer Science*. Vol. 140(9), ArtNo. e53545.

501. Electronic spectroscopy of trans-2-hexenal and 3-hexanol: Experimental and computational studies. Das A.K., K S., Rajasekhar B.N. *Journal of Quantitative Spectroscopy and Radiative Transfer*. Vol. 299, ArtNo. 108509.

502. Electronic structure and reactivity of dehydrobenzo[n]annulene incorporated two-dimensional metal-organic frameworks. Kancharlapalli S. *Journal of Chemical Sciences*. Vol. 135(2), ArtNo. 46.

503. Elevated Transition Temperature of VO2 Thin Films via Cr Doping: A Combined Electrical Transport and Electronic Structure Study. Zzaman M., Dawn R., Franklin J.B., et al. *Journal of Electronic Materials*. Vol. 52(6), pg. 3818-3830.

504. Emerging functionalized magnetic nanoparticles: from synthesis to nuclear fuel cycle application: where do we stand after two decade?. Patra K., Sengupta A., Mittal V.K., et al. *Materials Today Sustainability*. Vol. 24, ArtNo. 100489.

505. Emerging interfacial magnetization in isovalent manganite heterostructures driven by octahedral coupling. Kumar Y., Bhatt H., Kakkar S., et al. *Physical Review B*. Vol. 108(17), ArtNo. 174410.

506. Encapsulation of curcumin in alginate microbeads (AMB) for control release of curcumin. Shaikh S.A.M., Barik A. *Journal of Chemical Sciences*. Vol. 135(2), ArtNo. 39.

507. Endorsing Na+ storage mechanism in low tortuosity, high plateau capacity hard carbon towards development of high-performance sodium-ion pouch cells. Bhawana K., Gautam M., Mishra G.K., et al. *Carbon*. Vol. 214, ArtNo. 118319.

508. Energetic, Electronic, and Optical Behavior of Intrinsic Charge Carrier-Trapping Defects in Ge-Doped ZnGa2O4: Insights from a DFT Study. Modak B. *Journal of Physical Chemistry C*. Vol. 127(28), pg. 13918-13928.

509. Engineered triphenylphosphonium-based, mitochondrial-targeted liposomal drug delivery system facilitates cancer cell killing actions of chemotherapeutics. Sivagnanam S., Das K., Pan I., et al. *RSC Chemical Biology*. Vol., ArtNo. .

510. Engineering ZnO with Cu doping to lower the transition pressure: Experimental and theoretical investigations. Sharma B.B., Chakraborty B., Gohil S., et al. *AIP Advances*. Vol. 13(1), ArtNo. 15022.

511. Enhanced nitrobenzene sensing in metal anchored gamma-graphyne: predictions from density functional theory. Lakshmy S., Kalarikkal N., Chakraborty B. *Journal of Physics D: Applied Physics*. Vol. 56(49), ArtNo. 495104.

512. Enhanced optical and electronic properties of chlorobenzene-assisted perovskite CH3NH3PbI3−xClx film incorporated in p-i-n solar cells. Gupta D., Veerender P., Sridevi C., et al. *Journal of Materials Science: Materials in Electronics*. Vol. 34(1), ArtNo. 66.

513. Enhancement in Photoelectrochemical Efficiency and Modulation of Surface States in BiVO4 through the TiO2 Outer Layer Using the Atomic Layer Deposition Technique. Sharma A., Manna S., Satpati A.K. *Journal of Physical Chemistry C*. Vol. 127(9), pg. 4395-4406.

514. Enhancement in the Transport and Optoelectrical Properties of Spray Coated ZnO Thin Films by Nd Dopant. Srivathsa M., Kumar P., Goutam U.K., et al. *Electronic Materials Letters*. Vol. 19(2), pg. 138-160.

515. Enhancement of Hole Extraction in Carbon-Based Organic–Inorganic Hybrid Perovskite Solar Cells Using MAPbI3:NiO-NPs Composite. Daniel R.I., Govindaraj R., Ramasamy P., et al. *Journal of Electronic Materials*. Vol. 52(11), pg. 7459-7474.

516. Enhancement of Multiferroic and Optical Properties in BiFeO3 Due to Different Exchange Interactions Between Transition and Rare Earth Ions. Kumari S., Anand K., Alam M., et al. *Physica Status Solidi (B) Basic Research*. Vol. 260(9), ArtNo. 2300026.

517. Enhancing physical characteristics of thermotropic nematic liquid crystals by dispersing in various nanoparticles and their potential applications. Rastogi A., Mishra A., Pandey F.P., et al. *Emergent Materials*. Vol. 6(1), pg. 101-136.

518. Enhancing the PEC Efficiency in the Perspective of Crystal Facet Engineering and Modulation of Surfaces. Manna S., Satpati A.K., Patra C.N., et al. *ACS Omega*.

519. Enhancing the Ultrafast Third-Order Nonlinear Optical Response by Charge Transfer in VSe2-Reduced Graphene Oxide Hybrid. Kumar V., Afreen, Ka S.R., et al. *Journal of Physical Chemistry C*. Vol. 127(37), pg. 18485-18493.

520. Ensuring safety of new, advanced small modular reactors for fundamental safety and with an optimal main heat transport systems configuration. Gaikwad A.J., Maheshwari N.K., Chandrakar D.K., et al. *Kerntechnik*. Vol. 88(4), pg. 475-490.

521. Entrapping metal atom on hexagonal boron nitride monolayer for high performance single-atom-catalyst: Role of vacancy defects and metal support. Datta J., Majumder C. *Applied Surface Science*. Vol. 614, ArtNo. 156061.

522. Environmental isotope constraints and hydrogeochemical evolution of groundwater in the semi-arid national capital environs of Delhi, India. Gupta S., Nandimandalam J.R., Pant D., et al. *Urban Climate*. Vol. 49, ArtNo. 101481.

523. Equations of State and Crystal Structures of KCaPO4, KSrPO4, and K2Ce(PO4)2 under High Pressure: Discovery of a New Polymorph of KCaPO4. Errandonea D., Achary S.N., Diaz-Anichtchenko D., et al. *Crystal Growth and Design*. Vol. 23(4), pg. 2782-2794.

524. Equilibrium and thermodynamic study of trichloroethylene adsorption on activated carbon in a fluidized bed and its thermal regeneration. Nikam S., Mandal D. *Canadian Journal of Chemical Engineering*. Vol. 101(1), pg. 451-462.

525. Ergodic polar cluster state and its dynamics in K and Nb modified BaTiO3. Selvamani R., Rao R., Sastry P.U., et al. *Ceramics International*. Vol. 49(24), pg. 39926-39934.

526. Erratum: Battery-powered FPGA-based embedded system for ultrasonic pipe inspection and gauging systems (Rev. Sci. Instrum. (2023) 94 (034712) DOI: 10.1063/5.0142236). Kumar N.P., Patankar V.H. *Review of Scientific Instruments*. Vol. 94(4), ArtNo. 49901.

527. Erratum: Measurement of prompt and nonprompt charmonium suppression in PbPb collisions at 5.02 TeV (The European Physical Journal C, (2018), 78, 6, (509), 10.1140/epjc/s10052-018-5950-6). Sirunyan A.M., Tumasyan A., Adam W., et al. *European Physical Journal C*. Vol. 83(2), ArtNo. 145.

528. Erratum: Sensor position optimization for flux mapping in a nuclear reactor using compressed sensing (Annals of Nuclear Energy (2021) 159, (S0306454921001742), (10.1016/j.anucene.2021.108298)). Bahuguna S.K., Mukhopadhyay S., Tiwari A.P. *Annals of Nuclear Energy*. Vol. 183, ArtNo. 109588.

529. Establishment of ex vivo calibration curve for X-ray induced “dicentric + ring” and micronuclei in human peripheral lymphocytes for biodosimetry during radiological emergencies, and validation with dose blinded samples. Vijayalakshmi J., Chaurasia R.K., Srinivas K.S., et al. *Heliyon*. Vol. 9(6), ArtNo. e17068.

530. Estimating minimum energy requirement. Desai B.G., Bhattacharyya R., Singh K.K., et al. *Current Science*. Vol. 125(3), pg. 231-233.

531. Estimation of an empirical formula for efficiency of a BEGe type detector using machine learning based algorithm. Dey R., Chinnaesakki S., Dhumale M.R., et al. *Radiation Physics and Chemistry*. Vol. 206, ArtNo. 110761.

532. Estimation of effective thermal conductivity and heat transfer coefficient of lithium orthosilicate pebble bed in carbon dioxide–air medium. Ghuge N.S., Mandal D., Jadeja M.C., et al. *Experimental Heat Transfer*.

533. Estimation of fuzzy band for radon transport mechanism in earth crust. Rao T.D., Chakraverty S., Karunakar P., et al. *European Physical Journal Plus*. Vol. 138(3), ArtNo. 221.

534. Estimation of Lacustrine Groundwater Discharge (LGD) to an urban Himalayan lake using environmental tracers (222Rn, δ18O, EC). Pall I.A., Jeelani G., Noble J. *Journal of Hydrology*. Vol. 618, ArtNo. 129145.

535. Estimation of radionuclide concentrations and exhalation rates from soils of Patiala and Fatehgarh Sahib districts of Punjab. Kapil C., Mehta V., Shikha D., et al. *Journal of Radioanalytical and Nuclear Chemistry*. Vol. 332(11), pg. 4391-4401.

536. Estimation of radon in groundwater and analysis of radon and thoron exhalation rates of the soil in Mokokchung district, Nagaland, India. Jamir S., Sahoo B.K., Mishra R., et al. *Groundwater for Sustainable Development*. Vol. 20, ArtNo. 100874.

537. Estimation of rare earth elements in Indian coal fly ashes for recovery feasibility as a secondary source. Sandeep P., Maity S., Mishra S., et al. *Journal of Hazardous Materials Advances*. Vol. 10, ArtNo. 100257.

538. Estimation of Reference Gamma Radiation Field for Calibration of Radiation Monitors. Singh S.K., Shaiju L., Gupta A., et al. *Mapan - Journal of Metrology Society of India*.

539. Estimation of the buildup of He-3 and Li-6 poisoning, He-4 and tritium activity in beryllium oxide reflector block in APSARA-U reactor. Singha K., Singh T., Pandey P., et al. *Nuclear and Particle Physics Proceedings*. Vol. 341 pg. 104-109.

540. Estimation of238U and232Th in soil and water of prominent fault region of Mizoram. Thuamthansanga T., Sahoo B.K., Tiwari R.C. *Environmental Engineering Research*. Vol. 28(1), ArtNo. 210106.

541. Eu3+ as a spectroscopic probe to understand local site-luminescence correlation in novel Y2TiO5:Eu3+ phosphor. Jafar M., Balhara A., Gupta S.K. *Journal of Molecular Structure*. Vol. 1289, ArtNo. 135795.

542. Eutectoid phase transformation in U-Mo-X alloys. Rakesh R., Sinha V.P., Manikrishna K.V., et al. *Journal of Nuclear Materials*. Vol. 573, ArtNo. 154113.

543. Evaluation of a Phosphinate Functionalized Ionic Liquid for the Separation of Nb and Ta from Nitric Acid Feed Conditions. Goyal P., Sengupta A., Mohapatra P.K. *ACS Omega*. Vol. 8(39), pg. 36506-36520.

544. Evaluation of Conducted Electromagnetic Interference Behavior of Copper Vapor Laser. Singh D.K., Dikshit B., Vijayan R., et al. *IEEE Transactions on Electromagnetic Compatibility*. Vol. 65(1), pg. 58-68.

545. Evaluation of DNBR with neutronics calculation in LWR systems. Khan S.A., Kannan U. *Nuclear Energy and Technology*. Vol. 9(2), pg. 77-83.

546. Evaluation of hyperfine interactions in strontium titanate perovskite for low doses of electron beam radiation. Kumar A., Sahu M., Khader S.A., et al. *Journal of Radioanalytical and Nuclear Chemistry*. Vol. 332(8), pg. 2963-2970.

547. Evaluation of integral parameters of BAPL and AERE benchmarks using ν-TRAC code and ENDF/B VIII.0 library. Singh A., Pal U., Karthikeyan R. *Nuclear and Particle Physics Proceedings*. Vol. 339-340 pg. 78-87.

548. Evaluation of mixing performance and validation of CFD simulations in baffled anaerobic digesters using radiotracer technique. Goswami S., Kshirsagar V.S., Aswini V., et al. *Applied Radiation and Isotopes*. Vol. 192, ArtNo. 110570.

549. Evaluation of Neutron Cross-Section Data Using Gaussian Mixture Model and Digital Filter. Phatak T.S., Nair J., Prasanna Ram S., et al. *Nuclear Science and Engineering*.

550. Evaluation of Pendrin Expression Using Nuclear Imaging Modalities and Immunohistochemistry in Animal Thyroid Cancer Model. Gholve C.S., Shete Y., Rakshit S., et al. *Indian Journal of Nuclear Medicine*. Vol. 38(4), pg. 328-333.

551. Evaluation of seismic margins for nuclear power plant piping systems using ratcheting criterion. Ravi Kiran A., Agrawal M.K. *International Journal of Pressure Vessels and Piping*. Vol. 202, ArtNo. 104894.

552. Evaluation of simple algorithms for spatial interpolation of salinity hazard parameter in natural waters. Rafi A., Dauji S., Keesari T. *Journal of Earth System Science*. Vol. 132(4), ArtNo. 162.

553. Evaluation of Skin Absorption Potential of Chemicals Relevant to Painting Trades. Ghosh N., Vitti Krushna P., Sharma J.D., et al. *ACS Chemical Health and Safety*. Vol. 30(4), pg. 204-211.

554. Evaluation of uranium content and annual ingestion dose in the surface and ground water bodies of Chittorgarh, Rajasthan, India. Menaria T., Tiwari S.N., Patra A.K., et al. *Environmental Monitoring and Assessment*. Vol. 195(9), ArtNo. 1043.

555. Evidence for four-top quark production in proton-proton collisions at s=13TeV. Tumasyan A., Adam W., Andrejkovic J.W., et al. *Physics Letters, Section B: Nuclear, Elementary Particle and High-Energy Physics*. Vol. 844, ArtNo. 138076.

556. Evidence of Eu(III) Dual Binding in a PVC-Based Electrochemical Sensor with N,N,N',N'-Tetrapentyl Diglycolamide (TPDGA) as the Ionophore: Potentiometric and Luminescence studies. Mahanty B., Verma P.K., Mohapatra P.K. *ChemistrySelect*. Vol. 8(10), ArtNo. e202204681.

557. Evidence of Size Stratification in Colloidal Glass Microgranules Realized by Rapid Evaporative Assembly. Tiwari A.K., Sen D., Das A., et al. *Langmuir*. Vol. 39(44), pg. 15572-15586.

558. Evidence of vacancy ordered structures in PuO2−x and AmO2−x from first-principles calculations. Ghosh P.S., Arya A. *Physical Chemistry Chemical Physics*. Vol. 25(20), pg. 14117-14125.

559. Evolution of dislocations and grain boundaries during multi-axial forging of tantalum. Kedharnath A., Kapoor R., Sarkar A. *International Journal of Refractory Metals and Hard Materials*. Vol. 112, ArtNo. 106120.

560. Evolution of Local Structure and Pore Architecture during Zeolitic Imidazolate Framework-L to Zeolitic Imidazolate Framework-8 Phase Transformation Investigated Using Raman, Extended X-ray Absorption, and Positron Annihilation Lifetime Spectroscopy. Mor J., Utpalla P., Kumar R., et al. *Chemistry of Materials*. Vol. 35(17), pg. 6625-6636.

561. Evolution of static charge density wave order, amplitude mode dynamics, and suppression of Kohn anomalies at the hysteretic transition in EuTe4. Rathore R., Pathak A., Gupta M.K., et al. *Physical Review B*. Vol. 107(2), ArtNo. 24101.

562. Evolution of the valence state of Ru metal ions in correlation with the structural and electronic properties of double perovskite ruthenates; A2SmRuO6 (where A = Ba & Sr). Dani S., Pandit R., Sharma H., et al. *Journal of Materials Chemistry C*. Vol. 11(12), pg. 4081-4093.

563. Evolutionary conservation of protein dynamics: insights from all-atom molecular dynamics simulations of 'peptidase' domain of Spt16. Gaur N.K., Ghosh B., Goyal V.D., et al. *Journal of Biomolecular Structure and Dynamics*. Vol. 41(4), pg. 1445-1457.

564. Excitation Frequency Effect on Breast Cancer Cell Death by Atmospheric Pressure Cold Plasma. Chaturvedi Misra V., Pai B G., Tiwari N., et al. *Plasma Chemistry and Plasma Processing*. Vol. 43(2), pg. 467-490.

565. Excitation functions of the 197Au(p,pxn) and 197Au(p,xn) reactions. Naik H., Kim G., Lee C., et al. *Radiochimica Acta*.

566. Exciton many-body interactions and charge transfer in CsPbBr3 /graphene derivatives. Maurya N.C., Karmakar R., Yadav R.K., et al. *Physical Review B*. Vol. 108(15), ArtNo. 155417.

567. Expansion of a finite-size photoplasma in an electrostatic field with M-type electrode configuration using a novel adaptive mesh 2D-PIC code. Singh P., Sridhar G., Maiti N. *Current Applied Physics*. Vol. 47 pg. 30-43.

568. Experimental and computational investigation on the charge storage performance of a novel Al2O3-reduced graphene oxide hybrid electrode. Ratha S., Sahoo S., Mane P., et al. *Scientific Reports*. Vol. 13(1), ArtNo. 5283.

569. Experimental and Numerical Analysis of Pressure Gradient and Flow Characteristics of Cemented Paste Backfill Based on Carbonate-Rich Tailings. Panchal S., Deb D., Sreenivas T. *Journal of The Institution of Engineers (India): Series D*. Vol. 104(1), pg. 225-232.

570. Experimental and Theoretical Findings of the Concerted Effect of Dual Quantum Dots on a Graphene Matrix for Energy Storage Applications. Mohanty B., Pradhan L., Kandasamy M., et al. *Energy and Fuels*. Vol. 37(10), pg. 7530-7538.

571. Experimental and theoretical insight into biphasic extractive mass transfer of thorium into ionic liquid phase using chloroamide ligands. Deshmukh S., Bhatt A.M., Boda A., et al. *Journal of Molecular Liquids*. Vol. 371, ArtNo. 121074.

572. Experimental and theoretical insights into colossal supercapacitive performance of graphene quantum dots incorporated Ni3S2/CoS2/MoS2 electrode. Sangabathula O., Kandasamy M., Chakraborty B., et al. *Journal of Energy Storage*. Vol. 65, ArtNo. 107274.

573. Experimental and Theoretical Investigation on the Extractive Mass Transfer of Eu3+ Ions Using Novel Amide Ligands in 1-Hexyl-3-methylimidazolium Bis(trifluoromethylsulfonyl)imide. Ghosh A., Pandey A., Sengupta A., et al. *Inorganic Chemistry*. Vol. 62(36), pg. 14678-14693.

574. Experimental and theoretical revelation of a unique band topology in Sb2Te3 topological insulator by substitution of Cu—A high pressure study. Pal D., Sharma B.B., Garg N., et al. *Materials Science and Engineering: B*. Vol. 290, ArtNo. 116347.

575. Experimental and theoretical studies (DFT) on technetium extraction as HTcO4 using dicyclohexano-18-crown-6 in a blend of isodecyl alcohol and n-dodecane from acidic medium. Khan P.N., Sinharoy P., Bhattacharyya A. *Progress in Nuclear Energy*. Vol. 160, ArtNo. 104684.

576. Experimental and Theoretical Studies of the Gas-Phase Kinetics of Epichlorohydrin with Tropospheric Oxidants. Sharma A., Virmani A., Walavalkar M.P., et al. *ACS Earth and Space Chemistry*. Vol. 7(8), pg. 1567-1577.

577. Experimental and theoretical study of the Cu 65 (n,p) Ni 65 reaction cross section from reaction threshold up to 25 MeV. Singh R.K., Singh N.L., Mehta M., et al. *Physical Review C*. Vol. 107(5), ArtNo. 54607.

578. Experimental assessment of hydrogen removal rate for passive auto catalytic recombiners. Sharma S.K., Kansal M., Guptan R.K., et al. *Nuclear Engineering and Design*. Vol. 407, ArtNo. 112274.

579. Experimental Evaluation of Two-Phase Heat Transfer Coefficient Under Oscillatory Flow Conditions and Correlation Development. Kumar R., Chandraker D.K., Dasgupta A., et al. *Journal of Nuclear Engineering and Radiation Science*. Vol. 9(1), ArtNo. 11403.

580. Experimental evidence of large collective enhancement of nuclear level density and its significance in radiative neutron capture. Santhosh T., Rout P.C., Santra S., et al. *Physics Letters, Section B: Nuclear, Elementary Particle and High-Energy Physics*. Vol. 841, ArtNo. 137934.

581. Experimental Investigation and Crystal Plasticity Simulation with Damage for Single Crystal Copper Subjected to Tensile Load. Paik S., Naveen Kumar N., Dutta B.K., et al. *Metals and Materials International*. Vol. 29(3), pg. 618-633.

582. Experimental investigation of jet pump performance used for high flow amplification in nuclear applications. Kotak V., Pathrose A., Sengupta S., et al. *Nuclear Engineering and Technology*. Vol. 55(10), pg. 3549-3558.

583. Experimental investigation of the structural features of polycarbonate (PC) filled with bismuth nitrate pentahydrate (BNP) composite films in terms of free volume defects probed by positron annihilation lifetime spectroscopy. Mirji R., Lobo B., Dutta D., et al. *Applied Radiation and Isotopes*. Vol. 196, ArtNo. 110773.

584. Experimental Investigations on Heat Transfer Deterioration for Vertical Flow of Supercritical Carbon-Dioxide Under Natural Circulation. Bodkha K., Pilkhwal D.S., Maheshwari N.K. *ASME Journal of Heat and Mass Transfer*. Vol. 145(2), ArtNo. 22101.

585. Experimental investigations on magnetic pulse crimping of copper lug. Ali N., Sharma S.K., Chebolu R., et al. *Engineering Research Express*. Vol. 5(1), ArtNo. 15055.

586. Experimental observation of spin glass state in the highly disordered quaternary Heusler alloy FeRuMnGa. Gupta S., Chakraborty S., Pakhira S., et al. *Physical Review B*. Vol. 107(18), ArtNo. 184408.

587. Experimental strategy for acid-free plutonium recovery from assorted matrices: Non-aqueous leaching followed by selective solid phase extraction. Kumar S.S., Rao A., Srivastava A., et al. *Korean Journal of Chemical Engineering*. Vol. 40(11), pg. 2716-2723.

588. Experimental Study and 3-D PIC-MCC Simulation of DC Discharge in Various Concentrations of SF6Admixture. Gandi V.K., Verma R., Singh G., et al. *IEEE Transactions on Dielectrics and Electrical Insulation*. Vol. 30(3), pg. 1096-1104.

589. Experimental study of different innovative measurement methodologies applied to a canned pulsed eddy current testing probe suitable for dilation measurement of test specimens. Shyam T.V., Sharma A., Patankar V.H., et al. *Insight: Non-Destructive Testing and Condition Monitoring*. Vol. 65(2), pg. 80-86.

590. Experimental study on the mass transport characteristics of dilute iodine vapor from air to caustic soda solution in a packed column using different packing materials. Krishnan U., Mandal D. *Chemical Engineering Communications*.

591. Experimentation, modeling and optimisation studies of an integrated-packed bed reactor (PBR) for the decomposition of sulphuric acid. Sujeesh S., Shriniwas Rao A., Mukhopadhyay S. *International Journal of Hydrogen Energy*. Vol. 48(53), pg. 20176-20192.

592. Experiments and CFD modelling of bubble formation at a lateral hole in a top-submerged nozzle. Sen N., Sarkar S., Singh K.K. *Chemical Engineering Research and Design*. Vol. 200 pg. 134-145.

593. Exploratory analysis of 64CuCl2 PET-CT imaging in carcinoma prostate and its comparison with 68Ga-PSMA-11 and 18F-FDG PET-CT. Nazar A.K., Kalshetty A., Chakravarty R., et al. *Nuclear Medicine Communications*. Vol. 44(10), pg. 910-923.

594. Exploring effects of strain on newly synthesised two-dimensional polyaramid for hydrogen storage using DFT. Nair H.T., Jha P.K., Chakraborty B. *Surfaces and Interfaces*. Vol. 42, ArtNo. 103444.

595. Exploring the crystal structure and properties of ytterbium orthoantimonate under high pressure. Garg A.B., Lopez-Moreno S., Botella-Vives P., et al. *Dalton Transactions*. Vol. 52(40), pg. 14517-14526.

596. Exploring the effects of organic loading rate and domestic wastewater treatment by algal-bacterial granules under natural daylight conditions. Vincent F., Rao T.S., Kumar R., et al. *Water Environment Research*. Vol. 95(1), ArtNo. e10831.

597. Exploring the hygroscopicity and chemical composition evolution in organic-inorganic aerosols: A study on internally mixed malonic acid-metal (Na+, Ca2+, Mg2+) nitrates. Saha S., Mathi P. *Chemosphere*. Vol. 336, ArtNo. 139260.

598. Exploring the influence of lanthanides on the structure and thermodynamic stability of SrLnTh(PO4)3 (Ln = La, Nd, Sm, Eu, and Gd). Rawat D., Vats B.G. *Journal of Thermal Analysis and Calorimetry*. Vol. 148(21), pg. 12071-12081.

599. Exploring the perioperative infection control practices & incidence of surgical site infections in rural India. Nayan A., Sarang B., Khajanchi M., et al. *Antimicrobial Resistance and Infection Control*. Vol. 12(1), ArtNo. 65.

600. Expression of radish defensin (RsAFP2) gene in chickpea (Cicer arietinum L.) confers resistance to Fusarium wilt disease. Sadhu S.K., Jogam P., Gande K., et al. *Molecular Biology Reports*. Vol. 50(1), pg. 11-18.

601. Extent of glaucomatous damage on the first presentation. Bhedasgaonkar S., Nadkarni S.U. *Oman Journal of Ophthalmology*. Vol. 16(2).

602. Extraction of Group Velocity Dispersion Curves of Surface Waves Using Continuous Wavelet Transform. Gupta P., Mukhopadhyay S. *IEEE Geoscience and Remote Sensing Letters*. Vol. 20, ArtNo. 7503605.

603. Extraction of Np(IV/VI) from nitric acid medium using three different tripodal diglycolamide ligands in ionic liquid: Batch extraction, spectroscopic and electrochemical investigations. Gujar R.B., Verma P.K., Mahanty B., et al. *Journal of Molecular Liquids*. Vol. 369, ArtNo. 120922.

604. Extreme phonon anharmonicity underpins superionic diffusion and ultralow thermal conductivity in argyrodite Ag8SnSe6. Ren Q., Gupta M.K., Jin M., et al. *Nature Materials*. Vol. 22(8), pg. 999-1006.

605. Exudation of microplastics from commonly used face masks in COVID-19 pandemic. Bhangare R.C., Tiwari M., Ajmal P.Y., et al. *Environmental Science and Pollution Research*. Vol. 30(12), pg. 35258-35268.

606. Fabrication of RGO based bimetal oxides ternary composite for deterioration of handloom dye and pathogens from polluted water. Satya Sree G., Ranjitha K.V.B., Jagan Mohan Reddy B., et al. *Inorganic Chemistry Communications*. Vol. 155, ArtNo. 111054.

607. Fabrication of solution processable perovskite solar cells under high humid conditions via optimization of TiO2compact layer. Bhagat N., Saxena V., Singh A., et al. *International Journal of Modern Physics B*. Vol., ArtNo. 2450250.

608. Fabrication, characterization, and mechanical properties and wear characteristics of graphite nanoplatelets incorporated nanotwinned Cu composites. Shrivastava P., Alam S.N., Ghosh A., et al. *Diamond and Related Materials*. Vol. 140, ArtNo. 110530.

609. Fabry-Perot Interferometric Pressure Sensor With Thermally Stretched Ridged Metal Diaphragm for 0-1000-mbar Range. Ghildiyal S., Ranjan P., Mishra S. *IEEE Sensors Journal*. Vol. 23(9), pg. 9246-9253.

610. Facile and Scalable Development of High-Performance Carbon-Free Tin-Based Anodes for Sodium-Ion Batteries. Gandharapu P., Das A., Tripathi R., et al. *ACS Applied Materials and Interfaces*. Vol. 15(31), pg. 37504-37516.

611. Facile Hydrogenolysis of Sugars to 1,2-Glycols by Ru@PPh3/OPPh3 Confined Large-Pore Mesoporous Silica. Modak A., Gill D., Sharma K., et al. *Journal of Physical Chemistry Letters*. Vol. 14(48), pg. 10832-10846.

612. Facile in-situ grown spinel MnCo2O4/MWCNT and MnCo2O4/Ti3C2 MXene composites for high-performance asymmetric supercapacitor with theoretical insight. Pathak M., Mane P., Chakraborty B., et al. *Journal of Energy Storage*. Vol. 66, ArtNo. 107475.

613. Facile Synthesis of Graphitic Fungal Carbon Dots for Sensing of Food Adulterants and “Bio-Imaging” of Human Kidney Cell Line. Kumari P., Pratap R., Gautam V.S., et al. *ChemistrySelect*. Vol. 8(39), ArtNo. e202302437.

614. False-Positive 68Ga-DOTATATE PET/CT Findings in Hereditary Hypophosphatemia-Osteomalacia Mimicking Culprit Lesions of Tumor-Induced Osteomalacia. Parghane R.V., Basu S. *Journal of Nuclear Medicine Technology*. Vol. 51(1), pg. 73-74.

615. Fast and accurate determination of the curvature-corrected field emission current. Biswas D., Ramachandran R. *Journal of Applied Physics*. Vol. 133(9), ArtNo. 94304.

616. Fast ion conduction and stable [Na-Si-P] glass-ceramic solid electrolyte mixed with hafnium and scandium ions: Application to Na-ion full cell. Krishna Katta V., Kumar Katari N., Dutta D.P., et al. *Journal of Electroanalytical Chemistry*. Vol. 937, ArtNo. 117392.

617. Fate of 1,3-dioxolane in the troposphere: kinetics, mechanism with theoretical support, and atmospheric implications. Virmani A., Walavalkar M.P., Sharma A., et al. *Journal of Atmospheric Chemistry*. Vol. 80(3), pg. 173-189.

618. Fatigue experiments and life predictions of notched C-Mn steel tubes. Kumar Jena S., Gupta S.K., Arora P., et al. *International Journal of Fatigue*. Vol. 169, ArtNo. 107502.

619. Fe(TCNQ)2 nanorod arrays: an efficient electrocatalyst for electrochemical ammonia synthesis via the nitrate reduction reaction. Mukherjee N., Adalder A., Barman N., et al. *Journal of Materials Chemistry A*. Vol. 12(6), pg. 3352-3361.

620. Fe@g-C3N4: an effective photocatalyst for Baeyer-Villiger oxidation under visible light condition. Maru B.A., Bhatt G.J., Lad U., et al. *New Journal of Chemistry*. Vol. 47(20), pg. 9797-9805.

621. Feasibility Study of Uranium Mill Tailings as Construction Material by Making Bricks and Assessment of Its Radiological Significance. Rana B.K., Molla S., Kumar R., et al. *Mapan - Journal of Metrology Society of India*.

622. Fenton reaction by H2O2 produced on a magnetically recyclable Ag/CuWO4/NiFe2O4 photocatalyst. Kumar U., Shrivastava A., De A.K., et al. *Catalysis Science and Technology*. Vol. 13(8), pg. 2432-2446.

623. Ferrimagnetic (α-Mn3O4/MnO)@rGO nanocomposite as potential adsorbent for organic pollutant dye. Gangwar A., Shaw S.K., Sharma A., et al. *Applied Surface Science*. Vol. 612, ArtNo. 155778.

624. Fibril ZnO as an Electron Transporting Layer for Enhancing the Photovoltaic Performance of Inverted Polymer Solar Cells Based on Nonfullerene Acceptors. Putta V., Gupta D., Sridevi C., et al. *ACS Applied Electronic Materials*. Vol. 5(12), pg. 6746-6756.

625. Fibroblast activation protein (FAP)-targeted radionuclide therapy: which ligand is the best? Chakravarty R., Song W., Chakraborty S., et al. *European Journal of Nuclear Medicine and Molecular Imaging*. Vol. 50(10), pg. 2935-2939.

626. Field- and polarization-dependent quantum spin dynamics in the honeycomb magnet Na2Co2TeO6: Magnetic excitations and continuum. Pilch P., Peedu L., Bera A.K., et al. *Physical Review B*. Vol. 108(14), ArtNo. L140406.

627. Field electron emission performance of Janus MoSSe and MoSSe-MWCNTs composite: Corroboration by Hall measurement and DFT simulation. Mistari C.D., Mane P., Koinkar P., et al. *Journal of Alloys and Compounds*. Vol. 965, ArtNo. 171356.

628. Field Evaluation of an Encapsulated 226Ra–222Rn Source. Sethy N.K., Singh S., Jha V.N., et al. *Mapan - Journal of Metrology Society of India*.

629. Field-induced phase transitions and anisotropic magnetic properties of the Kitaev-Heisenberg compound Na2Co2Te O6. Bera A.K., Yusuf S.M., Orlandi F., et al. *Physical Review B*. Vol. 108(21), ArtNo. 214419.

630. Fine mesh pin-by-pin analysis of IPWR equilibrium core. Khan S.A., Kannan U. *Nuclear and Particle Physics Proceedings*. Vol. 341 pg. 6-11.

631. Fine-Tuning of the Pore Aperture and Framework Flexibility of Mixed-Metal (Zn/Co) Zeolitic Imidazolate Framework-8: An In Situ Positron Annihilation Lifetime Spectroscopy Study under CO2 Gas Pressure. Mor J., Nelliyil R.B., Sharma S.K. *Langmuir*. Vol. 39(29), pg. 10056-10065.

632. First exploratory survey of poloidal magnetic flux emission from a dense plasma focus. Upadhyay M., Choudhary M., Mishra M., et al. *Physics of Plasmas*. Vol. 30(8), ArtNo. 82502.

633. First measurement of the forward rapidity gap distribution in Formula Presented collisions at Formula Presented. Tumasyan A., Adam W., Ambrogi F., et al. *Physical Review D*. Vol. 108(9), ArtNo. 92004.

634. First principles study on yttrium decorated BeN4 monolayer for reversible hydrogen storage. Sanyal G., Nair H.T., Jha P.K., et al. *Journal of Energy Storage*. Vol. 68, ArtNo. 107892.

635. First-principles property assessment of hybrid formate perovskites. Popoola A., Ghosh P.S., Kingsland M., et al. *Journal of Chemical Physics*. Vol. 159(7), ArtNo. 74702.

636. Flow synthesis of 1-ethyl-3-methylimidazolium ethyl sulfate in a PTFE micro-capillary: an experimental and numerical study. Sen N., Singh K.K., Mukhopadhyay S., et al. *Microfluidics and Nanofluidics*. Vol. 27(12), ArtNo. 82.

637. Flow synthesis of intrinsically radiolabeled and renal-clearable ultrasmall [198Au]Au nanoparticles in a PTFE microchannel. Chakravarty R., Sen N., Ghosh S., et al. *Chemical Engineering Journal Advances*. Vol. 14, ArtNo. 100456.

638. Fluidization-based chemical vapour deposition for alumina coating on tubular carbon steel substrates—Modelling and validation. Dabhade P.A., Mandal D., Satre S.R., et al. *Canadian Journal of Chemical Engineering*. Vol. 101(2), pg. 845-869.

639. Fluorescence based studies on the interaction and characterization of surface-active ionic liquids with polarity sensitive intramolecular charge transfer probe. Ray D., Chamlagai D., Kumar S., et al. *Chemical Physics Impact*. Vol. 7, ArtNo. 100368.

640. Fluorescence correlation spectroscopy measurements on amyloid fibril reveal at least two binding modes for fluorescent sensors. Sarkar A., Namboodiri V., Kumbhakar M. *Chemical Physics Impact*. Vol. 7, ArtNo. 100369.

641. FOIL ACTIVATION TECHNIQUE-A TOOL FOR THE EVALUATION OF PHOTO-NEUTRON DOSE IN RADIOTHERAPY. Sathian D., Bakshi A.K., Kannan U., et al. *Radiation protection dosimetry*. Vol. 199(7), pg. 603-614.

642. Formation of B2-ordered FeRh alloy thin films on annealing of pure and nitrogen doped Fe/Rh multilayers. Negi P., Gupta M., Rawat R., et al. *Journal of Magnetism and Magnetic Materials*. Vol. 581, ArtNo. 170941.

643. Forming-free RRAM device based on HfO2 thin film for non-volatile memory application using E-beam evaporation method. Moirangthem B., Meitei P.N., Debnath A.K., et al. *Journal of Materials Science: Materials in Electronics*. Vol. 34(4), ArtNo. 306.

644. Fractal fatigue crack. Das A. *Philosophical Magazine*. Vol. 103(11), pg. 1048-1070.

645. Fracture complexions of a nanocrystalline microstructure. Das A. *Applied Physics A: Materials Science and Processing*. Vol. 129(9), ArtNo. 667.

646. Fracture Studies on Through-Wall Cracked Straight Pipes and Elbows under Internal Pressure and Bending. Saravanan M., Gandhi P., Vishnuvardhan S., et al. *Experimental Techniques*. Vol. 47(5), pg. 941-957.

647. Free convection from a single and a pair of spheres in power-law fluids at very small Grashof numbers. Suri P., Verma A., Patel S.A., et al. *Journal of Non-Newtonian Fluid Mechanics*. Vol. 320, ArtNo. 105109.

648. Free radical induced degradation and computational studies of hydroxychloroquine in aqueous solution. Rath M.C., Keny S.J., Upadhyaya H.P., et al. *Radiation Physics and Chemistry*. Vol. 206, ArtNo. 110785.

649. Freezing of water–ethanol mixture in nano-confinement: A positron annihilation study. Dutta D., Muthulakshmi T., Maheshwari P. *Chemical Physics Letters*. Vol. 826, ArtNo. 140644.

650. FtsZ phosphorylation brings about growth arrest upon DNA damage in Deinococcus radiodurans. Chaudhary R., Mishra S., Maurya G.K., et al. *FASEB BioAdvances*. Vol. 5(1), pg. 27-42.

651. Functional characterization of 5'-regulatory region of flavonoid 3',5'-hydroxylase-1 gene of banana plants. Negi S., Tak H., Madari S., et al. *Protoplasma*. Vol. 260(2), pg. 391-403.

652. Functional hBN decorated Ni(OH)2 nanosheets synthesized for remarkable adsorption performance for the elimination of fluoride ions. Choudhary D., Singh A., Giri A., et al. *Dalton Transactions*. Vol. 52(37), pg. 13199-13215.

653. Functional inhibition of RECQL5 helicase elicits non-homologous end joining response and sensitivity of breast cancers to PARP inhibitor. Philip K.T., Dutta K., Chakraborty S., et al. *International Journal of Biochemistry and Cell Biology*. Vol. 161, ArtNo. 106443.

654. Functional nanostructures in analytical chemistry: new insights into the optical and electrochemical sensing of animal hormones in food, environmental and biological samples. Raval J.B., Mehta V.N., Jha S., et al. *Sensors and Diagnostics*. Vol. 2(4), pg. 815-836.

655. Functionalized Carbon Nanotubes Encapsulated Alginate Beads for the Removal of Mercury Ions: Design, Synthesis, Density Functional Theory Calculation, and Demonstration in a Batch and Fixed-Bed Process. Singha Deb A.K., Mohan M., Govalkar S., et al. *ACS Omega*. Vol. 8(35), pg. 32204-32220.

656. Functionalized Fluorescent Nanostructures Generated from Self-Assembly of a Cationic Tripeptide Direct Cell-Selective Chemotherapeutic Drug Delivery. Sivagnanam S., Das K., Pan I., et al. *ACS Applied Bio Materials*. Vol. 6(2), pg. 836-847.

657. Functionalized graphene-based material as a nanofiller for high-performance thin film composite seawater reverse osmosis membrane. Bhoje R.S., Ghosh A.K., Nemade P.R. *Separation Science and Technology (Philadelphia)*. Vol. 58(15-16), pg. 2790-2805.

658. Fusion of Conventional and Modern Approaches for Spall Protection of Indian Concrete Structures. Srivastava P.K., Dauji S., Bhargava K. *Journal of The Institution of Engineers (India): Series A*. Vol. 104(3), pg. 747-762.

659. Gallium-substituted X-type hexagonal ferrites Sr2Co2GaxFe28−xO46: effect of substitution and heating temperature on phase formation and magnetic and dielectric properties. Patel A.G., Pullar R.C., Meena S.S., et al. *Journal of Materials Chemistry C*. Vol. 11(43), pg. 15035-15052.

660. Gamma (γ)-radiation stress response of the cyanobacterium Anabaena sp. PCC7120: Regulatory role of LexA and photophysiological changes. Srivastava A., Kumar A., Biswas S., et al. *Plant Science*. Vol. 326, ArtNo. 111529.

661. Gamma Phase Stability in U–Mo Alloys. Rakesh R., Jain A., Sinha V.P., et al. *Transactions of the Indian Institute of Metals*. Vol. 76(7), pg. 1997-2007.

662. Gamma radiation processing for extending shelf-life and ensuring quality of minimally processed ready-to-eat onions. Khade H.D., Saxena S., Hajare S.N., et al. *Journal of Food Science and Technology*. Vol. 60(8), pg. 2265-2274.

663. Gamma Ray Pulsars and Opportunities for the MACE Telescope. Pathania A., Singh K.K., Yadav K.K. *Galaxies*. Vol. 11(4), ArtNo. 91.

664. Gamma-irradiation of inulin improves its biological functionality and feasibility as a functional ingredient in synbiotic food. Sudesh, Maurya D.K., Jamdar S.N. *Food Chemistry*. Vol. 408, ArtNo. 135217.

665. Gamma-ray assisted synthesis of silver nanoparticles to improve advanced oxidation process for continuous flow catalysis and environmental remediation. Jadhav A.P., Gade M.D., Bagekari Y.G., et al. *Journal of Materials Science: Materials in Electronics*. Vol. 34(26), ArtNo. 1811.

666. Gas barrier properties of polyurethane nanocomposites. Pandey S., Maiti P., Jana K.K., et al. *Journal of Applied Polymer Science*. Vol. 140(32), ArtNo. e54256.

667. Gate Opening Induced High Pore Volume Expansion in Flexible Zeolitic Imidazole Frameworks during CO2 Adsorption: A Direct Observation Using Positron Annihilation Spectroscopy. Mor J., Utpalla P., Mukherjee S., et al. *Journal of Physical Chemistry C*. Vol. 127(5), pg. 2160-2172.

668. Generation of map on natural environmental background absorbed dose rate in India. Mishra M.K., Jha S.K., Patra A.C., et al. *Journal of Environmental Radioactivity*. Vol. 262, ArtNo. 107146.

669. Generation of Photoinduced Phenalenyl-Based Radicals: Towards Designing Reductive C−C Coupling Catalysis. Datta P., Goswami T., Kandoth N., et al. *ChemPhotoChem*. Vol. 7(6), ArtNo. e202300033.

670. Generative Adversarial Network based method for generation of synthetic image parameters for TACTIC γ-ray telescope. Das M.P., Dhar V.K., Yadav K.K. *Astronomy and Computing*. Vol. 44, ArtNo. 100741.

671. Genetic mapping and transcriptome profiling of a chickpea (Cicer arietinum L.) mutant identifies a novel locus (CaEl) regulating organ size and early vigor. Misra G., Joshi-Saha A. *Plant Journal*. Vol. 116(5), pg. 1401-1420.

672. Genetics, genomics, and breeding of black gram [Vigna mungo (L.) Hepper]. Nair R.M., Chaudhari S., Devi N., et al. *Frontiers in Plant Science*. Vol. 14, ArtNo. 1273363.

673. Genome-wide analysis of bromodomain gene family in Arabidopsis and rice. Abiraami T.V., Sanyal R.P., Misra H.S., et al. *Frontiers in Plant Science*. Vol. 14, ArtNo. 1120012.

674. Genome-wide identification of BONZAI (BON) genes in Glycine max L. and their regulated expression patterns under saline environment. Joshi S., Sahoo S.A., Khare T., et al. *Current Plant Biology*. Vol. 33, ArtNo. 100273.

675. Genotype x environment interaction in hybrids and parents of Sesame (Sesamum indicum L.). Rathod S.T., Gite V.K., Prakash J., et al. *Indian Journal of Genetics and Plant Breeding*. Vol. 83(4), pg. 605-608.

676. Genotype-by-environmental interaction effects on earliness, semi-dwarfism, and yield of rice (Oryza sativa L.) mutants in Tamil Nadu, India. Pillai M.A., Rajamadhan R., Murugan E., et al. *Crop Science*. Vol. 63(6), pg. 3402-3415.

677. Geodesics in geometrothermodynamics (GTD) type II geometry of 4D asymptotically anti-de-Sitter black holes. Gogoi N.J., Mahanta G.K., Phukon P. *European Physical Journal Plus*. Vol. 138(4), ArtNo. 345.

678. Geographic and socioeconomic inequities in cesarean delivery rates at the district level in Madhya Pradesh, India: A secondary analysis of the national family health survey-5. Dutta R., Tuli S., Shukla M., et al. *Global Health Action*. Vol. 16(1), ArtNo. 2203544.

679. Glucosinolates breakdown and enhanced nitrile formation in gamma irradiated minimally processed cauliflower (Brassica oleracia). Vaishnav J., Srivastava A.K., Mishra B.B., et al. *Radiation Physics and Chemistry*. Vol. 205, ArtNo. 110672.

680. Glutamate receptor like channels: Emerging players in calcium mediated signaling in plants. Ahmed I., Kumar A., Bheri M., et al. *International Journal of Biological Macromolecules*. Vol. 234, ArtNo. 123522.

681. Glutathione-Capped Hollow Silver Nanoparticles: Optimization of Surface Plasmon Resonance, Photothermal Effect, and In Vitro and In Vivo Biocompatibility. Bhavsar C., Joshi R., Fernandes T., et al. *ACS Applied Nano Materials*. Vol. 6(11), pg. 9276-9289.

682. G-quadruplex binding affinity variation on molecular encapsulation of ligands by porphyrin-tethered cyclodextrin. Alexander A., Pillai A.S., Varalakshmi G.S., et al. *Journal of Molecular Liquids*. Vol. 373, ArtNo. 121233.

683. Granular stability, nitrogen and phosphorus removal pathways of aerobic granular sludge treating real municipal wastewater at different temperatures. Nancharaiah Y.V., Sarvajith M. *Journal of Environmental Chemical Engineering*. Vol. 11(5), ArtNo. 110769.

684. Green Chemistry to Valorize Seafood Side Streams: An Ecofriendly Roadmap toward Sustainability. Venugopal V., Sasidharan A., Rustad T. *Journal of Agricultural and Food Chemistry*. Vol. 71(46), pg. 17494-17509.

685. Green emitting plastic scintillator with neutron/gamma pulse shape discrimination for fast neutron detection. Alex L., Paulraj R., Sonu, et al. *Journal of Materials Science: Materials in Electronics*. Vol. 34(7), ArtNo. 576.

686. Gross Alpha Activity Measurements: Investigating the Crucial Role of Self-Absorption Correction Factors. Verma G.P., Abhigyan, Prakash R., et al. *Mapan - Journal of Metrology Society of India*.

687. Growth, structural, optical, and thermal behavior of bibenzyl organic single crystal for scintillator applications. Ramprasath R.H., Kajamuhideen M.S., Tiwari B., et al. *Journal of Materials Science: Materials in Electronics*. Vol. 34(7), ArtNo. 620.

688. Guest Binding with Sulfated Cyclodextrins: Does the Size of Cavity Matter?. Singh G., Pandey S.P., Singh P.K. *ChemPhysChem*. Vol. 24(4), ArtNo. e202200421.

689. Gum tragacanth-mediated synthesis of metal nanoparticles, characterization, and their applications as a bactericide, catalyst, antioxidant, and peroxidase mimic. Kora A.J. *Green Processing and Synthesis*. Vol. 12(1).

690. H4K16ac activates the transcription of transposable elements and contributes to their cis-regulatory function. Pal D., Patel M., Boulet F., et al. *Nature Structural and Molecular Biology*. Vol. 30(7), pg. 935-947.

691. Harnessing CRISRP-Cas9 as an anti-mycobacterial system. Sodani M., Misra C.S., Rath D., et al. *Microbiological Research*. Vol. 270, ArtNo. 127319.

692. Harnessing salt stress to drive the efficient and inexpensive bioproduction of a valuable thermotolerant biocatalyst (Mn-catalase) from cyanobacterial biomass. Chakravarty D., Tewari H., Ballal A. *Bioresource Technology Reports*. Vol. 23, ArtNo. 101535.

693. Harvesting Plasmonic Near-Infrared Photons by Hot Hole Transfer in Nonstoichiometric-Semiconductor Plasmonic Heterojunctions. Ghorai N., Sachdeva M., Kharbanda N., et al. *ACS Photonics*. Vol. 10(3), pg. 733-742.

694. Health Physics in Applications of Radiation Technology. Seshadri M. *Japanese Journal of Health Physics*. Vol. 57(4), pg. 159-160.

695. Heat transfer characteristics and design aspects of thermolysis reactor in copper-chlorine thermochemical water splitting cycle. Thomas D., Kumar G., Ghuge N.S., et al. *International Journal of Hydrogen Energy*. Vol. 48(88), pg. 34286-34298.

696. Hellmann-Feynman theorem and internal pressure for atoms, molecules and plasmas under pressure. Mukherjee N., Patra C.N., Roy A.K. *Journal of Physics B: Atomic, Molecular and Optical Physics*. Vol. 56(6), ArtNo. 65001.

697. Hierarchical mesoporous spherical Zn(4-hzba) MOF for efficient adsorption of Strontium and Caesium ions from aqueous solution. Suresh K., Jagasia P., Babu M.S.S. *Surfaces and Interfaces*. Vol. 39, ArtNo. 102944.

698. Hierarchical Polyoxometallate Confined in Woven Thin Films for Single-Cluster Catalysis: Simplified Electrodes for Far-Fetched O2Evolution from Seawater. Kirti, Dobaria P., Maurya A., et al. *ACS Catalysis*. Vol. 13(7), pg. 4587-4596.

699. High capacity hydrogen storage on zirconium decorated γ-graphyne: A systematic first-principles study. Singh M., Shukla A., Chakraborty B. *International Journal of Hydrogen Energy*. Vol. 48(96), pg. 37834-37846.

700. High concentration quenching, improved PLQY and high color purity of novel Gd2TiO5:Eu3+ triggered by complete solubility of dopant. Jafar M., Balhara A., Sawant P., et al. *Optical Materials*. Vol. 142, ArtNo. 114059.

701. High power balanced TEM horn antenna for ultra wide band radiator. Singh S.K., Chandra R., Mitra S., et al. *Microwave and Optical Technology Letters*. Vol. 65(6), pg. 1686-1694.

702. High pressure studies of MgCu2O3 compound. Chandra S., Shukla B., Srihari V., et al. *Journal of Solid State Chemistry*. Vol. 327, ArtNo. 124249.

703. High spin polarization in the disordered quaternary Heusler alloy FeMnVGa. Gupta S., Chakraborty S., Bhasin V., et al. *Physical Review B*. Vol. 108(4), ArtNo. 45137.

704. High temperature CO2 capture in lithium orthosilicate packed fluidized bed: Gamma ray densitometry based numerical model and its experimental validation. Dabhade P.A., Mandal D., Ghuge N.S., et al. *Journal of the Taiwan Institute of Chemical Engineers*. Vol. 151, ArtNo. 105106.

705. High temperature structure and vibrational properties of GdVO4. Anitha M., Rao K.S., Syed R., et al. *Materials Chemistry and Physics*. Vol. 295, ArtNo. 127120.

706. High temperature thermo-chemical properties evolution of NaF-NiF2 system. Mukherjee S., Samui P., Das P. *Materials Chemistry and Physics*. Vol. 305, ArtNo. 127926.

707. High Thermally Stable Polyurethane Nanocomposite Foam Containing Polydimethyl Siloxane and Carbonaceous Nanofillers. Yadav G., Gupta S.K., Singh K., et al. *Silicon*. Vol. 15(6), pg. 2869-2878.

708. High thermoelectric performance of layered LaAgX O (X=Se,Te) from electrical and thermal transport calculations. Natarajan A.R., Ponvijayakanthan L., Gupta M.K., et al. *Physical Review Materials*. Vol. 7(2), ArtNo. 25405.

709. High Valent Mercury Fluoride Ions. Jayasekharan T. *ChemPhysChem*. Vol. 24(13), ArtNo. e202300036.

710. High-capacity hydrogen storage in zirconium decorated psi-graphene: acumen from density functional theory and molecular dynamics simulations. Nair H.T., Jha P.K., Chakraborty B. *International Journal of Hydrogen Energy*. Vol. 48(96), pg. 37860-37871.

711. High-homogeneity double-focusing stigmatic analyzer magnet for electromagnetic isotope separator. Teotia V., Mishra E., Malhotra S. *Journal of Magnetism and Magnetic Materials*. Vol. 580, ArtNo. 170908.

712. Highly Cross-Linked butene grafted poly (Vinyl Alcohol)–co-Vinyl pyridine based anion exchange membrane for improved acid recovery and desalination efficiency. Rathod N.H., Upadhyay P., Pal S., et al. *Separation and Purification Technology*. Vol. 308, ArtNo. 122895.

713. Highly efficient and selective 99TcO4– uptake from reprocessing low-level liquid waste using a zirconium-based metal−organic framework. Patra K., Mittal V.K., Valsala T.P., et al. *Separation Science and Technology (Philadelphia)*. Vol. 58(15-16), pg. 2837-2845.

714. Highly Efficient Extraction Chromatography Resin Containing Hexa-n-Octyl Nitrilotriacetamide (HONTA) for Selective Recovery of Plutonium from Acidic Feeds. Gujar R.B., Ansari S.A., Mohapatra P.K., et al. *Industrial and Engineering Chemistry Research*. Vol. 62(14), pg. 5954-5961.

715. Highly Efficient Pertraction of Tetravalent Neptunium Ions Across a Flat Sheet Supported Liquid Membrane Containing Two Different Aza-Crown Ether-Based Multiple Diglycolamide Ligands. Mahanty B., Mohapatra P.K., Egberink R.J.M., et al. *Solvent Extraction and Ion Exchange*. Vol. 41(2), pg. 143-159.

716. Highly efficient separation of Am(III) and Pu(IV) from lean feeds and soil using an extraction chromatographic resin containing a diglycolamide in an ionic liquid. Yadav A.G., Mohapatra P.K., Valsala T.P., et al. *Journal of Chromatography A*. Vol. 1707, ArtNo. 464299.

717. Highly efficient separation of Nb from Ta using a unique solvent system containing tri-n-octyl phosphine oxide in an ionic liquid. Sengupta A., Mohapatra P.K. *Journal of Molecular Liquids*. Vol. 390, ArtNo. 123033.

718. Highly Promising Method for the Decontamination of Europium from Americium Using an Extraction Chromatography Resin Containing a Tripodal Diglycolamide and SO3Ph-BTP as Eluent. Gujar R.B., Ansari S.A., Mohapatra P.K., et al. *Industrial and Engineering Chemistry Research*. Vol. 62(37), pg. 15157-15165.

719. Highly selective carrier mediated transport of plutonium(IV) across a supported liquid membrane using two substituted tripodal amides. Karak A., Mahanty B., Mohapatra P.K., et al. *Separation Science and Technology (Philadelphia)*. Vol. 58(2), pg. 382-393.

720. Highly selective H2S sensor realized via the facile synthesis of N-doped ZnO nanocrystalline films. Girija K.G., Kumar R., Debnath A.K. *Applied Physics A: Materials Science and Processing*. Vol. 129(5), ArtNo. 392.

721. Highly selective separation of plutonium using a mono-amide-based supported liquid membrane. Paul S., Vats B.G., Goswami P., et al. *Separation Science and Technology (Philadelphia)*. Vol. 58(15-16), pg. 2748-2758.

722. Highly Stable Electrochemical Supercapacitor Performance of Self-Assembled Ferromagnetic Q-Carbon. Karmakar S., Taqy S., Droopad R., et al. *ACS Applied Materials and Interfaces*. Vol. 15(6), pg. 8305-8318.

723. Highly water permeable 'reverse osmosis' polyamide membrane of folded nanoscale film morphology. Thummar U.G., Jayalakshmi J., Saxena M., et al. *Journal of Water Process Engineering*. Vol. 55, ArtNo. 104110.

724. High-pressure structural phase transition on Bi14MoO24. Botella P., Santamaria-Perez D., Otero-de-la-Roza A., et al. *Journal of Physics and Chemistry of Solids*. Vol. 182, ArtNo. 111598.

725. High-pressure structural transition and magnetic phase diagram of CuB2 O4. Sahoo S., Malavi P., Karmakar S. *Physical Review B*. Vol. 107(9), ArtNo. 94411.

726. High-Pressure Vibrational and Structural Studies of the Chemically Engineered Ferroelectric Phase of Sodium Niobate. Mishra S.K., Garg N., Gohil S., et al. *Crystals*. Vol. 13(8), ArtNo. 1181.

727. High-Pressure X-ray Diffraction Study of Orthorhombic Ca2Zr5Ti2O16. Garcia-Sanchez T., Diaz-Anichtchenko D., Muñoz A., et al. *Journal of Physical Chemistry C*. Vol. 127(4), pg. 2069-2077.

728. High-Throughput Screening of the CoRE-MOF-2019 Database for CO2 Capture from Wet Flue Gas: A Multi-Scale Modeling Strategy. Kancharlapalli S., Snurr R.Q. *ACS Applied Materials and Interfaces*. Vol. 15(23), pg. 28084-28092.

729. How is UVR8 relevant in plants? New evidence. Mishra V., Singh S., Dubey N.K., et al. *Plant Growth Regulation*. Vol. 100(1), pg. 1-5.

730. HPLC separation of REE, U and Pu from uranium silicide fuel. Telmore V.M., Kumar P., Jaison P.G. *Separation Science and Technology (Philadelphia)*. Vol. 58(15-16), pg. 2780-2789.

731. Human reliability analysis studies from simulator experiments using Bayesian inference. Garg V., Vinod G., Prasad M., et al. *Reliability Engineering and System Safety*. Vol. 229, ArtNo. 108846.

732. Hybrid DFM – Petri net approach for dynamic reliability analysis of smart transmitters. Garg V., Vinod G., Prasad M., et al. *Quality and Reliability Engineering International*. Vol. 39(6), pg. 2438-2453.

733. Hydrazones tethered disubstituted 1,2,3-triazoles: Design, synthesis, antitubercular and antimicrobial evaluation. Yadav A., Kaushik C.P., Kumar M. *Journal of Molecular Structure*. Vol. 1283, ArtNo. 135163.

734. Hydrochemical evolution of groundwater in northwestern part of the Indo-Gangetic Basin, India: A geochemical and isotopic approach. Prakash Rai S., Venyo Akpataku K., Noble J., et al. *Geoscience Frontiers*. Vol. 14(6), ArtNo. 101676.

735. Hydrogen spillover enhances alkaline hydrogen electrocatalysis on interface-rich metallic Pt-supported MoO3. Samanta R., Manna B.K., Trivedi R., et al. *Chemical Science*. Vol. 15(1), pg. 364-378.

736. Hydrogen-bonded linear chain assemblies of palladium(ii)-selenoether complexes: solid state aggregates as templates for nano-structural Pd17Se15 leading to efficient electrocatalytic activity. Kumbhare L.B., Udayan A.P.M., Singla H., et al. *Dalton Transactions*. Vol. 52(48), pg. 18302-18314.

737. Hydrogen-bonding and vibrational coupling of water in a hydrophobic hydration shell: Significance of alkyl chain configuration and charge on the hydrophobe. Bandyopadhyay A., Alam Mondal J. *Journal of Molecular Liquids*. Vol. 390, ArtNo. 122987.

738. Hydrogeochemical characterization of groundwater in the shallow aquifer system of Middle Ganga Basin, India. Patel A., Rai S.P., Akpataku K.V., et al. *Groundwater for Sustainable Development*. Vol. 21, ArtNo. 100934.

739. Hydrophobic MXene with enhanced electrical conductivity. Patra S., Kiran N.U., Mane P., et al. *Surfaces and Interfaces*. Vol. 39, ArtNo. 102969.

740. Hyperfine structure measurements on a forbidden transition of Bi I using fourier transform spectroscopy. Ashok C., Bhatt H., Babu S.H., et al. *Journal of Quantitative Spectroscopy and Radiative Transfer*. Vol. 309, ArtNo. 108688.

741. Hypoxia induces dichotomous and reversible attenuation of T cell responses through reactive oxygen species-dependent phenotype redistribution and delay in lymphoblast proliferation. Maurya D.K., Sharma D., Sandur S.K. *Free Radical Research*. Vol. 57(1), pg. 1-13.

742. Identification and characterization of aurintricarboxylic acid as a potential inhibitor of SARS-CoV-2 PLpro. Arya R., Prashar V., Kumar M. *International Journal of Biological Macromolecules*. Vol. 230, ArtNo. 123347.

743. Identifying Size-Segregated Particulate Matter (PM2.5, PM10 and SPM) Sources in an Industrial Town of India. Yadav A.K., Sahoo S.K., Kumar A.V., et al. Aerosol Science and Engineering. Vol. 7(4), pg. 455-473.

744. Imaging of bacterial infection: Harnessing positron emission tomography and Cherenkov luminescence imaging with UBI-derived octapeptide. Mitra J.B., Mukherjee A., Kumar A., et al. Drug Development Research. Vol. 84(7), pg. 1513-1521.

745. Imaging Recommendations for Diagnosis, Staging, and Management of Carcinoma of Unknown Origin (Lymph Node, Pulmonary, Liver, Skeletal, and Brain) with Emphasis on the Current Position of PET-CT in Carcinoma of Unknown Origin (CUP). Loharkar S., Basu S. Indian Journal of Medical and Paediatric Oncology. Vol. 44(2), pg. 194-206.

746. Imaging Recommendations for Theranostic PET-CT in Oncology. Parghane R.V., Mahajan A., Chakrabarty N., et al. *Indian Journal of Medical and Paediatric Oncology*. Vol. 44(3), pg. 314-321.

747. Impact of gamma irradiation and packaging on the storage quality of little millet (Panicum sumatrense) flour. Shobha D., Vasudevan S.N., Badigannavar A. *Cereal Research Communications*.

748. Impact of magnetic spinel ferrite content on the structure, morphology, optical, and magneto-dielectric properties of BaTiO3materials. Slimani Y., Meena S.S., Shirsath S.E., et al. *Zeitschrift fur Physikalische Chemie*. Vol. 237(11), pg. 1753-1774.

749. Impact of P3/P2 mixed phase on the structural and electrochemical performance of Na0.75Mn0.75Al0.25O2 cathode. Vasavan H.N., Badole M., Saxena S., et al. *Journal of Energy Storage*. Vol. 74, ArtNo. 109428.

750. Imparting Reprocessability, Quadruple Shape Memory, Self-Healing, and Vibration Damping Characteristics to a Thermosetting Poly(urethane-urea). Billa S., Vislavath P., Bahadur J., et al. *ACS Applied Polymer Materials*. Vol. 5(4), pg. 3079-3095.

751. Impedance stabilization by trigger modulation in copper vapor laser. Singh D.K., Dikshit B., Vijayan R., et al. *Optical and Quantum Electronics*. Vol. 55(1), ArtNo. 81.

752. Implication of nuclear analytical techniques for the assessment of coal quality in terms of ash content. Samanta S.K., Sharma V., Sengupta A., et al. *International Journal of Coal Preparation and Utilization*. Vol. 43(8), pg. 1387-1401.

753. Improved performance of LiFePO4F cathodes via V/Na-ion co-doping for application in lithium-ion batteries. Shinde P.V., Dutta D.P. *Ionics*. Vol. 29(12), pg. 5017-5027.

754. Improved Power Factor in Highly Textured n-Type Ag2Se Flexible Films. Sarkar P., Samanta S., Das D., et al. *ACS Applied Electronic Materials*. Vol. 5(3), pg. 1650-1659.

755. Improved recovery of cellulose nanoparticles from printed wastepaper and its reinforcement in guar gum films. Palanichamy P., Venkatachalam S., Gupta S. *Biomass Conversion and Biorefinery*. Vol. 13(15), pg. 14113-14125.

756. Improvement in Near Surface NWP Model Output using Kalman Filtering Technique: A Case Study for Trombay Site. Shrivastava R., Iyer I.S., Oza R.B. *Annals of Geophysics*. Vol. 66(45385).

757. Improvement of Electron Gun Breakdown Performance Through Surface Flashover and Discharge Studies. Goel V., Roy A., Maiti N. *IEEE Transactions on Electron Devices*. Vol. 70(7), pg. 3833-3841.

758. Improvement of high current performance of Li ion batteries with TiO2 thin film anodes by transition metal doping. Bhasin V., Halankar K.K., Biswas A., et al. *Journal of Alloys and Compounds*. Vol. 942, ArtNo. 169118.

759. Improving constraints on gluon spin-momentum correlations in transversely polarized protons via midrapidity open-heavy-flavor electrons in p ↑+p collisions at s =200 GeV. Abdulameer N.J., Acharya U., Aidala C., et al. *Physical Review D*. Vol. 107(5), ArtNo. 52012.

760. Improving perovskite/P3HT interface without an interlayer: Impact of perovskite surface topography on photovoltaic performance of P3HT-based perovskite solar cells. Koiry S.P., Jha P., Sridevi C., et al. *Materials Today Communications*. Vol. 36, ArtNo. 106418.

761. In house synthesized novel distyryl-BODIPY dye and polymer assembly as deep-red emitting probe for protamine detection. Gorai S., Mula S., Jonnalgadda P.N., et al. *Talanta*. Vol. 265, ArtNo. 124915.

762. In situ chamber for studying battery failure using high-speed synchrotron radiography. Pfaff J., Fransson M., Broche L., et al. *Journal of Synchrotron Radiation*. Vol. 30 pg. 192-199.

763. In situ time-resolved Raman spectroscopy of nitromethane under static and dynamic compression. Chaurasia S., Mohan A., Mishra A.K., et al. *Journal of Applied Physics*. Vol. 134(8), ArtNo. 85901.

764. In View of “On-Site” Nuclear Forensics and Assay of Fissile Materials in Sealed Packages by High-Resolution γ-Ray Spectrometry. Kumar S., Patra S., Mhatre A., et al. *Analytical Chemistry*. Vol. 95(6), pg. 3247-3254.

765. In Vitro Investigation Unveiling New Insights into the Antimalarial Mechanism of Chloroquine: Role in Perturbing Nucleation Events during Heme to β-Hematin Transformation. Singh R., Singh R., Srihari V., et al. *ACS Infectious Diseases*. Vol. 9(8), pg. 1647-1657.

766. Incidence of needlestick injury among healthcare workers in western India. Naidu R.T., Toal P., Mishra S.C., et al. *The Indian journal of medical research*. Vol. 158(56), pg. 552-558.

767. Inclusion phenomenon of β-carboline alkaloids with sulfonatocalix[4]arene: Photophysical, cytotoxicity and theoretical study. Thorave R., Kalyani V., Shelar A., et al. *Journal of Molecular Liquids*. Vol. 392, ArtNo. 123450.

768. Independent isomeric yield ratios of fission products in the epi-cadmium neutron induced fission of 241Pu. Naik H., Singh R.J., Dange S.P., et al. *Radiochimica Acta*. Vol. 111(11), pg. 793-800.

769. India's Participation Toward Timescale from Ancient Time to the Current Date: Nimesha to Universal Coordinated Time (UTC). Thorat P.P., Agarwal R., Aswal D.K. *Mapan - Journal of Metrology Society of India*. Vol. 38(1), pg. 231-240.

770. Indian traditional rice variety "Gathuwan" suppresses T-cell-mediated immune responses via activation of ERK/Nrf2/HO-1 signalling pathway. Chauhan A., Checker R., Nair S., et al. *Food and Function*. Vol. 14(11), pg. 5232-5250.

771. Inducing Selenium Vacancy in Nickel Selenide/Iron Selenide by Hydrazine-Ultrasonic Treatment for Electrocatalytic Water Splitting Reaction. Senapati S., Bal R., Mohapatra M., et al. *Energy Technology*.

772. Induction of stable, room-temperature ferromagnetism in WO3 by doping with K, Li, and Na: Theoretical investigations. Chakraborty B., Shivade R.K., Vaidyanathan A. *Journal of Magnetism and Magnetic Materials*. Vol. 565, ArtNo. 170244.

773. Inference of grain boundary sliding and co-rotation of α/β phases during superplastic deformation of Zr-2.5%Nb at 700 °C through EBSD measurements. Reddy G.B., Sarkar A., Sunil S., et al. *Scripta Materialia*. Vol. 234, ArtNo. 115567.

774. Influence of amorphous intermediate domains on the performance of Na2O–Bi2O3–GeO2 glass–ceramic anode material system. Yerranuka S.K., Katta V.K., Gandi S.S., et al. *Applied Physics A: Materials Science and Processing*. Vol. 129(12), ArtNo. 825.

775. Influence of defect dynamics on the nanoindentation hardness in NiCoCrFePd high entropy alloy under high dose Xe+3 irradiation. Hussain A., Khan S.A., Sharma S.K., et al. *Materials Science and Engineering: A*. Vol. 863, ArtNo. 144523.

776. Influence of guide tubes on configuration and heat-up behaviour for PHWR specific suspended debris bed – An analytical assessment. Rajaganesh S., Majumdar P., Mukhopadhyay D. *Nuclear Engineering and Design*. Vol. 405, ArtNo. 112219.

777. Influence of ion irradiation on the surface electronic structure of epitaxial lanthanum nickelate films. Sharma V., Singh I., Sunidhi, et al. *Surfaces and Interfaces*. Vol. 38, ArtNo. 102776.

778. Influence of Mn2O3 on the physical properties of metallic glass network. Vinothkumar P., Dhavamurthy M., Mohapatra M., et al. *Pramana - Journal of Physics*. Vol. 97(3), ArtNo. 137.

779. Influence of Molecular Separation on Through-Space Intervalence Transient Charge Transfer in Metal–Organic Frameworks with Cofacially arranged Redox Pairs. Nath A., Kumar V., Shukla A., et al. *Angewandte Chemie - International Edition*. Vol. 62(31), ArtNo. e202308034.

780. Influence of substrate-induced strain on exchange bias effect in YSMO/LSMO heterostructures. Waman P.T., Bhatt H., Rao R., et al. *Bulletin of Materials Science*. Vol. 46(3), ArtNo. 116.

781. Influence of synthesis atmosphere on the solid solubility of uranium at B-site of Nd2Zr2O7 pyrochlore. Nandi C., Phatak R., Kesari S., et al. *Journal of Nuclear Materials*. Vol. 574, ArtNo. 154175.

782. Influence of temperature and organic acid on self-assembly behavior of pluronic F127. Basu M., Hassan P.A. *Journal of Molecular Liquids*. Vol. 378, ArtNo. 121630.

783. Influence of vacancy defects on 2D BeN4 monolayer for NH3 adsorption: a density functional theory investigation. Lakshmy S., Sanyal G., Kalarikkal N., et al. *Nanotechnology*. Vol. 34(43), ArtNo. 435504.

784. Influence of weld repair on the residual stresses induced in austenitic stainless steel weld joints. Das Banik S., Kumar S., Singh P.K., et al. *Production Engineering*. Vol. 17(1), pg. 81-94.

785. Initial core loading pattern optimization studies using estimation of distribution algorithm for VVER type cores. Thakur A., Srivastava A., Kumar V., et al. *Nuclear Engineering and Design*. Vol. 412, ArtNo. 112458.

786. Innovative method of radiotracer data analysis to identify leaky heat exchangers. Walinjkar P.B., Yelgaonkar V.N. *Nuclear and Particle Physics Proceedings*. Vol. 339-340 pg. 102-105.

787. Inorganic polyphosphate accumulation protects a marine, filamentous cyanobacterium, Anabaena torulosa against uranium toxicity. Chandwadkar P., Acharya C. *Journal of Environmental Radioactivity*. Vol. 263, ArtNo. 107185.

788. In-plane magnetic anisotropy and magnetization reversal in phase-separated (La0.5Pr0.5)0.625Ca0.375Mn O3 thin films. Singh S., Olamit J., Fitzsimmons M.R., et al. *Physical Review B*. Vol. 107(2), ArtNo. 24420.

789. Insight into the negative magnetization and anomalous exchange-bias in DyFe5Al7 through neutron depolarization and neutron diffraction studies. Deepak, Kumar A., Yusuf S.M., et al. *Journal of Physics Condensed Matter*. Vol. 35(6), ArtNo. 65802.

790. Insights into fracture behavior of Ni-based superalloy single crystals: An atomistic investigation. Chandra S., Alankar A., Samal M.K., et al. *Journal of Alloys and Compounds*. Vol. 952, ArtNo. 169938.

791. Insights into Plasmon-Induced Dimerization of Rhodanine-A Surface-Enhanced Raman Scattering Study. Kumar N., Maiti N., Thomas S. *Journal of Physical Chemistry A*. Vol. 127(20), pg. 4429-4439.

792. Insights into the CO2 Capture Characteristics within the Hierarchical Pores of Carbon Nanospheres Using Small-Angle Neutron Scattering. Maity A., Singh S., Mehta S., et al. *Langmuir*. Vol. 39(12), pg. 4382-4393.

793. Insights into the evolution of mutations in SARS-CoV-2 non-spike proteins. Arya R., Tripathi P., Nayak K., et al. *Microbial Pathogenesis*. Vol. 185, ArtNo. 106460.

794. Insights into the presence of multiple RecQ helicases in the ancient cyanobacterium, Nostoc sp. strain PCC7120: bioinformatics and expression analysis approach. Kumar A., Rajaram H. *Molecular Genetics and Genomics*. Vol. 298(1), pg. 37-47.

795. Insights of nanomaterials integrated analytical approaches for detection of plant hormones in agricultural and environmental samples. Raval J.B., Mehta V.N., Singhal R.K., et al. *Trends in Environmental Analytical Chemistry*. Vol. 39, ArtNo. e00205.

796. In-situ construction of hierarchical 2D MoS2/1D Te hybrid for supercapacitor applications. Radhakrishnan S., Mane P., Sree Raj K.A., et al. *Journal of Energy Storage*. Vol. 60, ArtNo. 106703.

797. In-situ study of rules of nanostructure evolution, severe plastic deformations, and friction under high pressure. Lin F., Levitas V.I., Pandey K.K., et al. *Materials Research Letters*. Vol. 11(9), pg. 757-763.

798. Instrumental neutron activation analysis by utilizing pneumatic carrier facility at Dhruva reactor for estimation of minor and trace elements in antidiabetic ayurvedic formulations. George R.S., Datta A., Gupta S., et al. *Journal of Radioanalytical and Nuclear Chemistry*. Vol. 332(10), pg. 4301-4309.

799. Insulator-to-metal-like transition in thin films of a biological metal-organic framework. Sindhu P., Ananthram K.S., Jain A., et al. *Nature Communications*. Vol. 14(1), ArtNo. 2857.

800. Integrated experimental and modeling approach for hot deformation behavior of Co–Cr–Fe–Ni–V high entropy alloy. Jain R., Rahul M.R., Chakraborty P., et al. *Journal of Materials Research and Technology*. Vol. 25 pg. 840-854.

801. Integrated Genomic Selection for Accelerating Breeding Programs of Climate-Smart Cereals. Sinha D., Maurya A.K., Abdi G., et al. *Genes*. Vol. 14(7), ArtNo. 1484.

802. Interaction between oxidised state of quercetin and bovine serum albumin in presence of surfactant aggregates with different charges. Vigneshwari R., Anjali S., Rajesh P., et al. *Journal of Biomolecular Structure and Dynamics*. Vol. 41(22), pg. 12521-12531.

803. Interaction of lanthanide and actinide with BaHfO3 perovskite: A case study with cerium and uranium. Gupta S.K., Modak B., Tyagi M., et al. *Journal of the American Ceramic Society*. Vol. 106(2), pg. 1102-1112.

804. Interaction of β-lactoglobulin with gemcitabine based dansylated probe for its application in quantification of milk allergen. Gadly T., Patro B.S., Chakraborty G. *Journal of Molecular Liquids*. Vol. 391, ArtNo. 123259.

805. Interaction study of molten uranium with multilayer SiC/Y2O3 and Mo/Y2O3 coated graphite. Sharma S.K., Saify M.T., Majumdar S., et al. *Nuclear Engineering and Technology*. Vol. 55(5), pg. 1855-1862.

806. Intercorrelations of structural-magnetic properties of La0.7A0.3MnO3 (A=Ba, Sr, Pb) manganites and the energy harvesting applications of their flexible nanocomposite films. Koner S., Satapathy S., Deshmukh P., et al. *Journal of Alloys and Compounds*. Vol. 968, ArtNo. 172249.

807. Intergranular Corrosion Susceptibility of Alloy 800 Weldments. Abraham G.J., Kain V. *Journal of Materials Engineering and Performance*. Vol. 32(17), pg. 7905-7914.

808. Interlayer coupling in the superconducting state of iron-based superconductors. Hong W., Zhou H., Li Z., et al. *Physical Review B*. Vol. 107(22), ArtNo. 224514.

809. Interlink between ExoD (Alr2882), exopolysaccharide synthesis and metal tolerance in Nostoc sp. strain PCC 7120: Insight into its role, paralogs and evolution. Raghavan P.S., Potnis A.A., Gupta S., et al. *International Journal of Biological Macromolecules*. Vol. 242, ArtNo. 125014.

810. Intermediate valence and spin fluctuations near a quantum critical point in CeRu2-xCoxGe2. Pandey S., Mishra A.K., Saravanan M.P., et al. *Physical Review B*. Vol. 108(1), ArtNo. 14407.

811. Internal nitridation of Alloy 690 during creep deformation at 1100 °C. Sourabh K., Singh J.B., Ravikanth K.V., et al. *Materials Science and Engineering: A*. Vol. 867, ArtNo. 144719.

812. International Equivalence of 60Co: Sir Measurements of BIPM Comparison. Ravindra A., Kulkarni D.B., Sharma R., et al. *Mapan - Journal of Metrology Society of India*.

813. Interparticle interaction-dependent jamming in colloids: insights into glass transition and morphology modulation during rapid evaporation-induced assembly. Mehta S., Bahadur J., Sharma S.K., et al. *Soft Matter*. Vol. 20(2), pg. 375-387.

814. Interplay between the Pore Network Modifications and Dynamics of Confined Polyethyleneimine in Self-Assembled Polyethyleneimine-Silica Nanoparticle Microspheres. Sharma S.K., Mehta S., Utpalla P., et al. *Journal of Physical Chemistry C*. Vol. 127(21), pg. 10197-10206.

815. Interplay of dopant and polarons in trifunctional semimagnetic semiconductor for supercapacitor applications: Local structure and electronic structure investigations. Ponnusamy R., Venkatesan R., KaniAmuthan B., et al. *Journal of Energy Storage*. Vol. 60, ArtNo. 106655.

816. Inter-species competition of surface bacterial flora of pomegranate and their role in spoilage. Pant I., Shashidhar R. *World Journal of Microbiology and Biotechnology*. Vol. 39(10), ArtNo. 260.

817. Interstellar Carbonaceous Dust and Its Formation Pathways: From an Experimental Astrochemistry Perspective. Roy A., Surendra V.S., Ramachandran R., et al. *Journal of the Indian Institute of Science*. Vol. 103(3), pg. 919-938.

818. Interstitial Zinc Boosted Light Tunability, Afterglow, and Ultrabright White Emission in Zinc Germanate (Zn2GeO4). Gupta S.K., Sudarshan K., Modak B., et al. *ACS Applied Electronic Materials*. Vol. 5(2), pg. 1286-1294.

819. Intertwined crystal structure and electrical properties in layered battery materials A2Ni2Te O6 (A=Na/Li). Saha B., Bera A.K., Kesari S., et al. *Physical Review Materials*. Vol. 7(8), ArtNo. 85001.

820. Intertwined spin and phonon correlations across the magnetic compensation temperature in magnetoelectric Li0.5Fe2.5-xCrx O4. Patnaik P.S., Kumar A., Roy A., et al. *Physical Review B*. Vol. 108(1), ArtNo. 14438.

821. Intrinsically 69Ge-Labeled Gum Arabic Glycoprotein-Coated Gallium Oxide Nanoparticles: A New Nanoprobe for PET Imaging. Ghosh S., Patra S., Guleria A., et al. *Industrial and Engineering Chemistry Research*. Vol., ArtNo. .

822. Inverse 'intra-lattice' charge transfer in nickel-molybdenum dual electrocatalysts regulated by under-coordinating the molybdenum center. Parvin S., Bothra N., Dutta S., et al. *Chemical Science*. Vol. 14(11), pg. 3056-3069.

823. Investigating Cr dealloying and Li ingress in Ni-Mo-Cr alloys with different Mo/Cr ratio exposed to FLiNaK salt. Banerjee R.H., Singh V., Chakraborty P., et al. *Corrosion Science*. Vol. 212, ArtNo. 110929.

824. Investigating neutron transfer in the Li 6 + Sn 124 system. Parkar V.V., Parmar A., Prasanna M., et al. *Physical Review C*. Vol. 107(2), ArtNo. 24602.

825. Investigating the characteristics of 11 kHz excitation of EFCAP and its selective effect on breast cancer cell death. Misra V.C., Pai Bellare G., Tiwari N., et al. *Plasma Processes and Polymers*. Vol. 20(10), ArtNo. e2300081.

826. Investigating the impact of roller position on pressure tube-end fitting rolled joint performance using 3D explicit finite element analysis. Roy V., Chatterjee S., Halder P., et al. *International Journal of Pressure Vessels and Piping*. Vol. 206, ArtNo. 105057.

827. Investigating the Influence of Aromatic Counterions on the Micellar Structure and Aggregation Behavior of Morpholinium-Based Surface-Active Ionic Liquids in an Aqueous Solution. Viradiya R.A., Patel N., Aswal V.K., et al. *Langmuir*. Vol. 39(33), pg. 11684-11693.

828. Investigation of dog-boning & fishtailing defects in plate type dispersion fuel Rolling: Insights from finite element analysis and defect minimization techniques. Roy V., Sharma A. *Nuclear Engineering and Design*. Vol. 414, ArtNo. 112634.

829. Investigation of flow dynamics of molten glass in different solar glass production units using radiotracer method. Goswami S., Biswal J., Sharma V.K., et al. *Applied Radiation and Isotopes*. Vol. 193, ArtNo. 110662.

830. Investigation of Giant Cell Tumor of Bone and Tissue Engineering Approaches for the Treatment of Giant Cell Tumor of Bone. Anandan D., Kumar A., Jeyakkani M.N., et al. *ACS Applied Bio Materials*. Vol. 6(10), pg. 3946-3958.

831. Investigation of Magnetic and Transport Properties of Co2FeSi Spin Glass Heusler Alloy Under Extreme Conditions. Devarajan U., Sivaprakash P., Garg A.B., et al. *Journal of Superconductivity and Novel Magnetism*. Vol. 36(6), pg. 1611-1618.

832. Investigation of Photoelectrocatalytic and Magnetic Properties of Sr2YbRu1-xTaxO6 (x = 0, 0.25, 0.5, 0.75, and 1). Sarkar A., Das A., Ash S., et al. *Inorganic Chemistry*. Vol. 62(24), pg. 9324-9334.

833. Investigation of the low- and medium-spin level structure in As 77. Mondal A.K., Chakraborty A., Mandal K., et al. *Physical Review C*. Vol. 107(6), ArtNo. 64320.

834. Investigation of the Thermal Properties of Alkali Metal Thorium Phosphates and Their Application for the Sorption of Uranyl Ion from Acidic Medium. Patkare G., Shafeeq M., Sengupta A., et al. *European Journal of Inorganic Chemistry*. Vol. 26(17), ArtNo. e202300140.

835. Investigation of tribological and corrosion performance of electroplated hard chromium coating on 17-4 PH steel. Ghosh S.K., Limaye P.K., Srivastava C., et al. *Surface Engineering*. Vol. 39(5), pg. 521-531.

836. Investigation on integration of conducting polymers with Cu doped ZnO towards photocatalytic degradation of organic dye. Patil S.S., Amarnath C.A., Sukhdev A., et al. *Optical Materials*. Vol. 146, ArtNo. 114575.

837. Investigation on various properties of Dy0.7Ca0.3MnO3:TiO2 based nano-micro composites. Jambukiya U., Parmar M., Bhammar N.A., et al. *Journal of Alloys and Compounds*. Vol. 967, ArtNo. 171532.

838. Investigations on CuCl/HCl Electrolysis Using a Pt/C Electrocatalyst-based Membrane Electrode Assembly. Banerjee A.M., Antony R.P., Nadar A., et al. *Journal of the Electrochemical Society*. Vol. 170(12), ArtNo. 124515.

839. Ionic Liquid Assisted Exothermic Complexation of Trivalent Lanthanides with Fluorinated β Diketone: Multitechnique Approach with Theoretical Insight. Nagar A., Sengupta A., Sk M.A., et al. *Inorganic Chemistry*. Vol. 62(48), pg. 19631-19647.

840. Ionizing radiation-induced cancer: perplexities of the bystander effect. Gopinathan L., Gopinathan C. *ecancermedicalscience*. Vol. 17, ArtNo. 1579.

841. Iron-based fluorophosphate Na2FePO4F as a cathode for aqueous zinc-ion batteries. Singh D., Hu Y., Meena S.S., et al. *Chemical Communications*. Vol. 59(97), pg. 14391-14394.

842. Isolation of yellow vein mosaic virus (YVMV)-resistant mutants of okra (Abelmoschus esculentus L.) through applied mutagenesis. Hazra S., Gorai S., Roy S., et al. *Plant Breeding*.

843. Isotope effect on hydrogen storage properties of Ti and Nb co-substituted ZrCo alloy. Jat R.A., Rawat D., Sharma A. *International Journal of Hydrogen Energy*. Vol. 48(44), pg. 16802-16812.

844. Isotope hydrology tools in the assessment of arsenic contamination in groundwater: An overview. Ansari M.A., Saravana Kumar U., Noble J., et al. *Chemosphere*. Vol. 340, ArtNo. 139898.

845. Isotope selective three-step photoionization of 174Yb. Suryanarayana M.V., Sankari M. *Journal of the Optical Society of America B: Optical Physics*. Vol. 40(1), pg. 53-62.

846. Itraconazole Confers Cytoprotection Against Neurodegenerative Disease-Associated Abnormal Protein Aggregation. Dubey A.R., Mishra R., Jagtap Y.A., et al. *Molecular Neurobiology*. Vol. 60(5), pg. 2397-2412.

847. K+-doped P6̄ crystals of NIR-upconverting NaYF4:Yb3+/Ho3+ conform to the 'strain-intensity' relationship. Swain A., Verma P., Singh M.N., et al. *CrystEngComm*. Vol. 25(24), pg. 3528-3538.

848. Kinetic study of graphene oxide synthesis by electrochemical exfoliation of graphite. Biranje P.M., Patwardhan A.W., Joshi J.B., et al. *Journal of Industrial and Engineering Chemistry*. Vol. 119 pg. 335-345.

849. kNN based Machine Learning Model for Transient Detection in Nuclear Reactors. Arunprasath V., Santhosh T.V., Vinod G., et al. *IET Conference Proceedings*. Vol. 2023(5), pg. 104-109.

850. Label-free optical bio-sensing of non-cancerous and cancerous tissues from mice: Distinct spectroscopic features of thiazole orange. Gala R., Gandhi V.V., Barooah N., et al. *Sensors and Diagnostics*. Vol. 2(1), pg. 147-154.

851. Laser isotope separation of 192Ir. Suryanarayana M.V., Sankari M. *Applied Radiation and Isotopes*. Vol. 197, ArtNo. 110820.

852. Laser isotope separation of 223Ra. Suryanarayana M.V. *Scientific Reports*. Vol. 13(1), ArtNo. 7001.

853. Laser surface melting of 304L SS: increase in resistance to transpassive dissolution and pitting corrosion. Mahanti Ghosal A., Gupta R.K., Chandra K., et al. *Corrosion Engineering Science and Technology*. Vol. 58(5), pg. 508-520.

854. Laterally Grown Strain-Engineered Semitransparent Perovskite Solar Cells with 16.01% Efficiency. Ghosh T., Mane P., Chakraborty B., et al. *ACS Applied Materials and Interfaces*. Vol. 15(14), pg. 17994-18005.

855. Late-stage Ligand Modification After Coordination Strengthens Stereoselectively Self-Assembled Hemiaminal Ether Complexes. Raje S., Koner A., Ghosh S., et al. *Chemistry - An Asian Journal*. Vol. 18(20), ArtNo. e202300706.

856. Lattice dynamics and pressure induced metallization of solid iodanil (C6I4O2) studied using density functional theory. Mondal S., Ayadi T., Lebègue S., et al. *Physica Scripta*. Vol. 98(7), ArtNo. 75918.

857. LET spectrometry for p+nat(Li+C) system at different proton energies using CR-39: Development of autoLET code for automated generation of LET spectra and dose values. Sahoo G.S., Paul S., Tripathy S.P., et al. *Nuclear Instruments and Methods in Physics Research, Section A: Accelerators, Spectrometers, Detectors and Associated Equipment*. Vol. 1047, ArtNo. 167896.

858. Ligand engineering with heterocyclic aromatic thiol doped carbon quantum dots. Anthony A.M., Pandurangan P., Abbas S. *Carbon*. Vol. 211, ArtNo. 118086.

859. Light-particle-induced deexcitations of 31- and 22+ resonances of C 12 in extreme stellar conditions. Baishya A., Santra S., Rout P.C., et al. *Physical Review C*. Vol. 108(6), ArtNo. 65807.

860. Li-Ion Conduction Mechanism and Relaxation Dynamics in Sorosilicate Compound Li2Cu5(Si2O7)2. Chikara K.S., Bera A.K., Kumar A., et al. *ACS Applied Electronic Materials*. Vol. 5(9), pg. 5137-5150.

861. Linear and non-linear optical properties of boron carbide thin films. Bute A., Jena S., Sharma R.K., et al. *Applied Surface Science*. Vol. 608, ArtNo. 155101.

862. Linear and Nonlinear Stability Analysis of Molten Salt Natural Circulation Loop. Srivastava A.K., Saikrishna N., Maheshwari N.K. *Journal of Nuclear Engineering and Radiation Science*. Vol. 9(4), ArtNo. 41401.

863. Linear magnetoelectric coupling and type-II multiferroic order in NiMn2O4. Chatterjee A., Kumar A., Manna P.K., et al. *Journal of Applied Physics*. Vol. 134(10), ArtNo. 104103.

864. Linkage Isomers of Triangular Pd Metallacycles and Catalysis in Aqueous Suzuki Coupling Reaction. Chaudhari K.R., Wadawale A.P., Pathak A.K., et al. *Inorganic Chemistry*.

865. Liquid-liquid extraction of No-carrier-added 129Cs with various extractants. Ghosh K., Naskar N., Lahiri S. *Applied Radiation and Isotopes*. Vol. 196, ArtNo. 110777.

866. Lithium decorated Ψ-graphene as a potential hydrogen storage material: Density functional theory investigations. Dewangan J., Mahamiya V., Shukla A., et al. *International Journal of Hydrogen Energy*. Vol. 48(96), pg. 37908-37920.

867. Lithium titanate foam for tritium breeding application. Khan N., Sinha A., Sudarsan V. *Journal of Nuclear Materials*. Vol. 583, ArtNo. 154491.

868. Lithium–sulfur battery performance enhancement by optimal loading of graphene oxide on separator with MXene/reduced graphene oxide/sulfur cathode. Sandeep Rao K., Dutta Pathak D., Mandal B.P., et al. *Materials Today Sustainability*. Vol. 23, ArtNo. 100414.

869. Loading of alpha-tocopherol in a nonionic microemulsion: Phase behavior and structural characteristics. Kanike S., Sarolia J., Toor J., et al. *Colloids and Surfaces A: Physicochemical and Engineering Aspects*. Vol. 660, ArtNo. 130785.

870. Local Structure and Speciation-Driven UO22+ → Sm3+ Energy Transfer for Enhanced Luminescence in Li2B4O7. Balhara A., Gupta S.K., Modak B., et al. *Inorganic Chemistry*. Vol. 62(49), pg. 20258-20270.

871. Long-range and local structure evolution of Y1.8Eu0.2Ge2 O7 under static high pressures. Kaiwart R., Dwivedi A., Modak M., et al. *Physical Review B*. Vol. 108(17), ArtNo. 174108.

872. Low- pT direct-photon production in Au+Au collisions at sNN =39 and 62.4 GeV. Abdulameer N.J., Acharya U., Adare A., et al. *Physical Review C*. Vol. 107(2), ArtNo. 24914.

873. Low-cost, ecofriendly, and large-scale synthesis of nanostructured Co1−xMnxFe2O4 microgranules with enhanced magnetic performance by chemical spray drying processing. Ansari S.M., Sen D., Haritha K., et al. *Colloids and Surfaces A: Physicochemical and Engineering Aspects*. Vol. 672, ArtNo. 131697.

874. Luminescence and spectroscopic studies on Eu3+-doped borate and boro-phosphate glasses for solid state optical devices. Priya M., Dhavamurthy M., Suresh A.A., et al. *Optical Materials*. Vol. 142, ArtNo. 114007.

875. Luminescent Y2Zr2O7 for Ultrasensitive Detection of Volatile Organic Compounds Driven by Oxygen Vacancies. Parayil R.T., Gupta S.K., Rohilla R., et al. *ACS Applied Electronic Materials*. Vol. 5(9), pg. 5151-5163.

876. Machine learning approach for label-free rapid detection and identification of virus using Raman spectra. Alexander R., Uppal S., Dey A., et al. *Intelligent Medicine*. Vol. 3(1), pg. 22-35.

877. Machine learning based de-noising of electron back scatter patterns of various crystallographic metallic materials fabricated using laser directed energy deposition. Krishna K.V.M., Madhavan R., Pantawane M.V., et al. *Ultramicroscopy*. Vol. 247, ArtNo. 113703.

878. Macrophage targeted polymeric curcumin nanoparticles limit intracellular survival of Mycobacterium tuberculosis through induction of autophagy and augment anti-TB activity of isoniazid in RAW 264.7 macrophages. Gupta P.K., Jahagirdar P., Tripathi D., et al. *Frontiers in Immunology*. Vol. 14, ArtNo. 1233630.

879. Magnetic properties and coupled spin-phonon behavior in quasi-one-dimensional screw-chain compound BaMn2 V2 O8. Pal A., Anand K., Yen T.W., et al. *Physical Review Materials*. Vol. 7(1), ArtNo. 14402.

880. Magnetic studies of Mn2+substituted Zn-ferrite nanoparticles: Role of secondary phases, bond angles and magnetocrystalline anisotropy. Deepty M., Prasad G., Srinivas C., et al. *Solid State Communications*. Vol. 361, ArtNo. 115077.

881. Magnetism in A V3Sb5 (A=Cs, Rb, and K): Origin and Consequences for the Strongly Correlated Phases. Hasan M.N., Bharati R., Hellsvik J., et al. *Physical Review Letters*. Vol. 131(19), ArtNo. 196702.

882. Magnetism in A V3Sb5 (A=Cs, Rb, K): Complex landscape of dynamical magnetic textures. Karmakar D., Pereiro M., Hasan M.N., et al. *Physical Review B*. Vol. 108(17), ArtNo. 174413.

883. Magnetite interaction with arsenic during sorptive removal from groundwater: a mechanistic study. Ajith N., Satpati A.K., Debnath A.K., et al. *Journal of Environmental Science and Health - Part A Toxic/Hazardous Substances and Environmental Engineering*. Vol. 58(7), pg. 715-723.

884. Magneto-dielectric signature of Gd3+-substituted PbMg1/3Nb2/3O3 ceramics. Pandey A.H., Gupta S.M., Sahlot P., et al. *Journal of Materials Science: Materials in Electronics*. Vol. 34(17), ArtNo. 1349.

885. Magnetoelastic coupling with inverse magnetocaloric effect observed in Sr2YRuO6. Saha P., Nithya R., Sathyanarayana A.T., et al. *Journal of Magnetism and Magnetic Materials*. Vol. 574, ArtNo. 170682.

886. Magnetoimpedance effect in electrodeposited NiFe/Cu wire using trisodium citrate additive in plating bath. Tandon P., Sahu R., Mishra A.C., et al. *Journal of Magnetism and Magnetic Materials*. Vol. 570, ArtNo. 170490.

887. Magnetoimpedance effect in NiFeP thin films deposited on Cu microwire through electrodeposition. Tandon P., Kotti A.P., Venkatesh R., et al. *Materials Chemistry and Physics*. Vol. 309, ArtNo. 128304.

888. Magneto-strain effects in 2D ferromagnetic van der Waal material CrGeTe 3. Vijay K., Vavilapalli D.S., Arya A., et al. *Scientific Reports*. Vol. 13(1), ArtNo. 8579.

889. Malabaricone C, a constituent of spice Myristica malabarica, exhibits anti-inflammatory effects via modulation of cellular redox. Patwardhan R.S., Kundu K., Purohit V., et al. *Journal of Biosciences*. Vol. 48(2), ArtNo. 9.

890. Manganese cobalt-MOF@carbon nanofiber-based non-enzymatic histamine sensor for the determination of food freshness. Dey B., Ahmad M.W., Kim B.H., et al. *Analytical and Bioanalytical Chemistry*. Vol. 415(17), pg. 3487-3501.

891. Mapping the variation in indoor radon, thoron and their progeny concentration for different seasons. Mehta V., Kapil C., Shikha D., et al. *Indian Journal of Pure and Applied Physics*. Vol. 61(6), pg. 443-449.

892. Measurement of 58 co(n,xp) cross sections by a surrogate method. Gandhi R., Santra S., Rout P.C., et al. *European Physical Journal A*. Vol. 59(8), ArtNo. 187.

893. Measurement of alpha-induced reaction cross-sections for natZn with detailed covariance analysis. Choudhary M., Sharma A., Singh N., et al. *Nuclear Physics A*. Vol. 1038, ArtNo. 122720.

894. Measurement of differential cross sections for the production of a Z boson in association with jets in proton-proton collisions at Formula Presented. Tumasyan A., Adam W., Andrejkovic J.W., et al. *Physical Review D*. Vol. 108(5), ArtNo. 52004.

895. Measurement of Direct-Photon Cross Section and Double-Helicity Asymmetry at s =510 GeV in p → + p → Collisions. Abdulameer N.J., Acharya U., Adare A., et al. *Physical Review Letters*. Vol. 130(25), ArtNo. 251901.

896. Measurement of dose enhancement factor for Xoft Axxent electronic brachytherapy device using nanoparticle-embedded alginate film and radiochromic film. Kakade N.R., Das A., Kumar R., et al. *Journal of Cancer Research and Therapeutics*. Vol. 19(8), pg. S177-S182.

897. Measurement of excitation functions for natCu(α, x) reactions with detailed covariance analysis. Choudhary M., Sharma A., Gandhi A., et al. *Journal of Physics G: Nuclear and Particle Physics*. Vol. 50(1), ArtNo. 15103.

898. Measurement of flux distribution of an AmBe neutron source and estimation of two group integral capture cross-sections. Guruprasad, Shet S., Prajapati P.M., et al. *Nuclear and Particle Physics Proceedings*. Vol. 341 pg. 53-55.

899. Measurement of isomeric yield ratios for 104m,gAg and 106m,gAg isotopes using bremsstrahlung end-point energies of 45–75 MeV. Jang W., Naik H., Kim G., et al. *Nuclear Instruments and Methods in Physics Research, Section B: Beam Interactions with Materials and Atoms*. Vol. 537 pg. 111-118.

900. Measurement of natural radioactivity and radiation hazard assessment in the soil samples of Visakhapatnam, Andhra Pradesh, India. Satyanarayana G.V.V., Sivakumar N.S., VidyaSagar D., et al. *Journal of the Indian Chemical Society*. Vol. 100(1), ArtNo. 100856.

901. Measurement of neutron capture cross section on 71Ga at 2.15 and 3.19 MeV and uncertainty propagation and covariance analysis. Pachuau R., Gandhi A., Singh N., et al. *Chinese Physics C*. Vol. 47(7), ArtNo. 74001.

902. Measurement of neutron capture cross sections for the 174Yb(n,γ)175Yb reaction at thermal and epithermal energies. Hien N.T., Do N.V., Kim G., et al. *Radiation Physics and Chemistry*. Vol. 205, ArtNo. 110738.

903. Measurement of neutron induced reaction cross-section of 99Mo. Upadhyay M., Choudhary M., Singh N., et al. *Journal of Physics G: Nuclear and Particle Physics*. Vol. 50(12), ArtNo. 125107.

904. Measurement of residues from the Li 6 +Zn reaction: Analysis of fusion phenomena below 7.1 MeV/nucleon. Singh A., Maiti M., Nag T.N., et al. *Physical Review C*. Vol. 108(2), ArtNo. 24607.

905. Measurement of self-broadening coefficients and line intensities of ν1 + ν3 + ν4 – ν4 band of acetylene in 1.5 μm spectral region: External cavity diode laser based absorption study. Pal A.K., kumar N., Kshirsagar R.J. *Journal of Quantitative Spectroscopy and Radiative Transfer*. Vol. 300, ArtNo. 108510.

906. Measurement of the Bs 0→μ+μ− decay properties and search for the B0 → μ+μ− decay in proton-proton collisions at s=13TeV. Tumasyan A., Adam W., Andrejkovic J.W., et al. *Physics Letters, Section B: Nuclear, Elementary Particle and High-Energy Physics*. Vol. 842, ArtNo. 137955.

907. Measurement of the Dependence of the Hadron Production Fraction Ratios fs/fu and fd/fu on B Meson Kinematic Variables in Proton-Proton Collisions at Formula Presented. Tumasyan A., Adam W., Andrejkovic J.W., et al. *Physical Review Letters*. Vol. 131(12), ArtNo. 121901.

908. Measurement of the differential t t ¯ production cross section as a function of the jet mass and extraction of the top quark mass in hadronic decays of boosted top quarks. Tumasyan A., Adam W., Andrejkovic J.W., et al. *European Physical Journal C*. Vol. 83(7), ArtNo. 560.

909. Measurement of the electroweak production of Formula Presented in association with two jets in proton-proton collisions at Formula Presented. Tumasyan A., Adam W., Andrejkovic J.W., et al. *Physical Review D*. Vol. 108(3), ArtNo. 32017.

910. Measurement of the flux-weighted cross-sections for the natYb(γ,xn)175,169,167Yb reactions in the Bremsstrahlung end-point energies of 12–16 MeV and 60–70 MeV. Naik H., Kim G.N., Schwengner R., et al. *European Physical Journal A*. Vol. 59(10), ArtNo. 249.

911. Measurement of the isomeric yield ratios of 196m,gAu and 195m,gHg in the 197Au(p,x) reaction. Naik H., Kim G., Lee C., et al. *Radiochimica Acta*. Vol. 111(7), pg. 503-511.

912. Measurement of the mass dependence of the transverse momentum of lepton pairs in Drell–Yan production in proton–proton collisions at √s=13TeV. Tumasyan A., Adam W., Andrejkovic J.W., et al. *European Physical Journal C*. Vol. 83(7), ArtNo. 628.

913. Measurement of the N 14 (n,p) C 14 cross section at the CERN n_TOF facility from subthermal energy to 800 keV. Torres-Sánchez P., Praena J., Porras I., et al. *Physical Review C*. Vol. 107(6), ArtNo. 64617.

914. Measurement of the neutron-induced fission cross section of Th 230 at the CERN n_TOF facility. Michalopoulou V., Stamatopoulos A., Diakaki M., et al. *Physical Review C*. Vol. 108(1), ArtNo. 14616.

915. Measurement of the Se 77 (n,γ) cross section up to 200 keV at the n_TOF facility at CERN. Sosnin N.V., Lederer-Woods C., Krtička M., et al. *Physical Review C*. Vol. 107(6), ArtNo. 65805.

916. Measurement of the top quark mass using a profile likelihood approach with the lepton + jets final states in proton–proton collisions at √s=13TeV. Tumasyan A., Adam W., Andrejkovic J.W., et al. *European Physical Journal C*. Vol. 83(10), ArtNo. 963.

917. Measurement of the $t\bar{t}$ charge asymmetry in events with highly Lorentz-boosted top quarks in pp collisions at s=13 TeV. Tumasyan A., Adam W., Andrejkovic J.W., et al. *Physics Letters, Section B: Nuclear, Elementary Particle and High-Energy Physics*. Vol. 846, ArtNo. 137703.

918. Measurement of φ -meson production in Cu+Au collisions at sNN =200 GeV and U+ U collisions at sNN =193 GeV. Abdulameer N.J., Acharya U., Aidala C., et al. *Physical Review C*. Vol. 107(1), ArtNo. 14907.

919. Measurements of continuous spectra of photons from 4/6 MeV dual energy e-LINAC. Kumar A., Mishra G., De S., et al. *Radiation Physics and Chemistry*. Vol. 208, ArtNo. 110930.

920. Measurements of Higgs boson production in the decay channel with a pair of τ leptons in proton–proton collisions at √s=13 TeV. Tumasyan A., Adam W., Andrejkovic J.W., et al. *European Physical Journal C*. Vol. 83(7), ArtNo. 562.

921. Measurements of jet multiplicity and jet transverse momentum in multijet events in proton–proton collisions at √s=13TeV. Tumasyan A., Adam W., Andrejkovic J.W., et al. *European Physical Journal C*. Vol. 83(8), ArtNo. 742.

922. Measurements of second-harmonic Fourier coefficients from azimuthal anisotropies in p+p, p+Au, d+Au, and He 3 +Au collisions at sNN =200 GeV. Abdulameer N.J., Acharya U., Adare A., et al. *Physical Review C*. Vol. 107(2), ArtNo. 24907.

923. Measurements of the Higgs boson production cross section and couplings in the W boson pair decay channel in proton-proton collisions at √s=13TeV. Tumasyan A., Adam W., Andrejkovic J.W., et al. *European Physical Journal C*. Vol. 83(7), ArtNo. 667.

924. Mechanistic and evolutionary insights into alkaline phosphatase superfamily through structure-function studies on Sphingomonas alkaline phosphatase. Bihani S.C., Nagar V., Kumar M. *Archives of Biochemistry and Biophysics*. Vol. 736, ArtNo. 109524.

925. Mechanistic aspects of in - situ combustion synthesis: Low Temperature gadolinium oxide formation during the high temperature interactions between gadolinium nitrate hexahydrate and glycine through solid state route. Raje N., Kalekar B.B., Ghonge D.K. *Thermochimica Acta*. Vol. 720, ArtNo. 179415.

926. Mechanistic Study of Amphiphilic-Assisted Self-Assembled Cadmium Sulfide Quantum Dots into 3D Superstructures. Pathak S.S., Kedarnath G., Panchakarla L.S. *Journal of Physical Chemistry Letters*. Vol. 14(36), pg. 8114-8120.

927. Mechanochemical synthesis and structure analysis of binary cocrystals of extended bis-pyridyl spacers with resorcinol and orcinol. Kubendiran B., Pramanik G., Kumar M., et al. *Journal of Molecular Structure*. Vol. 1274, ArtNo. 134470.

928. Mesoporous Fe3O4 nanoparticle: A prospective nano heat generator for thermo-therapeutic cancer treatment modality. Shaw S.K., Sharma A., Kailashiya J., et al. *Journal of Magnetism and Magnetic Materials*. Vol. 578, ArtNo. 170817.

929. Meta-Analysis of Antioxidant Mutants Reveals Common Alarm Signals for Shaping Abiotic Stress-Induced Transcriptome in Plants. Mishra S., Ganapathi T.R., Pandey G.K., et al. *Antioxidants and Redox Signaling*. Vol., ArtNo. .

930. Metachronous Adenocarcinoma of the Lung in the Setting of Metastatic Gastric Neuroendocrine Tumor: Value of Elucidating Discordance on Dual-Tracer PET/CT with Ki-67 Index. Loharkar S., Basu S. *Journal of Nuclear Medicine Technology*. Vol. 51(1), pg. 75-77.

931. Metal-decorated γ-graphyne as a drug transporting agent for the mercaptopurine chemotherapy drug: a DFT study. Pallikkara Chandrasekharan S., Lakshmy S., Sanyal G., et al. *Physical Chemistry Chemical Physics*. Vol. 25(13), pg. 9461-9471.

932. meta-Topolin-induced regeneration and ameliorated rebaudioside-A production in genetically uniform candy-leaf plantlets (Stevia rebaudiana Bert.). Subrahmanyeswari T., Gantait S., Kamble S.N., et al. *South African Journal of Botany*. Vol. 159 pg. 405-418.

933. Methods and applications of 3-D SN neutron transport code ATES3. Gupta A. *Life Cycle Reliability and Safety Engineering*. Vol. 12(3), pg. 175-186.

934. Methods of Determining Irritable Bowel Syndrome and Efficiency of Probiotics in Treatment: A Review. Ahlawat G.M., Singh P.K. *Current Therapeutic Research - Clinical and Experimental*. Vol. 99, ArtNo. 100721.

935. Microalgae from wastewaters to wastelands: Leveraging microalgal research conducive to achieve the UN Sustainable Development Goals. Singh K., Ansari F.A., Ingle K.N., et al. *Renewable and Sustainable Energy Reviews*. Vol. 188, ArtNo. 113773.

936. Microdosimetry-based investigation of biological effectiveness of 252Cf brachytherapy source: TOPAS Monte Carlo study. Chattaraj A., Selvam T.P. *Physics in Medicine and Biology*. Vol. 68(22), ArtNo. 225005.

937. Microfluidic solvent extraction of no-carrier-added 64Cu from irradiated Zn target for radiopharmaceutical preparation. Chakravarty R., Sen N., Patra S., et al. *Chemical Engineering Journal Advances*. Vol. 13, ArtNo. 100433.

938. Micro-structural analysis of oxygen irradiated V-4Cr-4Ti by X-ray and electron back scattered diffraction. Dey S., Gayathri N., Dutta A., et al. *Fusion Engineering and Design*. Vol. 197, ArtNo. 114064.

939. Microstructural and mechanical property evolution of Ar9+ ion irradiated Zr-based alloys–effect of initial microstructure and alloying addition. Devi A., Menon R., Sharma S.K., et al. *Radiation Effects and Defects in Solids*. Vol. 178(45448), pg. 553-574.

940. Microstructural changes and enhanced biodiesel compatibility of radiation-processed Nitrile Butadiene Rubber in mixed fuel environments. Kyaw S.S., Chaudhari C.V., Maheshwari P., et al. *Journal of Polymer Research*. Vol. 30(10), ArtNo. 397.

941. Microstructure and magnetic properties of binary Mn54-Al46 alloy particulates obtained by severe plastic deformation processing via end-milling and annealing. Jo J., Vishwanadh B., Shankar M.R., et al. *Journal of Magnetism and Magnetic Materials*. Vol. 586, ArtNo. 171200.

942. Microwave absorption and hyperthermia properties of titanium dioxide–nickel zinc copper ferrite nanocomposite. Mallick A., Dey C.C., Sadhukhan S., et al. *Journal of Magnetism and Magnetic Materials*. Vol. 587, ArtNo. 171373.

943. Microwave-mediated One-step Synthesis of CeVO4-rGO Composites with Enhanced Photocatalytic Activity under Visible Light. Mishra S., Soren S., Debnath A.K., et al. *ChemistrySelect*. Vol. 8(12), ArtNo. e202203968.

944. Miniaturized double transit magnetic field measurement probe using the Faraday rotation principle. Kanchi S., Shukla R., Dey P., et al. *Applied Optics*. Vol. 62(4), pg. 1123-1129.

945. Mitochondria-Directing Fluorogenic Probe: An Efficient Amyloid Marker for Imaging Lipid Metabolite-Induced Protein Aggregation in Live Cells and Caenorhabditis elegans. Pandey S.P., Kavyashree P., Dutta T., et al. *Analytical Chemistry*. Vol. 95(15), pg. 6341-6350.

946. Mitochondria-targeted derivative of pterostilbene, a dietary phytoestrogen, exhibits superior cancer cell cytotoxicity via mitochondrial superoxide mediated induction of autophagy. Ibrahim M.K., Nandha S.R., Patil A.S., et al. *Advances in Redox Research*. Vol. 8, ArtNo. 100071.

947. Mitochondriotropic Derivative of Ethyl Ferulate, a Dietary Phenylpropanoid, Exhibits Enhanced Cytotoxicity in Cancer Cells via Mitochondrial Superoxide-Mediated Activation of JNK and AKT Signalling. Patil A.S., Ibrahim M.K., Sathaye S., et al. *Applied Biochemistry and Biotechnology*. Vol. 195(3), pg. 2057-2076.

948. Mixed Aggregates of Surface-Active Ionic Liquids and 14-2-14 Gemini Surfactants in an Aqueous Medium as Fluid Scaffolds for Enzymology of Cytochrome-c. Singh M., Kumar S., Aswal V.K., et al. *Langmuir*. Vol. 39(33), pg. 11582-11595.

949. Mixed Pluronic/lecithin micelles formulation for oral bioavailability of candesartan cilexetil drug: in vitro characterization and in vivo pharmacokinetic investigations. Mahajan H., Patel H.S., Ray D., et al. *Drug Development and Industrial Pharmacy*. Vol., ArtNo. .

950. MnNCN@C nanocomposite as an anode for Li-ion battery. Pradhan S., Anuraag N.S., Shaw S.K., et al. *Materials Science and Engineering: B*. Vol. 298, ArtNo. 116894.

951. MnxWO4 Nanostructure-Based Catalysts for Single-Step Oxidation of Cyclohexane and Methane to Oxygenates. Prabu M., Manikandan M., Samal P.P., et al. *ACS Applied Nano Materials*. Vol. 6(9), pg. 7245-7258.

952. Modeling and experimental investigation for development of Combined Electrolysis and Catalytic Exchange process for hydrogen isotope separation. Mistry K.A., Shenoy N.S., Bhanja K., et al. *Chemical Engineering Research and Design*. Vol. 192 pg. 487-499.

953. Modeling and Simulation of PGGP Electrode Configuration for Ion-Extraction Process Using 2.5D-PIC Code. Singh P., Sridhar G., Maiti N. *IEEE Transactions on Plasma Science*. Vol. 51(1), pg. 35-48.

954. Modelling and optimization of dosimeters in the product box for commissioning dosimetry at gamma irradiator using Voronoi Diagram algorithm. Singh M., Datta D., Gupta A. *Radiation Physics and Chemistry*. Vol. 210, ArtNo. 111011.

955. Modelling of Tarapur BWR lattice and core to estimate the required number of SB-BE startup neutron sources. Rai R., Singh I., Baraila P., et al. *Nuclear and Particle Physics Proceedings*. Vol. 339-340 pg. 110-113.

956. Modification and Functionalization of Polymers for Targeting to Bone Cancer and Bone Regeneration. Nimbalkar Y., Gharat S., Tanna V., et al. *Critical Reviews in Biomedical Engineering*. Vol. 51(3), pg. 21-58.

957. Modification of surface characteristics of functionalized multi-walled carbon nanotubes containing mixed matrix membrane using click chemistry. Mistry P., Nikita K., Aswal V.K., et al. *Desalination and Water Treatment*. Vol. 295 pg. 42-51.

958. Modifications in structure dependent magnetic parameters of Nd-doped Ba–Ca hexaferrites synthesized by sol gel using lemon extract as a fuel. Pujari V.C., Mhase P.D., Mahindrakar R.M., et al. *Ceramics International*. Vol. 49(24), pg. 40466-40477.

959. Modified Ion Exchange Resin Method for Extraction of Micronutrient Cations from Soils. Srivastava P.C., Shrivastava M. *Communications in Soil Science and Plant Analysis*. Vol. 54(11), pg. 1483-1491.

960. Modifying interprotein interactions for controlling heat-induced protein gelation. Kumar S., Saha D., Aswal V.K. Physical Review Materials. Vol. 7(1), ArtNo. 15601.

961. Modulated Ultrathin NiCo-LDH Nanosheet-Decorated Zr3+-Rich Defective NH2-UiO-66 Nanostructure for Efficient Photocatalytic Hydrogen Evolution. Sk S., Jamma A., Gavali D.S., et al. ACS Applied Materials and Interfaces. Vol. 15(48), pg. 55822-55836.

962. Modulation of photoluminescence and optical limiting properties of spray-coated tin oxide thin film through Eu doping. Hind P.A., Patil P.S., Gummagol N.B., et al. *Journal of Materials Research*. Vol. 38(22), pg. 4828-4847.

963. Modulation of Surface Ti-O Species in 2D-Ti3C2TX MXene for Developing a Highly Efficient Electrocatalyst for Hydrogen Evolution and Methanol Oxidation Reactions. Navjyoti N., Sharma V., Bhullar V., et al. *Langmuir*. Vol. 39(8), pg. 2995-3005.

964. Modulation of surfactant self-assembly in deep eutectic solvents and its relevance to drug delivery-A review. Basu M., Hassan P.A., Shelar S.B. *Journal of Molecular Liquids*. Vol. 375, ArtNo. 121301.

965. MOF (M=Zr, Zn, Co)@COFs hybrid composite as a potential adsorbent for UO22+ and Methylene blue (MB) from solutions.. Koppula S., Jagasia P., Manabolu Surya S.B. *Materials Today Communications*. Vol. 34, ArtNo. 105336.

966. Molecular Detection of Multidrug Resistance and Characterizations of Mutations in Mycobacterium Tuberculosis Using Polycarbonate Track-Etched Membrane Based DNA Bio-Chip. Jain B., Kulkarni S. *Indian Journal of Microbiology*.

967. Molecular dynamic simulations reveal anti-SARS-CoV-2 activity of mitocurcumin by potentially blocking innate immune evasion proteins NSP3 and NSP16. Pal D., Checker R., Kutala V.K., et al. *Molecular Diversity*. Vol. 27(2), pg. 635-649.

968. Molecular dynamics simulations of the decomposition and Us–Up relationship of RDX molecular crystal subjected to high velocity impact. Pahari P., Rao A.D.P., Warrier M. *Journal of Molecular Modeling*. Vol. 29(2), ArtNo. 50.

969. Molecular growth of PANH via intermolecular Coulombic decay. Barik S., Behera N.R., Dutta S., et al. *Science Advances*. Vol. 9(30), ArtNo. eadi0230.

970. Molecular imaging of tumor hypoxia: Evolution of nitroimidazole radiopharmaceuticals and insights for future development. Mittal S., Mallia M.B. *Bioorganic Chemistry*. Vol. 139, ArtNo. 106687.

971. Molecular insights into the aggregation and solubilizing behavior of biocompatible amphiphiles Gelucire® 48/16 and Tetronics® 1304 in aqueous media. Bhalani D., Kakkad H., Modh J., et al. *RSC Advances*. Vol. 13(41), pg. 28590-28601.

972. Molecular mapping of two recessive genes controlling resistance to bacterial leaf pustule disease in soybean (Glycine max). Totade S.P., Gupta S.K., Manjaya J.G. *Plant Breeding*. Vol. 142(2), pg. 184-194.

973. Molecular Mechanistic of Zn-Solubilizing Bacteria for Agronomic Eminence: Recent Updates and Futuristic Development. Rani N., Chauhan A., Kaur S., et al. *Journal of Plant Growth Regulation*.

974. Molecular precursor approach to develop catalytically relevant nanosized metals, palladium chalcogenides and ternary/quaternary metal chalcogenides. Kedarnath G., Jain V.K. New Journal of Chemistry. Vol. 47(45), pg. 20688-20702.

975. Molecular precursor mediated selective synthesis of phase pure cubic InSe and hexagonal In2Se3 nanostructures: new anode materials for Li-ion batteries. Karmakar G., Dutta Pathak D., Tyagi A., et al. Dalton Transactions. Vol. 52(20), pg. 6700-6711.

976. Molecular Precursor-Driven Synthesis of Copper Telluride Nanostructures for LIB Anode Application. Kushwah N., Kedarnath G., Wadawale A., et al. *Inorganic Chemistry*. Vol. 62(23), pg. 8823-8834.

977. Monte Carlo analysis of the contributions of long-lived positronium to the spectra of positron-impact-induced secondary electrons measured using an annihilation-gamma-triggered time-of-flight spectrometer. Lotfimarangloo S., Chirayath V.A., Mukherjee S., et al. *Nuclear Instruments and Methods in Physics Research, Section B: Beam Interactions with Materials and Atoms*. Vol. 542 pg. 99-109.

978. Morphology-controlled synthesis of MoO3 nanostructures and its effect on heavy metal ion detection. Choudhari U., Gadekar P., Ramgir N., et al. *Journal of Materials Science: Materials in Electronics*. Vol. 34(25), ArtNo. 1759.

979. MpSNAC67 transcription factor of banana regulates stress induced senescence through salicylic acid dependent pathway. Negi S., Bhakta S., Ganapathi T.R., et al. *Environmental and Experimental Botany*. Vol. 205, ArtNo. 105104.

980. MSA-based seismic fragility analysis of RC structures considering soil nonlinearity effects and time histories compatible to uniform hazard spectra. Bandyopadhyay S., Parulekar Y.M., Sengupta A. *Structures*. Vol. 54 pg. 330-347.

981. Multi-anionic polymer templated aggregation induced emission of berberine and its application for protamine sensing. Chakraborty G., Mal D.K., Potnis A., et al. *Journal of Molecular Liquids*. Vol. 388, ArtNo. 122729.

982. Multifunctional ZnO nanostructures: a next generation nanomedicine for cancer therapy, targeted drug delivery, bioimaging, and tissue regeneration. Gupta J., Hassan P.A., Barick K.C. *Nanotechnology*. Vol. 34(28), ArtNo. 282003.

983. Multigroup form of simplified spherical harmonics (SPN) equations for neutron transport. Mishra A., Ray A., Singh T. *Nuclear and Particle Physics Proceedings*. Vol. 341 pg. 81-83.

984. Multi-institutional dose audit in radiotherapy facilities using in-house developed optically stimulated luminescence disc dosimeters. Kumar P., Sharma S.D., Dhabekar B., et al. *Journal of Cancer Research and Therapeutics*. Vol. 19(8), pg. S361-S367.

985. Multiple Carbon Morphologies Derived from Polyion Complex-Based Double Hydrophilic Block Copolymers as Templates and Phenol as a Carbon Precursor. Sivanantham M., Senthamaraikannan R., Dirisala A., et al. *Langmuir*. Vol. 39(31), pg. 10756-10768.

986. Multiple Magnetic Phases and Anomalous Hall Effect in Sb1.9Fe0.1Te2.85S0.15 Topological Insulators. Pal D., Verma A., Alam M., et al. Journal of Physical Chemistry C. Vol. 127(5), pg. 2508-2517.

987. MusaNAC29-like transcription factor improves stress tolerance through modulation of phytohormone content and expression of stress responsive genes. Negi S., Bhakta S., Ganapathi T.R., et al. Plant Science. Vol. 326, ArtNo. 111507.

988. Mutation induction in aromatic Joha rice of Assam for improvement of morpho-agronomic traits through M1 to M3 generation. Bordoloi D., Sarma D., Sarma Barua N., et al. International Journal of Radiation Biology. Vol. 99(11), pg. 1760-1777.

989. MXene supported nickel-cobalt layered double hydroxide as efficient bifunctional electrocatalyst for hydrogen and oxygen evolution reactions. Navjyoti, Sharma A.K., Sharma V., et al. *Journal of Alloys and Compounds*. Vol. 939, ArtNo. 168779.

990. Nanocomposites of ZnO Nanostructures and Reduced Graphene Oxide Nanosheets for NO2 Gas Sensing. Pathak A., Samanta S., Bhangare B., et al. *ACS Applied Nano Materials*. Vol. 6(9), pg. 7649-7657.

991. Nanostructured CeO2 ultrathin film deposited by the Langmuir Blodgett technique for highly sensitive and specific detection of sub ppm level NO2 gas at room temperature. Choudhury S., Kanth S., Saxena V., et al. *Journal of Materials Chemistry C*. Vol. 11(34), pg. 11620-11630.

992. Nanostructured metal oxide semiconductors and composites for reliable trace gas sensing at room temperature. Betty C.A., Choudhury S., Shah A. *Surfaces and Interfaces*. Vol. 36, ArtNo. 102560.

993. National Audit for Traceable 131I Activity Measurements with Radionuclide Calibrators Among Nuclear Medicine Centers in India. Ravindra A., Kulkarni D.B., Sharma R., et al. *Mapan - Journal of Metrology Society of India*.

994. Near-infrared detection and line intensity measurements of H2S with ECDL source based off-axis integrated cavity output spectroscopy. Kumar N., Kumar Pal A., Kshirsagar R.J. *Chemical Physics*. Vol. 567, ArtNo. 111804.

995. Need for enrichment of lutetium isotope and design of a laser based separator module. Majumder A., Pulhani A.K., Ghosh A., et al. *Applied Radiation and Isotopes*. Vol. 202, ArtNo. 111038.

996. Need of Quantum Biology to Investigate Beneficial Effects at Low Doses (< 100 mSv) and Maximize Peaceful Applications of Nuclear Energy. Chandra A., Aswal D.K. *Mapan - Journal of Metrology Society of India*.

997. Neutron spectrometry and dosimetry using a multi-shell Single Sphere Neutron Spectrometer with thermo-luminescent and optically stimulated luminescent detectors. Paul S., Tripathy S.P., Sahoo G.S., et al. *Nuclear Instruments and Methods in Physics Research, Section A: Accelerators, Spectrometers, Detectors and Associated Equipment*. Vol. 1053, ArtNo. 168395.

998. Neutronic and burn up analysis of VVER 1000 benchmark using EXCEL and TRIHEX-FA code system. Srivastava A., Karthikeyan R., Pal U., et al. *Nuclear Engineering and Design*. Vol. 414, ArtNo. 112601.

999. Neutronics study of chloride fuel salts for experimental design of small Molten Salt Reactor. Dwivedi D.K., Srivastava A.K., Gupta A., et al. *Nuclear and Particle Physics Proceedings*. Vol. 339-340 pg. 129-132.

1000. Neutron-induced fission cross sections of Th 232 and U 233 up to 1 GeV using parallel plate avalanche counters at the CERN n_TOF facility. Tarrío D., Tassan-Got L., Duran I., et al. *Physical Review C*. Vol. 107(4), ArtNo. 44616.

1001. New approach for efficient separation of U and Mo using a task-specific ionic liquid from hydrochloric acid medium: extraction and electrochemical investigation. Pathak S., Srivastava A., Biswas S., et al. *New Journal of Chemistry*. Vol. 47(9), pg. 4552-4564.

1002. Next generation gamma ray shielding blocks developed using alumina industry waste. Arya R., Paulose R., Agrawal V., et al. *Construction and Building Materials*. Vol. 373, ArtNo. 130895.

1003. N-graphene synthesized in astrochemical ices. Sivaraman B., Rahul K.K., Ambresh M., et al. *European Physical Journal D*. Vol. 77(2), ArtNo. 24.

1004. Ni1-xZnxFe2O4@CoO (x = 0.25 and 0.50) Nanoparticles for Magnetic Resonance Imaging. Konwar K., Bora M., Kaushik S.D., et al. *ACS Applied Nano Materials*. Vol. 6(21), pg. 20440-20457.

1005. Ni3InSb: Synthesis, Crystal Structure, Electronic Structure, and Magnetic Properties. Kuila S.K., Harshit N., Roy N., et al. *Inorganic Chemistry*. Vol. 62(19), pg. 7304-7314.

1006. Nitrogen containing reductants for the corrosion control of alloys relevant to nuclear reactors. Kumar P.S., Rufus A.L. *Annals of Nuclear Energy*. Vol. 192, ArtNo. 109938.

1007. Nocardiopsis lucentensis and thiourea co-application mitigates arsenic stress through enhanced antioxidant metabolism and lignin accumulation in rice. AbdElgawad H., Negi P., Zinta G., et al. *Science of the Total Environment*. Vol. 873, ArtNo. 162295.

1008. Noncanonical Relationship between Heterogeneity and the Stokes-Einstein Breakdown in Deep Eutectic Solvents. Srinivasan H., Sharma V.K., Sakai V.G., et al. *Journal of Physical Chemistry Letters*. Vol. 14(43), pg. 9766-9773.

1009. Non-invasive mixing time estimation in unbaffled stirred tank: An ultrasonic approach. Mukherjee D., Sen N., Singh K.K., et al. *AIChE Journal*. Vol. 69(3), ArtNo. e17966.

1010. Non-linear dose response of DNA double strand breaks in response to chronic low dose radiation in individuals from high level natural radiation areas of Kerala coast. Jain V., Saini D., Soren D.C., et al. *Genes and Environment*. Vol. 45(1), ArtNo. 16.

1011. Nonlinear multivariate constitutive equations for modeling hot deformation behavior. Ahmedabadi P.M. *Materials Research Express*. Vol. 10(9), ArtNo. 10.

1012. Nonlocal Probing of Amplitude Mode Dynamics in Charge-Density-Wave Phase of EuTe4. Rathore R., Singhal H., Dwij V., et al. *Ultrafast Science*. Vol. 3, ArtNo. 41.

1013. Non-potable water for sustainable concrete: strength compliance in India for varying pH of mixing water and future scope. Dauji S. *Sadhana - Academy Proceedings in Engineering Sciences*. Vol. 48(4), ArtNo. 221.

1014. Nose to brain delivery of radiolabeled chemotherapeutic micelles: Meeting the unmet needs of brain tumors. Upadhaya P., Panwar Hazari P., Mishra A.K., et al. *Journal of Drug Delivery Science and Technology*. Vol. 86, ArtNo. 104700.

1015. Novel application of sodium manganese oxide in removing acidic gases in ambient conditions. Gupta N.K., Achary S.N., Viltres H., et al. *Scientific Reports*. Vol. 13(1), ArtNo. 2330.

1016. Novel Complex Fractional Order Speed Controller for IM Drive Under Varying Operating Conditions With Enhanced Robustness. Adigintla S., Aware M.V., Bingi K., et al. *IEEE Transactions on Industrial Electronics*. Vol. pg. 1-10.

1017. Novel detection method to rapidly quantify toxic cucurbitacin in Lagenaria siceraria (bottle gourd). Saurabh C.K., Ghosh S.K., Sanyal B. *Journal of Food Science and Technology*. Vol. 60(1), pg. 160-170.

1018. Novel merocyanine-derived receptor: Synthesis, crystal structure and picric acid recognition, spectroscopic and theoretical study. Bhusanur D.I., Nanubolu J.B., Singh P.K., et al. *Journal of Molecular Structure*. Vol. 1284, ArtNo. 135382.

1019. Novel N-Substituted 2,2'-Oxydiacetic Acid Diamide-Functionalized Silica Resins: An Efficient Sorbent for Removal of U(VI) and Th(IV) Present in Nitric Acid-Rich Effluents. Khan P.N., Pahan S., Sengupta A., et al. *Industrial and Engineering Chemistry Research*. Vol. 62(35), pg. 13953-13965.

1020. Novel Schiff base as Fe3+ sensor as well as an antioxidant and its theoretical studies. Sehrawat S., Mahajan A., Sandhu N., et al. *Main Group Chemistry*. Vol. 22(3), pg. 389-401.

1021. Novel thorium borides and their hardness and superconductivity under pressure: Ab initio calculations. Sahoo B.D., Joshi K.D. *Journal of Applied Physics*. Vol. 134(6), ArtNo. 65903.

1022. NtcA, LexA and heptamer repeats involved in the multifaceted regulation of DNA repair genes recF, recO and recR in the cyanobacterium Nostoc PCC7120. Pradhan M., Kumar A., Kirti A., et al. *Biochimica et Biophysica Acta - Gene Regulatory Mechanisms*. Vol. 1866(1), ArtNo. 194907.

1023. Nuclear Factor-Y (NF-Y): Developmental and Stress-Responsive Roles in the Plant Lineage. Kavi Kishor P.B., Ganie S.A., Wani S.H., et al. *Journal of Plant Growth Regulation*. Vol. 42(5), pg. 2711-2735.

1024. Nucleation kinetics of reactive crystallization of ammonium di-uranate. Paik S., Satpati S.K., Singh D.K. *Indian Chemical Engineer*. Vol. 65(6), pg. 527-542.

1025. Nucleation-Growth Versus Spinodal Decomposition in Fe-Cr Alloys: An Experimental Verification by Atom Probe Tomography and Small Angle Neutron Scattering. Sarkar S.K., Ray D., Sen D., et al. *Microscopy and Microanalysis*. Vol. 29(2), pg. 437-450.

1026. Numerical analysis of thermal-hydraulic safety for a reactor containment in the event of a main steam line break. Verma A., Dutta G., Kumar M. *Annals of Nuclear Energy*. Vol. 183, ArtNo. 109631.

1027. Numerical Experimentation and Validation of Shrinking Particle - Gas Reaction in a Pilot Plant Downer Reactor. Govindan B., Tiwari A.K., J.N U.K., et al. *Combustion Science and Technology*. Vol. 195(2), pg. 398-418.

1028. Numerical investigation on convective heat transfer in a pool with submerged heat source under seismic condition. Chauhan S.P., Kumar N., Chandraker D.K. *Journal of Thermal Analysis and Calorimetry*. Vol. 148(7), pg. 2765-2779.

1029. Numerical Study of the Hydride Embrittlement in Zirconium Alloy using XFEM. Jha A., Duhan N., Singh I.V., et al. *International Journal of Structural Stability and Dynamics*. Vol., ArtNo. 2440002.

1030. Observation of charge transfer induced large enhancement of magnetic moment in a structurally disordered inverse Heusler alloy Fe2RuGe. Chakraborty S., Gupta S., Bhasin V., et al. *Physical Review B*. Vol. 108(24), ArtNo. 245151.

1031. Observation of electroweak W+W− pair production in association with two jets in proton-proton collisions at s=13TeV. Tumasyan A., Adam W., Andrejkovic J.W., et al. *Physics Letters, Section B: Nuclear, Elementary Particle and High-Energy Physics*. Vol. 841, ArtNo. 137495.

1032. Observation of Same-Sign WW Production from Double Parton Scattering in Proton-Proton Collisions at Formula Presented. Tumasyan A., Adam W., Andrejkovic J.W., et al. *Physical Review Letters*. Vol. 131(9), ArtNo. 91803.

1033. Observation of triple J/ψ meson production in proton-proton collisions. Tumasyan A., Adam W., Andrejkovic J.W., et al. *Nature Physics*. Vol. 19(3), pg. 338-350.

1034. Observation of τ Lepton Pair Production in Ultraperipheral Pb-Pb Collisions at Formula Presented. Tumasyan A., Adam W., Andrejkovic J.W., et al. *Physical Review Letters*. Vol. 131(15), ArtNo. 151803.

1035. Off axis integrated cavity output spectroscopy of deuterated water isotopologues in 7178–7196 cm−1 spectral region. Gupta A., Udupa D.V. *Spectrochimica Acta - Part A: Molecular and Biomolecular Spectroscopy*. Vol. 299, ArtNo. 122772.

1036. Oligothiophene-Ring-Strapped Perylene Bisimides: Functionalizable Coaxial Donor–Acceptor Macrocycles. Dnyaneshwar Veer S., Chandrakant Wakchaure V., Asokan K., et al. *Angewandte Chemie - International Edition*. Vol. 62(3), ArtNo. e202212934.

1037. On characterization of shock propagation and radiative preheating in x-ray driven high-density carbon foils. Mishra G., Ghosh K. *Physics of Plasmas*. Vol. 30(4), ArtNo. 42712.

1038. On enhancing the Li-ion conductivity of quasi-solid-state electrolytes by suppressing the flexibility of zeolitic imidazolate framework-8 via a mixed ligand strategy. Utpalla P., Mor J., Sharma S.K. *Physical Chemistry Chemical Physics*. Vol. 25(5), pg. 3959-3968.

1039. On synthesis, stability and superconductivity of ThNb2H12under pressure: ab-inito calculations. Sahoo B.D., Joshi K.D. *Journal of Physics and Chemistry of Solids*. Vol. 175, ArtNo. 111193.

1040. On the Maximum Energy Release from Formation of Static Compact Objects. Mitra A., Singh K.K. *Galaxies*. Vol. 11(6), ArtNo. 116.

1041. On the modification of wire wrapping process for fast Breeder reactor fuel Pins: Replacing hydraulic crimping with resistance spot welding. Kumar A., Kulshrestha A., Aher S., et al. *Nuclear Engineering and Design*. Vol. 411, ArtNo. 112441.

1042. On the Propensity of Excess Hydroxide Ions at the Alcohol Monolayer-Water Interface. Bandyopadhyay D., Bhanja K., Choudhury N. *Journal of Physical Chemistry B*. Vol. 127(3), pg. 783-793.

1043. On the role of shape and distribution of secondary voids in the mechanism of coalescence. Dwivedi A.K., Khan I.A., Chattopadhyay J. *Engineering Fracture Mechanics*. Vol. 289, ArtNo. 109399.

1044. One-pot synthesis of unsubstituted and methyl substituted-pyrazinyl diselenides and monoselenides: structural, optical property characterization and DFT calculations. Kushwah N., Chopade S.M., Wadawale A., et al. *RSC Advances*. Vol. 13(51), pg. 36392-36402.

1045. Operational characteristics of LWR core fuelled with thorium-based fuel. Raj D., Kannan U. *Annals of Nuclear Energy*. Vol. 188, ArtNo. 109801.

1046. Optimisation of solids concentration in wet rod mill grinding of limestone ore through modelling and simulation. Serajuddin M., Mukhopadhyay S., Kacham A.R. *International Journal of Mining and Mineral Engineering*. Vol. 13(3), pg. 231-255.

1047. Optimization of Ball Mill Grinding of a Limestone-Type Brecciated Uranium Ore. Serajuddin M., Mukhopadhyay S., Kacham A.R. *Transactions of the Indian Institute of Metals*. Vol. 76(8), pg. 2253-2261.

1048. Optimization of Praseodymium-Based Perovskites as Electrocatalysts for Oxygen Reduction Reaction. Nayak B.B., Soren S., Hota I., et al. *ACS Applied Energy Materials*. Vol. 6(19), pg. 9951-9962.

1049. Orientation Filtering of Fluorescence by Plasmon-Coupled Waveguide. Dutta Choudhury S. *Journal of Physical Chemistry C*. Vol. 127(30), pg. 14822-14829.

1050. Origin of magnetic ordering in half-Heusler RuMnGa. Chakraborty S., Gupta S., Pakhira S., et al. *Physical Review B*. Vol. 108(5), ArtNo. 54430.

1051. Origin of Strong Hydrogen Bonding and Preferred Orientation of Water at Uncharged Polyethylene Glycol Polymer/Water Interface. Patra A., Bandyopadhyay A., Roy S., et al. *Journal of Physical Chemistry Letters*. Vol. 14(50), pg. 11359-11366.

1052. Origin of the long-range ferrimagnetic ordering in cubic Mn(Co)Cr2 O4 spinels. Das A., Pal P., Ranaut D., et al. *Physical Review B*. Vol. 107(10), ArtNo. L100414.

1053. Output feedback Model Reference Adaptive Control of nuclear reactor. Reddy P.M.S., Shimjith S.R., Tiwari A.P., et al. *Nuclear Engineering and Design*. Vol. 407, ArtNo. 112276.

1054. Overview of Method of ChAracteristics based Neutron TRAnsport Code (MANTRA) and its validation. Mazumdar T., Singh T. *Nuclear and Particle Physics Proceedings*. Vol. 341 pg. 84-87.

1055. Overview of the physics challenges in design of new energy systems. Kannan U. *Nuclear and Particle Physics Proceedings*. Vol. 339-340 pg. 38-42.

1056. Oxidation behaviour of uranium and U–10wt.%Mo alloy in air. Rakesh R., Roy S.P., Jain A., et al. *Journal of Radioanalytical and Nuclear Chemistry*. Vol. 332(8), pg. 3181-3190.

1057. Oxidation studies of (U1−yGdy)O2.00; (y ≤ 0.2) under different oxygen partial pressures by thermogravimetry and in situ X-ray diffraction. Shafeeq M., Patkare G.R., Phatak R., et al. *Journal of Thermal Analysis and Calorimetry*. Vol. 148(14), pg. 6687-6698.

1058. Oxidation studies of SiC-coated 2.5D carbon fibre preforms. Tammana S.R.C.M., Venkatachalam V., Zou J., et al. *Open Ceramics*. Vol. 15, ArtNo. 100385.

1059. Oxygen ion vacancies in strontium cobalt oxides: neutron and X-ray diffraction study. Narayanan A.M., Wajhal S., Shinde A.B., et al. *Journal of Chemical Sciences*. Vol. 135(3), ArtNo. 76.

1060. Oxygen vacancy induced luminescence in Y2Zr2O7 and its removal on Eu3+ doping leading to enhanced quantum efficiency. Parayil R.T., Gupta S.K., Modak B., et al. *Materials Today Chemistry*. Vol. 33, ArtNo. 101744.

1061. Paediatric and adolescent ectopic Cushing's syndrome: systematic review. Yami Channaiah C., Karlekar M., Sarathi V., et al. *European Journal of Endocrinology*. Vol. 189(4), pg. S75-S87.

1062. Palladium-based membranes for potential application in bio-jet fuel production unit. Parashar R., Nailwal B.C., Goswami N., et al. Indian Chemical Engineer. Vol. 65(6), pg. 556-573.

1063. Parametric optimization of Sm(III) extraction from nitrate media by employing hollow fiber membrane using Taguchi analysis. Yadav K.K., Choudhury D., Singh D.K., et al. Separation Science and Technology (Philadelphia). Vol. 58(15-16), pg. 2655-2664.

1064. Pd “Kills Two Birds with One Stone” for the Synthesis of Catalyst: Dual Active Sites of Pd Triggers the Kinetics of O2 Electrocatalysis. Kumar G., Das S.K., Nayak C., et al. *Small*.

1065. Pd encapsulated core-shell ZIF-8/ZIF-67 for efficient oxygen evolution reaction. Varangane S., Jamma A., Prabhu Y.T., et al. *Electrochimica Acta*. Vol. 447, ArtNo. 142100.

1066. Pd-functionalized 2D TMDC MoTe2 monolayer as an efficient glucose Sensor: A First-principles DFT study. Lakshmy S., Kundu A., Kalarikkal N., et al. *Applied Surface Science*. Vol. 631, ArtNo. 157525.

1067. Peak Cyclic Stress and Ratcheting Response of a Low Alloy Steel for Reactor Pressure Vessel Applications. Gupta C. *Metallurgical and Materials Transactions A: Physical Metallurgy and Materials Science*. Vol. 54(4), pg. 1414-1427.

1068. Pechini citrate-gel synthesised In3+ substituted X-type barium zinc hexaferrites: An investigation on structural, optical, magnetic and dielectric properties. Patel A.G., Pullar R.C., Meena S.S., et al. *Materials Chemistry and Physics*. Vol. 293, ArtNo. 126947.

1069. Peptide receptor radionuclide therapy in neuroendocrine neoplasms and related tumors: from fundamentals to personalization and the newer experimental approaches. Loharkar S., Basu S. *Expert Review of Precision Medicine and Drug Development*. Vol. 8(1), pg. 1-32.

1070. Performance evaluation of an indigenously-designed high performance dynamic feeding robotic structure using advanced additive manufacturing technology, machine learning and robot kinematics. Parikh P., Sharma A., Trivedi R., et al. *International Journal on Interactive Design and Manufacturing*.

1071. Performance of small- and wide-angle x-ray scattering beamline at Indus-2 synchrotron. Das A., Bahadur J., Kumar A., et al. *Review of Scientific Instruments*. Vol. 94(4), ArtNo. 43902.

1072. Performance of the local reconstruction algorithms for the CMS hadron calorimeter with Run 2 data. Tumasyan A., Adam W., Andrejkovic J.W., et al. *Journal of Instrumentation*. Vol. 11, ArtNo. P11017.

1073. Perspectives of different colour-emissive nanomaterials in fluorescent ink, LEDs, cell imaging, and sensing of various analytes. Atulbhai S.V., Singhal R.K., Basu H., et al. *Luminescence*. Vol. 38(7), pg. 867-895.

1074. Perspectives on phage therapy for health management in aquaculture. Rai S., Kaur B., Singh P., et al. *Aquaculture International*.

1075. PET-Computed Tomography in Bone and Joint Infections. Loharkar S., Basu S. *PET Clinics*. Vol. 18(1), pg. 49-69.

1076. pH assisted modulation in the binding affinity for BODIPY-benzimidazole conjugate with anionic cyclodextrin. Chakraborty G., Chattaraj S., Pal H. *Journal of Photochemistry and Photobiology A: Chemistry*. Vol. 434, ArtNo. 114266.

1077. pH tolerant metal ion controlled luminescence behaviour of supramolecular assembly and its application in bioimaging and supramolecular logic gate. Prasad N., Shelar S., Sayed M. *Journal of Molecular Liquids*. Vol. 369, ArtNo. 120834.

1078. Phase Engineering of Molybdenum Dichalcogenide to Anion-Tunable Polyphasic Quaternary Chalcogenide (2H/1T/1T') MoSxSeyTez (x + y + z = 2) Amplifies the Growth of H2 Electrolytically. Sarkar A., Sanyal G., Chakraborty B., et al. *ACS Applied Energy Materials*. Vol. 6(15), pg. 8017-8031.

1079. Phase Evolution and Microstructural Behavior in Plasma-sprayed YPO4 Coating upon Thermal Cycling. Bhandari S., Chakravarthy Y., Misra V.C., et al. *Journal of Thermal Spray Technology*. Vol. 32(1), pg. 46-58.

1080. Phase evolution in the UO2–CeO2 system under oxidizing and reducing conditions: X-ray diffraction and spectroscopic studies. Nandi C., Grover V., Kesari S., et al. *Journal of Physics and Chemistry of Solids*. Vol. 180, ArtNo. 111444.

1081. Phase matching in quantum search algorithm. Chowdhury S.R., Baruah S., Dikshit B. *EPL*. Vol. 141(5), ArtNo. 58001.

1082. Phase relations and lattice parameter trends in Nd3+−substituted UO2 system under reducing and oxidizing conditions. Nandi C., Phatak R., Shafeeq M., et al. *Journal of Nuclear Materials*. Vol. 579, ArtNo. 154396.

1083. pH-Induced Biophysical Perspectives of Binding of Surface-Active Ionic Liquid [BMIM][OSU] with HSA and Dynamics of the Formed Complex. Ravikanth Reddy R., Saha D., Pan A., et al. *Langmuir*. Vol. 39(10), pg. 3729-3741.

1084. Phonon anharmonicity and equation of state parameters of orthovanadate Mg3(VO4)2: Raman Spectroscopy and X-ray diffraction investigation. Kesari S., Garg A.B., Rao R. *Solid State Sciences*. Vol. 139, ArtNo. 107186.

1085. Phosphorization Engineering on a MOF-Derived Metal Phosphide Heterostructure (Cu/Cu3P@NC) as an Electrode for Enhanced Supercapacitor Performance. Hussain N., Abbas Z., Ansari S.N., et al. *Inorganic Chemistry*. Vol. 62(42), pg. 17083-17092.

1086. Phosphorous/Fluorine Co-doped Biomass-derived Carbon for Enhanced Sodium-ion and Lithium-ion Storage. Dutta D.P., Modak B., Ravuri B.R. *ChemNanoMat*. Vol. 9(5), ArtNo. e202300077.

1087. Photoluminescence and third-order nonlinear optical limiting properties of Sn1-xNdxO2 thin films deposited via spray pyrolysis. Hind P.A., Patil P.S., Gummagol N.B., et al. *Ceramics International*. Vol. 49(18), pg. 30060-30075.

1088. Photophysical Modulation of Rhodamine-B via π-π stacking with GQD and Its Further Tuning by Cucurbit[7]uril**. Chakraborty G., Bondarde M.P., Ray A.K., et al. *ChemistrySelect*. Vol. 8(1), ArtNo. e202203689.

1089. Phthalimide/Naphthalimide containing 1,2,3-triazole hybrids: Synthesis and Antimicrobial Evaluation. Yadav P., Kaushik C.P., Kumar M., et al. *Journal of Molecular Structure*. Vol. 1276, ArtNo. 134688.

1090. Phylogenomics of transcriptionally active AP2/ERF and bHLH transcription factors and study of their promoter regions in Nothapodytes nimmoniana (J.Graham) Mabb. Godbole R.C., Kadam S.B., Pable A.A., et al. *Genome*. Vol. 66(9), pg. 235-250.

1091. Physicochemical Characterization, Stability, and In Vitro Evaluation of Curcumin-Loaded Solid Lipid Nanoparticles Prepared Using Biocompatible Synthetic Lipids. Patra S., Dey J., Chakraborty A. *ACS Applied Bio Materials*. Vol. 6(7), pg. 2785-2794.

1092. Physiochemical insight into the solution behavior of cationic gemini surfactant in water and ethanol–water systems. Kumar V., Patel P., Ray D., et al. *Journal of Surfactants and Detergents*. Vol. 26(5), pg. 623-632.

1093. Phytochemical profiling of Nothapodytes nimmoniana to understand camptothecin biosynthesis using tandem mass spectrometry. Godbole R.C., Pable A.A., Singh S., et al. *South African Journal of Botany*. Vol. 156 pg. 169-176.

1094. Picosecond laser-induced hybrid groove structures on Ti-6Al-4V bio-alloy to accelerate osseointegration. Kedia S., Checker R., Sandur S.K., et al. *Journal of Biomedical Materials Research - Part B Applied Biomaterials*. Vol. 111(10), pg. 1775-1784.

1095. Piezoelectric properties and structural evolution in La- and Al-modified K0.5Bi0.5TiO3 ceramics. Badole M., Vasavan H.N., Saxena S., et al. *Journal of Alloys and Compounds*. Vol. 944, ArtNo. 169204.

1096. Pilot-scale aerobic granular sludge reactors with granular activated carbon for effective nitrogen and phosphorus removal from domestic wastewater. Nancharaiah Y.V., Sarvajith M., Mohan T.V.K. *Science of the Total Environment*. Vol. 894, ArtNo. 164822.

1097. Plant regeneration through somatic embryogenesis in cell suspensions of Cenchrus ciliaris L.. Goyal S., Chatterjee V., Kulkarni V.M., et al. *Plant Methods*. Vol. 19(1), ArtNo. 110.

1098. Plastic scintillator detector for qualitative and quantitative measurements of gamma radiation. Thakur V.M., Bhosale N., Jain A., et al. *Radiation Detection Technology and Methods*. Vol. 7(4), pg. 578-588.

1099. Play of molecular host: guest assembly on a G-quadruplex binder. Alexander A., Pillai A.S., Grace S.R., et al. *Journal of Inclusion Phenomena and Macrocyclic Chemistry*. Vol. 103(45385), pg. 147-159.

1100. Pluronic Induced Interparticle Attraction and Re-entrant Liquid-Liquid Phase Separation in Charged Silica Nanoparticle Suspensions. Kumar S., Ganguly R., Nath S., et al. *Langmuir*. Vol. 39(23), pg. 8109-8119.

1101. PM1, PM2.5 and PM10 size fraction distribution under steady-state conditions in a walk-in type 222Rn calibration chamber facility. Vijith A.P., Mayya Y.S., Mishra R., et al. *Radiation Protection Dosimetry*. Vol. 199(20), pg. 2401-2405.

1102. Polyacrylonitrile support impregnated with amine-functionalized graphitic carbon nitride/magnetite composite nanofibers towards enhanced arsenic remediation: A mechanistic approach. Tripathy M., Padhiari S., Ghosh A.K., et al. *Journal of Colloid and Interface Science*. Vol. 640 pg. 890-907.

1103. Polyaniline modified waste-derived graphene/sulfur nanocomposite cathode for lithium–sulfur batteries. Ponmani P., Bahadur J., Tewari C., et al. *Journal of Polymer Science*. Vol. 61(18), pg. 2149-2162.

1104. Polyaniline/rGO/S composite cathode with GO modified separator for lithium sulfur battery: A multipronged approach to tackle the shuttle effect. Rao K.S., Pathak D.D., Mandal B.P., et al. *Materials Today Communications*. Vol. 36, ArtNo. 106708.

1105. Polyether phases of formic acid revealed under high pressure. Bhatt H., Verma A.K., Modak P. *Chemical Communications*. Vol. 59(65), pg. 9888-9891.

1106. Polyethylene terephthalate track etched membrane for recovery of helium from helium-nitrogen system. Nailwal B.C., Goswami N., Nair J.P., et al. *Express Polymer Letters*. Vol. 17(6), pg. 596-609.

1107. Polyethyleneimine-assisted formation of Ag-SiO2 hybrid microspheres for H2O2 sensing and SERS applications. Mehta S., Bahadur J., Sen D., et al. *RSC Advances*. Vol. 13(42), pg. 29086-29098.

1108. Polymer-based nanocomposites as defence material. Singh K., Jaiswal R., Kumar R., et al. *Bulletin of Materials Science*. Vol. 46(2), ArtNo. 79.

1109. Polymer-mediated tuning of the monomer-aggregate equilibrium of a coumarin derivative for ratiometric sensing of protamine. Mal D.K., Chittela R.K., Chakraborty G. *Organic and Biomolecular Chemistry*. Vol. 21(24), pg. 5079-5089.

1110. POP-Pincer Xantphos Pd Complex of 4-Pyridylthiolate: Cyclocarbonylative Reaction for the Synthesis of Flavones Using Cobalt Carbonyl as a C1 Source. Lokolkar M.S., Pal M.K., Dey S., et al. *Catalysis Letters*. Vol. 153(8), pg. 2359-2367.

1111. Pore anisotropy in shale and its dependence on thermal maturity and organic carbon content: A scanning SAXS study. Bahadur J., Chandra D., Das A., et al. *International Journal of Coal Geology*. Vol. 273, ArtNo. 104268.

1112. Pore morphology in thermally-treated shales and its implication on CO2 storage applications: A gas sorption, SEM, and small-angle scattering study. Chandra D., Bakshi T., Bahadur J., et al. *Fuel*. Vol. 331, ArtNo. 125877.

1113. Pore-Confined π-Chromophoric Tetracene as a Visible Light Harvester toward MOF-Based Photocatalytic CO2 Reduction in Water. Parambil S.R.V., Rahimi F.A., Ghosh R., et al. *Inorganic Chemistry*. Vol. 62(47), pg. 19312-19322.

1114. Pore-Structure Investigation of Bimetallic Zeolitic Imidazolate Framework-8 Films with Varying Co/Zn Nodes Ratio Using Depth Sensitive Positronium Annihilation Lifetime Spectroscopy. Nelliyil R.B., Mor J., Thota M., et al. *Journal of Physical Chemistry C*.

1115. Porosimetry of zeolitic imidazolate frameworks using positron annihilation lifetime spectroscopy. Mor J., Utpalla P., Bahadur J., et al. *Microporous and Mesoporous Materials*. Vol. 348, ArtNo. 112389.

1116. Porosity control of CNT aerogel and its conversion to CNT fiber in floating catalyst chemical vapour deposition. Alexander R., Kaushal A., Prakash J., et al. *Journal of Porous Materials*. Vol. 30(2), pg. 507-520.

1117. Portable and Room Temperature Operating H2S Gas Detection and Alert System Using Nanocrystalline SnO2Thin Films. Kanth S., Chikara A.K., Choudhury S., et al. *IEEE Sensors Letters*. Vol. 7(5), ArtNo. 5501704.

1118. Post-Neutron Fission Product Yield Distribution in the Spontaneous Fission of 244Cm. Naik H., Singh R.J., Jang W. *Nuclear Science and Engineering*. Vol. 197(1), pg. 25-44.

1119. Post-Neutron Mass Yield Distribution in the Epi-Cadmium Neutron-Induced Fission of 229Th. Naik H., Singh R.J., Dange S.P., et al. *Nuclear Science and Engineering*. Vol. 197(7), pg. 1265-1278.

1120. Post-Neutron Mass Yield Distribution in the Epi-Cadmium Neutron-Induced Fission of 233U. Naik H., Dange S.P., Singh R.J., et al. *Nuclear Science and Engineering*.

1121. Post-Neutron Mass Yield Distribution in the Epi-Cadmium Neutron–Induced Fission of 238Pu. Naik H., Singh R.J., Dange S.P., et al. *Nuclear Science and Engineering*.

1122. Post-Neutron Mass Yield Distribution in the Epi-Cadmium Neutron-Induced Fission of 241Pu. Naik H., Singh R.J., Dange S.P., et al. *Nuclear Science and Engineering*. Vol. 197(12), pg. 3110-3124.

1123. Post-Neutron Mass Yield Distribution in the Epi-Cadmium Neutron-Induced Fission of 245Cm. Naik H., Singh R.J., Jang W., et al. *Nuclear Science and Engineering*. Vol. 197(7), pg. 1279-1292.

1124. Post-Neutron Mass Yield Distribution in the Thermal Neutron Induced Fission of 233U. Naik H., Dange S.P., Singh R.J., et al. *Nuclear Science and Engineering*. Vol. 197(6), pg. 1133-1158.

1125. Post-Neutron Mass Yield Distribution in the Thermal Neutron–Induced Fission of 235U. Naik H., Dange S.P., Singh R.J., et al. *Nuclear Science and Engineering*. Vol. 197(4), pg. 485-509.

1126. Post-radiation treatment of 3,3'-diselenodipropionic acid augments cell kill by modulating DNA repair and cell migration pathways in A549 cells. Gandhi V.V., Gandhi K.A., Goda J.S., et al. *IUBMB Life*. Vol. 75(10), pg. 811-829.

1127. Post-synthetic modulation of UiO-66-NH2 with a cobaloxime catalyst for efficient hydrogen production. Sk S., Shelake S.P., Dolui D., et al. *Energy Advances*. Vol. 2(8), pg. 1116-1121.

1128. Potency of Extended X-ray Absorption Fine Structure Spectroscopy toward the Determination of Individual Bond Grüneisen Parameter for High Thermoelectric Performance. Basu R., Nayak C., Kumar R., et al. *ACS Applied Energy Materials*. Vol. 6(5), pg. 2981-2988.

1129. Potential behaviour of (Fe, Y) sites due to self-irradiation, as resolved through XAFS of natural metamict gadolinite. Lahiri D., Sengupta P., Rajput P., et al. *Ceramics International*. Vol. 49(18), pg. 30647-30655.

1130. Potential reversible hydrogen storage in Li-decorated carbon allotrope PAI-Graphene: A first-principles study. Mahamiya V., Shukla A., Chakraborty B. *International Journal of Hydrogen Energy*. Vol. 48(96), pg. 37898-37907.

1131. Prebiotic chemical origin of biomolecular complementarity. Sajeev Y. *Communications Chemistry*. Vol. 6(1), ArtNo. 259.

1132. Precipitation isotopes' response to the atmospheric processes over the mainland and the island region in the northern Indian Ocean: Implications to the paleo-monsoon study. Datye A., Chakraborty S., Chattopadhyay R., et al. *Mausam*. Vol. 74(2), pg. 503-512.

1133. Precise determination of quadrupole and hexadecapole deformation parameters of the sd-shell nucleus, 28Si. Gupta Y.K., Katariya V.B., Prajapati G.K., et al. *Physics Letters, Section B: Nuclear, Elementary Particle and High-Energy Physics*. Vol. 845, ArtNo. 138120.

1134. Precision measurement of the Z boson invisible width in pp collisions at s=13 TeV. Tumasyan A., Adam W., Andrejkovic J.W., et al. *Physics Letters, Section B: Nuclear, Elementary Particle and High-Energy Physics*. Vol. 842, ArtNo. 137563.

1135. Precision studies of QCD in the low energy domain of the EIC. Burkert V.D., Elouadrhiri L., Afanasev A., et al. *Progress in Particle and Nuclear Physics*. Vol. 131, ArtNo. 104032.

1136. Predicting porosity distribution effects on the orientation induced plastic anisotropy of ductile solids: A crystal plasticity investigation. Chandra S., Kumar S., Samal M.K., et al. *International Journal of Plasticity*. Vol. 171, ArtNo. 103781.

1137. Predicting the pair correlation functions of silicate and borosilicate glasses using machine learning. Ayush K., Sahu P., Ali S.M., et al. *Physical Chemistry Chemical Physics*. Vol. 26(2), pg. 1094-1104.

1138. Prediction of donor-acceptor-type novel noble gas complexes in the triplet electronic state. Kuntar S.P., Ghosh A., Ghanty T.K. *Physical Chemistry Chemical Physics*. Vol. 25(9), pg. 6987-6994.

1139. Prediction of electron beam weld quality from weld bead surface using clustering and support vector regression. Jaypuria S., Bondada V., Kumar Gupta S., et al. *Expert Systems with Applications*. Vol. 211, ArtNo. 118677.

1140. Preface. Sengupta A. *Separation Science and Technology (Philadelphia)*. Vol. 58(15-16), pg. 2603-2604.

1141. Pressure driven polymorphic transitions in nanocrystalline Lu2O3, Tm2O3 and Eu2O3. Bura N., Bhoriya A., Yadav D., et al. *Scientific Reports*. Vol. 13(1), ArtNo. 17365.

1142. Pressure tube replica imaging system for PHWR reactors based on optical coherence tomography. Goud B.K., Shinde D.D., Kamath M.P., et al. *Annals of Nuclear Energy*. Vol. 189, ArtNo. 109837.

1143. Pressure tuning of structure, magnetic frustration, and carrier conduction in the Kitaev spin liquid candidate Cu2IrO3. Pal S., Malavi P., Sinha A., et al. *Physical Review B*. Vol. 107(8), ArtNo. 85105.

1144. Pressure-induced electride phase formation in calcium: A key to its strange high-pressure behavior. Modak P., Verma A.K., Oppeneer P.M. *Physical Review B*. Vol. 107(12), ArtNo. 125152.

1145. Pressure-Induced Monoclinic to Tetragonal Phase Transition in RTaO4 (R = Nd, Sm): DFT-Based First Principles Studies. Banerjee S., Tyagi A., Garg A.B. *Crystals*. Vol. 13(2), ArtNo. 254.

1146. Pressure-induced multiple phase transitions in the magnetoelectric Co4Nb2 O9. Jana R., Garg A.B., Joseph B., et al. *Physical Review B*. Vol. 108(11), ArtNo. 115107.

1147. Pressure-Induced Phase Transition in MultilayeredVanadium Diselenide Nanosheets. Mishra K.K., Pandey K.K., Sree Raj K.A., et al. *Journal of Physical Chemistry C*. Vol. 127(1), pg. 368-380.

1148. Pressure-induced phase transition, its mechanism and compressibility studies on nanocrystalline and bulk U3O8. Shukla B., Kumar N.R.S., Maji D., et al. *Journal of Solid State Chemistry*. Vol. 328, ArtNo. 124340.

1149. Pressure-Induced Phase Transitions and Amorphization in HgCN(NO3). Jain A., Garg N., Chitnis A., et al. *Journal of Physical Chemistry C*. Vol. 127(43), pg. 21250-21260.

1150. Pressure-Induced Structural Phase Transitions in the Chromium Spinel LiInCr4O8 with Breathing Pyrochlore Lattice. Varma M., Krottenmüller M., Poswal H.K., et al. *Crystals*. Vol. 13(2), ArtNo. 170.

1151. Pressure-induced superconductivity in the weak topological insulator BiSe. Malavi P., Paul A., Bera A., et al. *Physical Review B*. Vol. 107(2), ArtNo. 24506.

1152. Pressure–temperature phase diagram of calcium up to 50 GPa pressure. Nayak B., Modak P. *Solid State Communications*. Vol. 360, ArtNo. 114993.

1153. Pristine and metal decorated biphenylene monolayer for enhanced adsorption of nitrobenzene: A DFT approach. Lakshmy S., Sanyal G., Kalarikkal N., et al. *Applied Surface Science*. Vol. 613, ArtNo. 155995.

1154. Pristine and transition metal decorated holey graphyne monolayer as an ammonia sensor: insights from DFT simulations. Lakshmy S., Kundu A., Kalarikkal N., et al. *Journal of Physics D: Applied Physics*. Vol. 56(5), ArtNo. 55402.

1155. Probabilistic Assessment of Groundwater Quality and Fluoride Exposure Risk for North-Eastern Rajasthan, India. Dauji S., Pant D., Keesari T. *Journal of Hazardous, Toxic, and Radioactive Waste*. Vol. 27(4), ArtNo. 4023030.

1156. Probable maximum tropical cyclone parameters for east and west coast of India. Kumar D.S., Behera M.R., Nadella S., et al. *Natural Hazards*. Vol. 116(2), pg. 2437-2455.

1157. Probing Heavy Majorana Neutrinos and the Weinberg Operator through Vector Boson Fusion Processes in Proton-Proton Collisions at Formula Presented. Tumasyan A., Adam W., Andrejkovic J.W., et al. *Physical Review Letters*. Vol. 131(1), ArtNo. 11803.

1158. Probing Microscale Structuring-Induced Phase Separation with Fluorescence Recovery Diffusion Dynamics in Poly(ethylene glycol) Solutions. Bhatt S., Bagchi D., Das A., et al. *ACS Omega*. Vol. 8(38), pg. 35219-35231.

1159. Probing Morphology-Dependent CdS/MoS2 Heterostructures for Photocatalytic and Light-Sensing Applications. Kundu B., Shajahan A.S., Chakraborty B., et al. *ACS Applied Nano Materials*. Vol. 6(24), pg. 23078-23089.

1160. Probing reaction mechanisms through residual cross section measurement for 7Li+Zn system. Singh A., Maiti M., Nag T.N., et al. *Physica Scripta*. Vol. 98(2), ArtNo. 25306.

1161. Probing room-temperature reactivity of H2S, SO2, and NO on the Li2MnO3 crystal surface by experimental and first-principles studies. Rajput K., Hernández-Fontes C., Gupta N.K., et al. *New Journal of Chemistry*. Vol. 47(39), pg. 18400-18410.

1162. Probing site-selective doping and charge compensating defects in KMgF3: insights from a hybrid DFT study. Modak P., Modak B., Arya A. *Physical Chemistry Chemical Physics*. Vol. 25(43), pg. 29968-29981.

1163. Probing Small Bjorken-x Nuclear Gluonic Structure via Coherent J=ψ Photoproduction in Ultraperipheral Pb-Pb Collisions at √sNN = 5.02 TeV. Tumasyan A., Adam W., Andrejkovic J.W., et al. *Physical Review Letters*. Vol. 131(26), ArtNo. 262301.

1164. Probing stability of the charge-reversed nanoparticles in electrolyte and surfactant solutions. Singh H., Kumar S., Aswal V.K. *Chemical Physics Letters*. Vol. 818, ArtNo. 140433.

1165. Probing structural evolutions in GdVO4 under extreme thermodynamic conditions. Bhoriya A., Bura N., Yadav D., et al. *Journal of Solid State Chemistry*. Vol. 324, ArtNo. 124072.

1166. Probing the effect of Y3+/Gd3+ on the optical properties of Gd2-xYxTiO5:Eu3+: Insight into local site-luminescence correlation. Jafar M., Balhara A., Sawant P., et al. *Inorganic Chemistry Communications*. Vol. 157, ArtNo. 111344.

1167. Probing the effect of Zn2+ on the local structure, dielectric and magnetic properties of La2CuMnO6 by solid state synthesis. Singh D.N., Shamim M.K., Panchal G., et al. *Journal of Alloys and Compounds*. Vol. 936, ArtNo. 168241.

1168. Probing the IC/CMB interpretation for the X-ray knots of AGNs through VHE observations. Rahman A.A., Sahayanathan S., Malik Z., et al. *Monthly Notices of the Royal Astronomical Society*. Vol. 524(3), pg. 3335-3343.

1169. Process identification and discrimination in the environmental dose rate time series of a radiopharmaceutical facility using machine learning techniques. Chandra A., Saindane S., Murali S. *Applied Radiation and Isotopes*. Vol. 198, ArtNo. 110878.

1170. Process temperature-dependent interface quality and Maxwell-Wagner interfacial polarization in atomic layer deposited Al2O3/TiO2 nanolaminates for energy storage applications. Padhi P.S., Ajimsha R.S., Rai S.K., et al. *Nanoscale*. Vol. 15(18), pg. 8337-8355.

1171. Production of Bauxite Certified Reference Material (BARC-B1201) for Nine Property Values (Al2O3, Fe2O3, SiO2, TiO2, V2O5, MnO, Cr2O3, MgO and LOI) Traceable to SI Units. Prasad A.D., Rastogi L., Verma V.K., et al. *Geostandards and Geoanalytical Research*. Vol. 47(3), pg. 629-636.

1172. Production of bottomonia states in proton+proton and heavy-ion collisions. Kumar V., Shukla P., Bhattacharyya A. *Progress in Particle and Nuclear Physics*. Vol. 131, ArtNo. 104044.

1173. Profiling of conserved orthologs and miRNAs for understanding their role in salt tolerance mechanism of Sesuvium portulacastrum L.. Nikalje G.C., Srivastava A.K., Shelake R.M., et al. *Molecular Biology Reports*. Vol. 50(11), pg. 9731-9738.

1174. Prognostic predictors for recurrence following curative resection in grade I/II pancreatic neuroendocrine tumours. Chopde A., Gupta A., Chaudhari V., et al. *Langenbeck's Archives of Surgery*. Vol. 408(1), ArtNo. 204.

1175. Programmed cell death in Xanthomonas axonopodis pv. glycines is associated with modulation of gene expression resulting in altered states of motility, biofilm and virulence. Bandyopadhyay N.C., Gautam S. *Research in Microbiology*. Vol. 174(8), ArtNo. 104137.

1176. Progress on boron nitride nanostructure materials: properties, synthesis and applications in hydrogen storage and analytical chemistry. Revabhai P.M., Singhal R.K., Basu H., et al. *Journal of Nanostructure in Chemistry*. Vol. 13(1), pg. 1-41.

1177. Properties of alginate-like exopolymers recovered from flocculent and granular microbial sludges of different biological treatment systems treating real municipal wastewater. Sarvajith M., Nancharaiah Y.V. *Separation and Purification Technology*. Vol. 313, ArtNo. 123460.

1178. Prospects of additional contribution at optical-NIR band of EBL in the light of VHE spectra. Mankuzhiyil N., Persic M., Franceschini A. *Monthly Notices of the Royal Astronomical Society*. Vol. 524(1), pg. 133-142.

1179. Proton reconstruction with the CMS-TOTEM Precision Proton Spectrometer. Tumasyan A., Adam W., Andrejkovic J.W., et al. *Journal of Instrumentation*. Vol. 18(9), ArtNo. P09009.

1180. Proton Relay Mediated Electrocatalytic Hydrogen Evolution by an Economic Co(III) Complex. Majumder D., Kolay S., Tripathi V.S. *Electrocatalysis*. Vol. 14(4), pg. 602-610.

1181. Prussian blue nanoparticles–mediated sensing and removal of 137Cs. Pandey P.C., Yadav H.P., Tiwari A.K., et al. *Frontiers in Environmental Science*. Vol. 11, ArtNo. 1230983.

1182. PSMA Receptor-Based PET-CT: The Basics and Current Status in Clinical and Research Applications. Adnan A., Basu S. *Diagnostics*. Vol. 13(1), ArtNo. 158.

1183. PSMA-targeted radioligand therapy in prostate cancer: current status and future prospects. Parghane R.V., Basu S. *Expert Review of Anticancer Therapy*. Vol. 23(9), pg. 959-975.

1184. p-T-dependent structural transformations of Zn-monochalcogenides to switch their semiconductor–metal transition: a DFT study. Das P.K., Mondal S.K., Mandal N., et al. *Applied Physics A: Materials Science and Processing*. Vol. 129(7), ArtNo. 497.

1185. Publisher Correction: Charge-transfer interface of insulating metal-organic frameworks with metallic conduction (Nature Communications, (2022), 13, 1, (7665), 10.1038/s41467-022-35429-5). Sindhu P., Ananthram K.S., Jain A., et al. *Nature Communications*. Vol. 14(1), ArtNo. 187.

1186. Publisher Correction: Observation of triple J/ψ meson production in proton-proton collisions (Nature Physics, (2023), 19, 3, (338-350), 10.1038/s41567-022-01838-y). Tumasyan A., Adam W., Andrejkovic J.W., et al. *Nature Physics*. Vol. 19(3).

1187. Publisher Correction: Observation of triple J/ψ meson production in proton-proton collisions (Nature Physics, (2023), 19, 3, (338-350), 10.1038/s41567-022-01838-y). Tumasyan A., Adam W., Andrejkovic J.W., et al. *Nature Physics*. Vol., ArtNo. .

1188. Purification, characterization and proteolytic processing of mosquito larvicidal protein Cry11Aa from Bacillus thuringiensis subsp. israelensis ISPC-12. Kinkar O.U., Prashar A., Yadav B., et al. *International Journal of Biological Macromolecules*. Vol. 242, ArtNo. 124979.

1189. Purple-blue luminescence and magnetic properties of visible-light active novel BiMn2O5 photocatalyst by ultrasonication assisted sol–gel method. Dubey K., Dubey S., Modi A., et al. *Applied Physics A: Materials Science and Processing*. Vol. 129(10), ArtNo. 715.

1190. Pyrethroid pesticides: An overview on classification, toxicological assessment and monitoring. Ahamad A., Kumar J. *Journal of Hazardous Materials Advances*. Vol. 10, ArtNo. 100284.

1191. Quantification of 1.75 MeV Xe5+ induced defects in zirconia doped ceria (Ce0.8Zr0.2O2). Kumar V., Sharma S.K., Singh Y., et al. *Journal of Applied Physics*. Vol. 134(6), ArtNo. 65902.

1192. Quantifying nematic order in the evaporation-driven self-assembly of halloysite nanotubes: nematic islands and the critical aspect ratio. Dadwal A., Prasher M., Sengupta P., et al. *Soft Matter*. Vol. 19(46), pg. 9050-9058.

1193. Quantum error correction beyond the toric code: dynamical systems meet encoding. Rajpoot G., Kumari K., Jain S.R. *European Physical Journal: Special Topics*.

1194. Qubit control using quantum Zeno effect: Action principle approach. Kumari K., Rajpoot G., Joshi S., et al. *Annals of Physics*. Vol. 450, ArtNo. 169222.

1195. Quest for understanding neutron emission in nuclear fission: The case of Po 210. Dhuri S., Mahata K., Ramachandran K., et al. *Physical Review C*. Vol. 108(5), ArtNo. 54609.

1196. Quick Classification and Prediction of CO2, NH3, H2S, and NO2 Gases from Their Mixture Using a ZnO Nanowire-Based Electronic Nose. Sinju K.R., Bhangare B.K., Debnath A.K., et al. *Journal of Electronic Materials*. Vol. 52(7), pg. 4686-4698.

1197. Quintinite: A Mg–Al-layered double hydroxide as an efficient amido black dye adsorbent. Bokka S., Achary S.N., Chowdhury A. *Ceramics International*. Vol. 49(24), pg. 40866-40874.

1198. Radiation assisted hydrophobization of jute fiber. Jha A., Thite A., Chowdhury S.R., et al. *Journal of Applied Polymer Science*. Vol. 140(46), ArtNo. e54690.

1199. Radiation crosslinking and grafting of chitosan: Conversion of biowaste to an efficient adsorbent for removal of cationic dyes. Kumar S., Tiwari A., Chaudhari C.V., et al. *Analytical Chemistry Letters*. Vol. 13(6), pg. 682-698.

1200. Radiation effects and hardening of electronic components and systems: an overview. Ray A. *Indian Journal of Physics*. Vol. 97(10), pg. 3011-3031.

1201. Radiation processing in India: The voyage and present status. Bhardwaj Y.K., Dubey K.A. *Radiation Physics and Chemistry*. Vol. 212, ArtNo. 111171.

1202. Radiation processing of papad – A sustainable method to improve safety and shelf life. Bhoir S.A., Kanatt S.R. *Applied Radiation and Isotopes*. Vol. 201, ArtNo. 111017.

1203. Radiation response of Y3Al5O12 and Nd3+-Y3Al5O12 to Swift heavy ions: insight into structural damage and defect dynamics. Bhandari K., Grover V., Kalita P., et al. *Physical Chemistry Chemical Physics*. Vol. 25(30), pg. 20495-20509.

1204. Radiolabeled nanoporous hydroxyapatite microspheres: An advanced material for potential use in radiation synovectomy. Patra S., Chakravarty R., Bahadur J., et al. *Materials Chemistry and Physics*. Vol. 295, ArtNo. 127115.

1205. Radiolabelled folate micellar carriers as proposed diagnostic aid for CNS tumors by nasal route. Upadhaya P., Hazari P.P., Mishra A.K., et al. *Drug Delivery and Translational Research*. Vol. 13(10), pg. 2604-2613.

1206. Radio-Sensitivity Assessment of In Vitro Tissues of Stevia (Stevia rebaudiana Bert.) for Induced Mutagenesis. Subrahmanyeswari T., Gantait S., Kamble S.N., et al. *Sugar Tech*. Vol. 25(6), pg. 1520-1530.

1207. Radiosensitivity of seedling traits to varying gamma doses, optimum dose determination and variation in determined doses due to different time of sowings after irradiation and methods of irradiation in faba bean genotypes. Guha Mallick R., Pramanik S., Pandit M.K., et al. *International Journal of Radiation Biology*. Vol. 99(3), pg. 534-550.

1208. Radon build-up in a prototype dwelling using uranium mill tailings as construction material. Rana D., Jha V.N., Patnaik R.L., et al. *Journal of Radioanalytical and Nuclear Chemistry*. Vol. 332(8), pg. 3113-3120.

1209. Rapid and precise determination of the 238Pu/239Pu isotope ratio using thermal ionization mass spectrometry. Goswami P., Paul S., Bhushan K.S., et al. *Journal of Analytical Atomic Spectrometry*. Vol. 39(2), pg. 500-507.

1210. Rapid and reliable assaying of Tc-99 in sediment samples with novel MTPN polymeric resin. Pant A.D., Ruhela R., Pilllai A.S., et al. *Journal of Environmental Radioactivity*. Vol. 270, ArtNo. 107297.

1211. Reaction-Diffusion-Driven Stoichiometric Gradient in Coevaporated Superconducting NiBi3 Thin Films. Das B., Senapati T.R., Yadav A.K., et al. *Crystal Growth and Design*. Vol. 23(2), pg. 980-988.

1212. Reactivity of oxidants towards phenyl and benzyl substituted 5-selanylpentanoic acids: radiolytic and theoretical insights. Singh B.G., Prasanthkumar K.P., Mangiavacchi F., et al. *New Journal of Chemistry*. Vol. 48(1), pg. 36-44.

1213. Reactor physics calculation and measurement during first approach to criticality of Apsara-U research reactor. Singh T., Pandey P., Kumar J., et al. *Annals of Nuclear Energy*. Vol. 182, ArtNo. 109636.

1214. Reactor physics of research reactors at BARC: Aspects and scopes. Singh T. *Nuclear and Particle Physics Proceedings*. Vol. 339-340 pg. 160-167.

1215. Realizing an Optical Micro-Cavity in a CuCo2O4-W-CuCo2O4 Thin Film Stack for Spectrally Selective Solar Absorbers. Silpa S., Srinivas G., Biswas A., et al. *Advanced Optical Materials*. Vol. 11(19), ArtNo. 2300567.

1216. Recent advances in arsenic mitigation in rice through biotechnological approaches. Singh S., Srivastava S. *International Journal of Phytoremediation*. Vol. 25(3), pg. 305-313.

1217. Recent advances in Targeted Radionuclide therapy for Cancer treatment. Goel M., Mishra M.K., Kumar D. *Chemical Biology Letters*. Vol. 10(3), ArtNo. 544.

1218. Recent advances in ultra-trace determination of uranium in natural water using total reflection X-ray fluorescence (TXRF) spectrometry. Sanyal K., Dhara S. *X-Ray Spectrometry*.

1219. Recent development of two-dimensional tantalum dichalcogenides and their applications. kumar S., Pratap S., Joshi N., et al. *Micro and Nanostructures*. Vol. 181, ArtNo. 207627.

1220. Recent developments and future perspectives on energy storage and conversion applications of nickel molybdates. Sanyal G., Mondal B., Rout C.S., et al. *Energy Storage*. Vol. 5(6), ArtNo. e432.

1221. Recognising socio-cultural barriers while seeking early detection services for breast cancer: a study from a Universal Health Coverage setting in India. Sawhney R., Nathani P., Patil P., et al. *BMC Cancer*. Vol. 23(1), ArtNo. 881.

1222. Recombinant full-length Bacillus Anthracis protective antigen and its 63 kDa form elicits protective response in formulation with addavax. Sharma S., Bahl V., Srivastava G., et al. *Frontiers in Immunology*. Vol. 13, ArtNo. 1075662.

1223. Reconstruction of decays to merged photons using end-to-end deep learning with domain continuation in the CMS detector. Tumasyan A., Adam W., Andrejkovic J.W., et al. *Physical Review D*. Vol. 108(5), ArtNo. 52002.

1224. Recovery and enrichment of acid from metallurgical wastewater model by electrodialysis integrated diffusion dialysis system using poly(ethylene) based IEMs. Upadhyay P., Mishra S., Sharma J., et al. *Separation and Purification Technology*. Vol. 304, ArtNo. 122353.

1225. Recovery of Rare Earth Values from Micro-granite Type Hard Rocks Using Deep Eutectic Solvents. Karan R., Sreenivas T. *Transactions of the Indian Institute of Metals*.

1226. Red and NIR emitting ring-fused BODIPY/aza-BODIPY dyes. Shukla V.K., Chakraborty G., Ray A.K., et al. *Dyes and Pigments*. Vol. 215, ArtNo. 111245.

1227. Red light-activable biotinylated copper(II) complex-functionalized gold nanocomposite (Biotin-Cu@AuNP) towards targeted photodynamic therapy. Musib D., Upadhyay A., Pal M., et al. *Journal of Inorganic Biochemistry*. Vol. 243, ArtNo. 112183.

1228. Redox Potentials of Uranyl Ions in Macrocyclic Complexes: Quantifying the Role of Counter-Ions. Sundararajan M. *ACS Omega*. Vol. 8(20), pg. 18041-18046.

1229. Redox-labelled detection probe enabled immunoassay for simultaneous detection of multiple cancer biomarkers. Chellachamy Anbalagan A., Sawant S.N. *Microchimica Acta*. Vol. 190(3), ArtNo. 86.

1230. Reduction-sensitive shell crosslinked TPGS micelles: Formulation and colloidal characterizations. Sarolia J., Shah S.A., Aswal V.K., et al. *Colloids and Surfaces A: Physicochemical and Engineering Aspects*. Vol. 677, ArtNo. 132321.

1231. Re-engineered theranostic gold nanoparticles for targeting tumor hypoxia. Mittal S., Kumar C., Mallia M.B., et al. *Materials Advances*. Vol. 5(2), pg. 513-520.

1232. Relation of ηpl and γpl with separation parameter (S) and their usefulness for fracture toughness evaluation. Bind A.K., Singh R.N. *Engineering Fracture Mechanics*. Vol. 289, ArtNo. 109487.

1233. Relativistic coupled-cluster study of SrF for low-energy precision tests of fundamental physics. Talukdar K., Buragohain H., Nayak M.K., et al. *Theoretical Chemistry Accounts*. Vol. 142(2), ArtNo. 15.

1234. Release of an encrypted, highly potent ACE-inhibitory peptide by enzymatic hydrolysis of moth bean (Vigna aconitifolia) protein. Goyal N., Hajare S.N., Gautam S. *Frontiers in Nutrition*. Vol. 10, ArtNo. 1167259.

1235. Reliable liquified petroleum gas sensing at room temperature by nanocrystalline SnO2 thin film deposited by Langmuir–Blodgett method. Shah A.Y., Choudhury S., Betty C.A. *Applied Physics A: Materials Science and Processing*. Vol. 129(7), ArtNo. 478.

1236. Remarkable enhancement in CNT fiber synthesis by reducing convection vortex in floating catalyst chemical vapour deposition. Kaushal A., Alexander R., Mandal D., et al. *Chemical Engineering Journal*. Vol. 452, ArtNo. 139142.

1237. Remarkable enhancement in durability of ZrCo alloy against hydrogen induced disproportionation by Ti and Nb co-substitution. Jat R.A., Rawat D., Sharma A., et al. *International Journal of Hydrogen Energy*. Vol. 48(20), pg. 7431-7441.

1238. Remarkably enhanced upconversion luminescence in Na+ codoped spinel nanoparticles for photothermal cancer therapy and SPECT imaging. Balhara A., Gupta S.K., Aggarwal N., et al. *Materials Advances*. Vol. 4(21), pg. 5338-5352.

1239. Remediation and recycling of inorganic acids and their green alternatives for sustainable industrial chemical processes. Agarwal C., Pandey A.K. *Environmental Science: Advances*. Vol. 2(10), pg. 1306-1339.

1240. Removal of NOx using ozone injection and subsequent absorption in water. Bhowmick S., Badiwal A., Shenoy K.T. *Chemical Engineering Journal Advances*. Vol. 15, ArtNo. 100511.

1241. Reply to discussion of "Probable maximum tropical cyclone parameters for east and west coast of India" by Li and Kumar (2023). Kumar D.S., Behera M.R., Nadella S., et al. *Natural Hazards*. Vol. 118(1), pg. 867-870.

1242. Resonance nucleon scattering amplitude in the photonuclear reaction. Das S. *Nuclear Physics A*. Vol. 1035, ArtNo. 122657.

1243. Resonance Photoemission Spectroscopic Study of Thermally Evaporated NiTiO3 Thin Films. Singh N.K., Kumar A., Dawn R., et al. *Journal of Electronic Materials*. Vol. 52(1), pg. 669-678.

1244. Response of different cultivars of apricots to gamma irradiation under different storage conditions. Raja J., Masoodi F.A., Hussain P.R., et al. *Radiation Physics and Chemistry*. Vol. 202, ArtNo. 110518.

1245. Retention of Am(III) by montmorillonite: effect of sulphate. Kar A.S., Patel M.A., Tomar B.S. *Journal of Radioanalytical and Nuclear Chemistry*. Vol. 332(8), pg. 3069-3077.

1246. Retraction notice to 'Coupling between Ho and Mn/Cr moments and its influence on the structural and magnetic properties of HoMn1-xCrxO3 ($0 < x = 1$) compounds' [J. Mag. Mag. Mater. (2018) 70–80, (S0304885318305213), (10.1016/j.jmmm.2018.05.080)]. Prakash P., Singh R., Mishra S.K., et al. *Journal of Magnetism and Magnetic Materials*. Vol. 587, ArtNo. 170936.

1247. Retrieval and processing of radioactive muck settled in the bottom of radioactive liquid waste storage tanks. Prakash A.D., Sonar N.L., Sah R.K., et al. *Annals of Nuclear Energy*. Vol. 194, ArtNo. 110102.

1248. Reversible hydrogen adsorption in Ti-functionalized porous holey graphyne: Insights from first-principles calculation. Dewangan J., Mahamiya V., Shukla A., et al. *Energy Storage*. Vol. 5(1), ArtNo. e391.

1249. Reversion of strain induced martensite to achieve high strength and ductility in AISI 304 L. Sunil S., Kapoor R., Singh J.B. *Materials Characterization*. Vol. 205, ArtNo. 113353.

1250. rGO supported cobalt-manganese based nanocomposite with improved electrochemical water oxidation catalysis. Tavar D., Sharma R.K., Ashiq M., et al. *Journal of Materials Science*. Vol. 58(27), pg. 11270-11285.

1251. Rich magnetic phase diagram of putative helimagnet Sr3Fe2O7. Andriushin N.D., Grumbach J., Kim J.-H., et al. *Physical Review B*. Vol. 108(17), ArtNo. 174420.

1252. Role of ammonium ionic liquid and Pd nanoparticles in cavitation-based graphite decontamination and recycling process. Lahiri S., Mandal D. *Ultrasonics Sonochemistry*. Vol. 100, ArtNo. 106607.

1253. Role of Crystal Structure on the Ionic Conduction and Electrical Properties of Germanate Compounds A2Cu3Ge4O12(A = Na, K). Chikara K.S., Bera A.K., Kumar A., et al. *ACS Applied Electronic Materials*. Vol. 5(5), pg. 2704-2717.

1254. Role of dopant local structure and defects in optical properties of SrHfO3:Ln3+ perovskite: experimental and theoretical studies. Gupta S.K., Modak B., Meena G., et al. *Journal of Materials Science: Materials in Electronics*. Vol. 34(24), ArtNo. 1729.

1255. Role of Gemini Surfactants with Variable Spacers and SiO2 Nanoparticles in ct-DNA Compaction and Applications toward In Vitro/In Vivo Gene Delivery. Halder S., Paul M., Dyagala S., et al. *ACS Applied Bio Materials*. Vol. 6(7), pg. 2795-2815.

1256. Role of impedance plethysmography in detecting dysautonomia and vascular changes in the dysglycemic milieu of gestational diabetes - A case-Control study. Bhat S., Sudeep K., Jain R.K. *Medical Journal of Dr. D.Y. Patil Vidyapeeth*. Vol. 16(7), pg. S102-S109.

1257. Role of neutron transfer in the reaction mechanism of 9Be+169Tm, 181Ta, 187Re and 197Au systems. M. P., Parkar V.V., Jha V., et al. *Nuclear Physics A*. Vol. 1029, ArtNo. 122570.

1258. Role of PET/Computed Tomography in Elderly Thyroid Cancer: Tumor Biology and Clinical Management. Sonavane S.N., Basu S. *PET Clinics*. Vol. 18(1), pg. 81-101.

1259. Role of Plant-Derived Flavonoids in Cancer Treatment. Tiwari P., Mishra K.P. *Nutrition and Cancer*. Vol. 75(2), pg. 430-449.

1260. Role of Sm in tuning the third-order nonlinear optical properties of spray coated Sn1-xSmxO2 films. Asha Hind P., Patil P.S., Gummagol N.B., et al. *Optical Materials*. Vol. 137, ArtNo. 113513.

1261. Room temperature d 0 ferromagnetism in carbon doped LaH3: insights from density functional theory simulations. Sharma P., Shukla A., Chakraborty B. *Journal of Physics D: Applied Physics*. Vol. 56(9), ArtNo. 95001.

1262. Room-Temperature Absorption of Carbon Dioxide on an Improved Soda Lime-Based Absorber. Ghuge N.S., Mandal D. *Industrial and Engineering Chemistry Research*.

1263. Rotational and deperturbation analysis of the interacting A2Π1/2, v = 11 ~ B2Σ+, v = 6 states of yttrium monoxide (YO) molecule. Mukund S., Nakhate S.G. Journal of Quantitative Spectroscopy and Radiative Transfer. Vol. 296, ArtNo. 108452.

1264. Salt induced micellization conduct in PEO-PPO-PEO-based block copolymers: a thermo-responsive approach. Tripathi N., Ray D., Aswal V.K., et al. Soft Matter. Vol. 19(37), pg. 7227-7244.

1265. Saturated nucleate flow boiling over a horizontal single and multi-cylinder under cross-flow condition. Silvi L.D., Chandraker D.K., Ghosh S., et al. Applied Thermal Engineering. Vol. 234, ArtNo. 121252.

1266. Search for a heavy composite Majorana neutrino in events with dilepton signatures from proton-proton collisions at s=13 TeV. Tumasyan A., Adam W., Andrejkovic J.W., et al. *Physics Letters, Section B: Nuclear, Elementary Particle and High-Energy Physics*. Vol. 843, ArtNo. 137803.

1267. Search for a massive scalar resonance decaying to a light scalar and a Higgs boson in the four b quarks final state with boosted topology. Tumasyan A., Adam W., Andrejkovic J.W., et al. *Physics Letters, Section B: Nuclear, Elementary Particle and High-Energy Physics*. Vol. 842, ArtNo. 137392.

1268. Search for a vector-like quark T' → tH via the diphoton decay mode of the Higgs boson in proton-proton collisions at √s = 13 TeV. Tumasyan A., Adam W., Andrejkovic J.W., et al. *Journal of High Energy Physics*. Vol. 2023(9), ArtNo. 57.

1269. Search for CP violating top quark couplings in pp collisions at √s = 13 TeV. Tumasyan A., Adam W., Bergauer T., et al. *Journal of High Energy Physics*. Vol. 2023(7), ArtNo. 23.

1270. Search for CP violation in t t ¯ H and tH production in multilepton channels in proton-proton collisions at √s = 13 TeV. Tumasyan A., Adam W., Andrejkovic J.W., et al. *Journal of High Energy Physics*. Vol. 2023(7), ArtNo. 92.

1271. Search for CP violation using (Formula presented.) events in the lepton+jets channel in pp collisions at √s = 13 TeV. Tumasyan A., Adam W., Andrejkovic J.W., et al. *Journal of High Energy Physics*. Vol. 2023(6), ArtNo. 81.

1272. Search for direct pair production of supersymmetric partners of τ leptons in the final state with two hadronically decaying τ leptons and missing transverse momentum in proton-proton collisions at Formula Presented. Tumasyan A., Adam W., Andrejkovic J.W., et al. *Physical Review D*. Vol. 108(1), ArtNo. 12011.

1273. Search for electroweak production of charginos and neutralinos at s=13TeV in final states containing hadronic decays of WW, WZ, or WH and missing transverse momentum. Tumasyan A., Adam W., Andrejkovic J.W., et al. *Physics Letters, Section B: Nuclear, Elementary Particle and High-Energy Physics*. Vol. 842, ArtNo. 137460.

1274. Search for Exotic Higgs Boson Decays Formula Presented with Events Containing Two Merged Diphotons in Proton-Proton Collisions at Formula Presented. Tumasyan A., Adam W., Andrejkovic J.W., et al. *Physical Review Letters*. Vol. 131(10), ArtNo. 101801.

1275. Search for heavy resonances and quantum black holes in eμ, eτ, and μτ final states in proton-proton collisions at √s = 13 TeV. Tumasyan A., Adam W., Andrejkovic J.W., et al. *Journal of High Energy Physics*. Vol. 2023(5), ArtNo. 227.

1276. Search for Higgs Boson and Observation of Z Boson through Their Decay into a Charm Quark-Antiquark Pair in Boosted Topologies in Proton-Proton Collisions at Formula Presented. Tumasyan A., Adam W., Andrejkovic J.W., et al. *Physical Review Letters*. Vol. 131(4), ArtNo. 41801.

1277. Search for Higgs Boson Decay to a Charm Quark-Antiquark Pair in Proton-Proton Collisions at sqrt[s]=13 TeV. Tumasyan A., Adam W., Andrejkovic J.W., et al. *Physical review letters*. Vol. 131(6).

1278. Search for Higgs boson decays into Z and J/ψ and for Higgs and Z boson decays into J/ψ or Y pairs in pp collisions at s=13 TeV. Tumasyan A., Adam W., Andrejkovic J.W., et al. *Physics Letters, Section B: Nuclear, Elementary Particle and High-Energy Physics*. Vol. 842, ArtNo. 137534.

1279. Search for high-mass exclusive γγ → WW and γγ → ZZ production in proton-proton collisions at √s = 13 TeV. Tumasyan A., Adam W., Andrejkovic J.W., et al. *Journal of High Energy Physics*. Vol. 2023(7), ArtNo. 229.

1280. Search for light Higgs bosons from supersymmetric cascade decays in pp collisions at √s=13TeV. Tumasyan A., Adam W., Andrejkovic J.W., et al. *European Physical Journal C*. Vol. 83(7), ArtNo. 571.

1281. Search for long-lived particles decaying to a pair of muons in proton-proton collisions at √s = 13 TeV. Tumasyan A., Adam W., Andrejkovic J.W., et al. *Journal of High Energy Physics*. Vol. 2023(5), ArtNo. 228.

1282. Search for medium effects using jets from bottom quarks in PbPb collisions at sNN=5.02TeV. Tumasyan A., Adam W., Andrejkovic J.W., et al. *Physics Letters, Section B: Nuclear, Elementary Particle and High-Energy Physics*. Vol. 844, ArtNo. 137849.

1283. Search for narrow resonances in the Formula Presented-tagged dijet mass spectrum in proton-proton collisions at Formula Presented. Tumasyan A., Adam W., Andrejkovic J.W., et al. *Physical Review D*. Vol. 108(1), ArtNo. 12009.

1284. Search for new heavy resonances decaying to WW, WZ, ZZ, WH, or ZH boson pairs in the all-jets final state in proton-proton collisions at s=13TeV. Tumasyan A., Adam W., Andrejkovic J.W., et al. *Physics Letters, Section B: Nuclear, Elementary Particle and High-Energy Physics*. Vol. 844, ArtNo. 137813.

1285. Search for new physics in the τ lepton plus missing transverse momentum final state in proton-proton collisions at √s = 13 TeV. Tumasyan A., Adam W., Andrejkovic J.W., et al. *Journal of High Energy Physics*. Vol. 2023(9), ArtNo. 51.

1286. Search for new physics using effective field theory in 13 TeV pp collision events that contain a top quark pair and a boosted Z or Higgs boson. Tumasyan A., Adam W., Andrejkovic J.W., et al. *Physical Review D*. Vol. 108(3), ArtNo. 32008.

1287. Search for nonresonant Higgs boson pair production in final state with two bottom quarks and two tau leptons in proton-proton collisions at s=13 TeV. Tumasyan A., Adam W., Andrejkovic J.W., et al. *Physics Letters, Section B: Nuclear, Elementary Particle and High-Energy Physics*. Vol. 842, ArtNo. 137531.

1288. Search for nonresonant Higgs boson pair production in the four leptons plus twob jets final state in proton-proton collisions at √s = 13 TeV. Tumasyan A., Adam W., Andrejkovic J.W., et al. *Journal of High Energy Physics*. Vol. 2023(6), ArtNo. 130.

1289. Search for Nonresonant Pair Production of Highly Energetic Higgs Bosons Decaying to Bottom Quarks. Tumasyan A., Adam W., Andrejkovic J.W., et al. *Physical Review Letters*. Vol. 131(4), ArtNo. 41803.

1290. Search for pair-produced vector-like leptons in final states with third-generation leptons and at least three b quark jets in proton-proton collisions at s=13TeV. Tumasyan A., Adam W., Andrejkovic J.W., et al. *Physics Letters, Section B: Nuclear, Elementary Particle and High-Energy Physics*. Vol. 846, ArtNo. 137713.

1291. Search for the Higgs boson decay to a pair of electrons in proton-proton collisions at s=13TeV. Tumasyan A., Adam W., Andrejkovic J.W., et al. *Physics Letters, Section B: Nuclear, Elementary Particle and High-Energy Physics*. Vol. 846, ArtNo. 137783.

1292. Search for top squarks in the four-body decay mode with single lepton final states in proton-proton collisions at √s = 13 TeV. Tumasyan A., Adam W., Andrejkovic J.W., et al. *Journal of High Energy Physics*. Vol. 2023(6), ArtNo. 60.

1293. Seasonal Variability in Key Radiological Attributes in U-Processing Plant and Solid Waste Disposal Sites at Jaduguda, India. Rana D., Jha V.N., Patnaik R.L., et al. *Mapan - Journal of Metrology Society of India*. Vol., ArtNo. .

1294. Seasonal variability of 222Rn and 220Rn equilibrium factors in indoor environment of Kumaun Himalaya, India. Ahamad T., Nautiyal O.P., Joshi M., et al. *Journal of Radioanalytical and Nuclear Chemistry*. Vol., ArtNo. .

1295. Selective detection of Cd (II) and Cr (VI) ions using rGO functionalized metal doped SnO2 nanocomposites. Choudhari U., Ramgir N., Late D., et al. *Microchemical Journal*. Vol. 190, ArtNo. 108728.

1296. Selective Electrocatalytic Oxidation of Nitrogen to Nitric Acid Using Manganese Phthalocyanine. Adalder A., Paul S., Ghorai B., et al. *ACS Applied Materials and Interfaces*. Vol. 15(29), pg. 34642-34650.

1297. Selective Extraction of Thorium(IV) from Uranium and Rare Earth Elements Using Tetraphenylethane-1,2-diylbis(phosphoramidate). Saha A., Kumari K., Sharma S., et al. *Inorganic Chemistry*. Vol. 62(24), pg. 9391-9399.

1298. Selective extraction of zirconium from zirconium nitrate solution in a pulsed stirred column. Pandey G., Darekar M., Singh K.K., et al. *Separation Science and Technology (Philadelphia)*. Vol. 58(15-16), pg. 2710-2717.

1299. Selective Ion Transport through a Self-Standing Protein-Based Biopolymer. Deshmukh S., Deore A., Mani A.M., et al. *ACS Applied Polymer Materials*. Vol. 5(9), pg. 7060-7068.

1300. Selective removal of uranium from aqueous streams using synergistic adsorbents. Das A., Gupta J., Gupta N., et al. *Inorganic Chemistry Communications*. Vol. 156, ArtNo. 111284.

1301. Selective targeting of gold nanoparticles for radiosensitization of somatostatin 2 receptor-expressing cancer cells. Shelar S.B., Barick K.C., Dutta B., et al. *Journal of Drug Delivery Science and Technology*. Vol. 82, ArtNo. 104381.

1302. Selenite reduction and biogenesis of selenium-nanoparticles by different size groups of aerobic granular sludge under aerobic conditions. Sudharsan G., Sarvajith M., Nancharaiah Y.V. *Journal of Environmental Management*. Vol. 334, ArtNo. 117482.

1303. Self-assembly generation triggered in highly hydrophilic Pluronics® by sugars/ polyols. Patel D., Tripathi N., Ray D., et al. *Journal of Molecular Liquids*. Vol. 378, ArtNo. 121614.

1304. Self-assembly modulation in star block copolymers by amphiphilic diol: A scattering insight. Patel A., Ray D., Parekh P., et al. *Journal of Molecular Liquids*. Vol. 380, ArtNo. 121726.

1305. Self-assembly of reverse poloxamine induced by saccharide excipients: Insights from fluorescence. Anilkumar A., Dutta Choudhury S. *Journal of Molecular Liquids*. Vol. 381, ArtNo. 121792.

1306. Sensitive turn-off detection of nitroaromatics using fluorescent tetraphenylethylene phosphonate derivative. Malegaonkar J.N., Al Kobaisi M., Singh P.K., et al. *Journal of Photochemistry and Photobiology A: Chemistry*. Vol. 438, ArtNo. 114530.

1307. Sensitivity of β4 values extracted from quasi elastic barrier distribution to the 2n transfer channel. Mohanto G., Parihari A., Gupta Y.K., et al. *European Physical Journal A*. Vol. 59(10), ArtNo. 234.

1308. Separation and determination of boron, chlorine, fluorine and molybdenum in uranium silicide using pyrohydrolysis and ion chromatography. Mishra V.G., Thakur U.K., Shah D.J., et al. *Journal of Radioanalytical and Nuclear Chemistry*. Vol. 332(1), pg. 15-22.

1309. Separation and determination of trace level terbium in gadolinium matrix by ion interaction chromatography. Mishra V.G., Das M.K., Raut V.V., et al. *Separation Science and Technology (Philadelphia)*. Vol. 58(15-16), pg. 2704-2709.

1310. Separation of fluoride in the presence of large amounts of organic acids by ion chromatography. Arul Suganthi C., Raut V.V., Bharti N.K., et al. *Separation Science and Technology (Philadelphia)*. Vol. 58(15-16), pg. 2759-2766.

1311. Sequestration of Actinides by an Extraction Chromatography Resin Containing a Triaza-9-crown-3 Functionalized Diglycolamide. Banerjee P., Ansari S.A., Mohapatra P.K., et al. Industrial and Engineering Chemistry Research. Vol. 62(35), pg. 13966-13973.

1312. Sequestration of Np4+ and NpO22+ ions by using diglycolamide-functionalized azacrown ethers in C8mim•NTf2 ionic liquid: Extraction, spectroscopic, electrochemical and DFT studies. Gujar R.B., Verma P.K., Mahanty B., et al. Journal of Molecular Liquids. Vol. 370, ArtNo. 120872.

1313. Shell effect driven fission modes in fragment mass and total kinetic energy distribution of Hg ∗ 192. Kumar R., Maiti M., Pal A., et al. Physical Review C. Vol. 107(3), ArtNo. 34614.

1314. Shell effect on fission fragment mass distribution at Ecn∗ up to 70 MeV: Role of multichance fission. Santra S., Pal A., Chattopadhyay D., et al. Physical Review C. Vol. 107(6), ArtNo. L061601.

1315. Sigma phase precipitation and growth in solution annealed 321 stainless steel during thermal aging: Effects on toughness & intergranular corrosion. Bonagani S.K., Chandra K., Ravikanth K.V., et al. Materials Science and Engineering: A. Vol. 888, ArtNo. 145763.

1316. Silver impregnated novel adsorbents for capture of elemental Mercury: A review. Shukla P., Singhal P., Manivannan S., et al. Environmental Nanotechnology, Monitoring and Management. Vol. 20, ArtNo. 100825.

1317. Silver nanoparticles-immobilized-radiation grafted polypropylene fabric as breathable, antibacterial wound dressing. Mehta K., Kumar V., Rai B., et al. *Radiation Physics and Chemistry*. Vol. 204, ArtNo. 110683.

1318. Silver zeolite in ultrasonically welded packed beds for enhanced elemental mercury capture from contaminated air stream: Adsorption and kinetics study. Shukla P., Manivannan S., Mandal D. *Microporous and Mesoporous Materials*. Vol. 359, ArtNo. 112651.

1319. Simple, Fast, and Selective Dissolution of Eu2O3 in an Ionic Liquid as a Sustainable Paradigm for Lanthanide-Actinide Separations in Radioactive Waste Remediation. Verma P.K., Mahanty B., Sengupta A., et al. *Inorganic Chemistry*. Vol. 62(1), pg. 87-97.

1320. Simulation of coupled flow and contaminant transport in an unconfined aquifer using the local radial point interpolation meshless method. Swetha K., Eldho T.I., Singh L.G., et al. *Hydrogeology Journal*. Vol. 31(2), pg. 485-500.

1321. Simulation of random medium of fuel pebble with liquid salt coolant using PebMC code. Singh I., Mallick A.K., Gupta A., et al. *Physics Open*. Vol. 17, ArtNo. 100190.

1322. Simulation study to assess the effectiveness of gamma radiation for inactivation of viruses on food packaging material. Tripathi J., Saxena S., Gautam S. *Radiation Physics and Chemistry*. Vol. 204, ArtNo. 110678.

1323. Simulations and experimentation of ultrasonic wave propagation and flaw characterisation for underwater concrete structures. Jain H., Patankar V.H. *Nondestructive Testing and Evaluation*.

1324. Simultaneous determination of flouride, iodate and iodide by ion chromatography in caustic off-gas scrubber of nuclear recycle facilities by employing dual detectors. Das M.K., Mishra V.G., Umadevi K., et al. *Separation Science and Technology (Philadelphia)*. Vol. 58(15-16), pg. 2867-2873.

1325. Single Stretch Wire and vibrating wire measurement system for characterization of multipole accelerator magnets. Teotia V., Malhotra S. *Journal of Instrumentation*. Vol. 18(7), ArtNo. P07029.

1326. Single-Atom Ru Catalyst-Decorated CNF(ZnO) Nanocages for Efficient H2 Evolution and CH3OH Production. Vennapoosa C.S., Varangane S., Abraham B.M., et al. *Journal of Physical Chemistry Letters*. Vol. 14(50), pg. 11400-11411.

1327. Single-Molecule Orientation Imaging Reveals Two Distinct Binding Configurations on Amyloid Fibrils. Sarkar A., Namboodiri V., Kumbhakar M. *Journal of Physical Chemistry Letters*. Vol. 14(21), pg. 4990-4996.

1328. Single-pot modus operandi for 2-amino-4H-chromenes synthesis utilizing amine functionalized graphene oxide decorated with zirconium oxide. Trivedi K., Kane S.R., Goutam U.K., et al. *Molecular Catalysis*. Vol. 550, ArtNo. 113591.

1329. Single-Wall-Carbon-Nanotube- VSe2 Nanohybrid for Ultrafast Visible-To-Near-Infrared Third-Order Nonlinear Optical Limiters. Kumar V., Mandal D., Sree Raj K.A., et al. *Physical Review Applied*. Vol. 19(4), ArtNo. 44081.

1330. SiNPLs/CoPc hybrid heterostructures based photodetector with low dark current and enhanced sensitivity. Kumar A., Karadan P., Samanta S., et al. *Materials Science in Semiconductor Processing*. Vol. 165, ArtNo. 107602.

1331. SIRT1 inhibits mitochondrial hyperfusion associated mito-bulb formation to sensitize oral cancer cells for apoptosis in a mtROS-dependent signalling pathway. Patra S., Singh A., Praharaj P.P., et al. *Cell Death and Disease*. Vol. 14(11), ArtNo. 732.

1332. Site preference-based luminescence studies in Eu doped calcium magnesium silicate phosphor: A combined experimental and DFT approach. Kuriyan N.S., Ghosh P.S., Arya A., et al. *Journal of Luminescence*. Vol. 260, ArtNo. 119901.

1333. Site-specific characterisation of hydrogeological parameters for low-level solid radioactive waste disposal facility at Tarapur, India. Goel S., Chopra M., Patra A.C., et al. *Journal of Earth System Science*. Vol. 132(3), ArtNo. 94.

1334. Size-segregated aerosol measurements during Diwali festival in an elevated background location. Buwaniwal A., Joshi M., Sharma V., et al. *Atmospheric Environment*. Vol. 314, ArtNo. 120078.

1335. Smart Magnetic Nanocarriers for Codelivery of Nitric Oxide and Doxorubicin for Enhanced Apoptosis in Cancer Cells. Dutta B., Shelar S.B., Nirmalraj A., et al. *ACS Omega*. Vol. 8(47), pg. 44545-44557.

1336. Sodium/lithium 3d transition metalates for chemisorption of gaseous pollutants: a review. Gupta N.K., Hernández-Fontes C., Achary S.N. *Materials Today Chemistry*. Vol. 27, ArtNo. 101329.

1337. Soil and Plant Enzymes Responses to Zinc Oxide Nanoparticles in Submerged Rice (Oryza sativa L.) Ecosystem. Srivastav A., Shukla A., Singhal R.K., et al. *Trends in Sciences*. Vol. 20(9), ArtNo. 5558.

1338. Sol-gel mediated synthesis and characterization of hierarchically porous Fe2O3/SiO2 monolithic catalyst for high temperature sulfuric acid decomposition. Kumar N., Banerjee A.M., Pai M.R., et al. *Catalysis Communications*. Vol. 179, ArtNo. 106686.

1339. Solid Flow Mapping at the Bottom Section of a Pilot-Plant Scale Riser with the Help of a Radioactive Particle Tracking Technique. Tribedi T., Tiwari P., Pant H.J., et al. *Industrial and Engineering Chemistry Research*.

1340. Solid solution of Cr3+ doped ZnGa2O4 and Zn2SnO4 to create cation inversion and its role on persistent deep red emission. Gupta S.K., Sudarshan K., Chandrashekhar D., et al. *Journal of Luminescence*. Vol. 257, ArtNo. 119697.

1341. SOLUTION OF FRACTIONAL-ORDER REACTION-ADVECTION-DIFFUSION EQUATION ARISING IN POROUS MEDIA. Biswas C., Das S., Singh A., et al. *Journal of Porous Media*. Vol. 26(1), pg. 15-29.

1342. Solution processable polypyrrole nanotubes as an alternative hole transporting material in perovskite solar cells. Jha P., Koiry S.P., Sridevi C., et al. *Materials Today Communications*. Vol. 35, ArtNo. 105994.

1343. Solvation Structure and Dynamics of Aqueous Solutions of Au+ Ions: A Molecular Dynamics Simulation Study. Saha S., Bhadyopadhyay D., Choudhury N. *Journal of Solution Chemistry*. Vol. 52(3), pg. 326-342.

1344. Solvent wash studies for the removal of di-butyl phosphate from spent solvent under simulated PUREX condition. Mishra S., Anand P.V., Patra C., et al. *Journal of Radioanalytical and Nuclear Chemistry*. Vol. 332(2), pg. 343-353.

1345. Somatostatin Receptor Targeted PET-CT and Its Role in the Management and Theranostics of Gastroenteropancreatic Neuroendocrine Neoplasms. Adnan A., Basu S. *Diagnostics*. Vol. 13(13), ArtNo. 2154.

1346. Sorption behavior studies of Cs and its migration in soil samples around Visakhapatnam, India. Maity S., Sandeep P., Mishra S., et al. *Environmental Monitoring and Assessment*. Vol. 195(6), ArtNo. 685.

1347. Sorption of long-lived 94Nb on magnetite: spectroscopic and electrochemical investigation of the associated mechanism. Ghosh M., Yadav A.K., Debnath A.K., et al. *Journal of Radioanalytical and Nuclear Chemistry*. Vol. 332(6), pg. 1969-1979.

1348. Sorption of ruthenium on aniline-siloxane composites. Ajith N., Dalvi A.A., Remya Devi P.S., et al. *Separation Science and Technology (Philadelphia)*. Vol. 58(15-16), pg. 2726-2737.

1349. Sorption study of long-lived 94Nb on laterite: Effects of physicochemical parameters on sorption. Ghosh M., Swain K.K. *Journal of Environmental Radioactivity*. Vol. 264, ArtNo. 107201.

1350. Spatio-temporal species kinetics, thermal and electrical field evolution in an argon EFCAP under different rates of nitrogen seeding: A one-dimensional simulation study. Chaturvedi Misra V., Ghorui S. *Vacuum*. Vol. 215, ArtNo. 112371.

1351. Spectroscopic features of a perylenediimide probe for sensing amyloid fibrils: in vivo imaging of Aβ-aggregates in a Drosophila model organism. Barooah N., Karmakar P., Sharanya M.K., et al. *Journal of Materials Chemistry B*. Vol. 11(39), pg. 9545-9554.

1352. Spectroscopic Investigation of Structural Perturbations in CsPbCl3 Perovskite Nanocrystals: Temperature- and Excitation-Energy-Dependent Study. Shukla A., Kaur G., Babu K.J., et al. *ACS Photonics*. Vol. 10(6), pg. 1906-1915.

1353. Speed Breeding Opportunities and Challenges for Crop Improvement. Sharma S., Kumar A., Dhakte P., et al. *Journal of Plant Growth Regulation*. Vol. 42(1), pg. 46-59.

1354. Sponge-Supported Low-Temperature Chemical Synthesis of the Hybrid Bi2O3@Ppy Electrode Material for Energy-Storage Devices. Shaikh Z.A., Shinde N.M., Shinde P.V., et al. *Energy and Fuels*. Vol. 37(5), pg. 4048-4057.

1355. Stability and morphology of cyanonaphthalene icy mantles on ISM cold dust analogues. Ramachandran R., Rahul K.K., Meka J.K., et al. *Journal of Chemical Sciences*. Vol. 135(3), ArtNo. 77.

1356. Stabilizing Polar Domains in MAPbBr3 via the Hydrostatic Pressure-Induced Liquid Crystal-like Transition. Maity S., Verma S., Ramaniah L.M., et al. *Journal of Physical Chemistry Letters*. Vol. 14(24), pg. 5497-5504.

1357. Steady state performance of molten salt natural circulation loop with different orientations of heater and cooler. Srivastava A.K., Saikrishna N., Maheshwari N.K. *Applied Thermal Engineering*. Vol. 218, ArtNo. 119318.

1358. Sterile neutrino searches with reactor antineutrinos using coherent neutrino-nucleus scattering experiments. Behera S.P., Mishra D.K., Netrakanti P.K., et al. *Physical Review D*. Vol. 108(11), ArtNo. 113002.

1359. Stochastic modelling of diffused and specular reflector efficiencies for scintillation detectors. Pany S.S., Singh S.G., Kar S., et al. *Journal of Optics (India)*. Vol. 52(4), pg. 1950-1961.

1360. Strategy to minimize induced 24Na, 56Mn activity in concrete composites used for fast neutron shielding: impact of cement and rock aggregates. Shanbhag A.A., Paul S., Sharma S.C., et al. *Journal of Radioanalytical and Nuclear Chemistry*. Vol. 332(8), pg. 3093-3102.

1361. Stress relaxation and thermal management in highly filled flexible styrene butadiene styrene copolymer-tungsten composites for high-energy radiation attenuation. Suman S.K., Sharma R., Kaul B.N., et al. *Polymer Composites*. Vol. 44(9), pg. 5819-5829.

1362. Structural and characterization assessment of clay ceramic water filter materials from locations near the Thar Desert in India. Duhan S., Gupta S., Agrawal A.K., et al. *Desalination and Water Treatment*. Vol. 309 pg. 236-248.

1363. Structural and magnetic properties of LaVO3 - Absence of anomalous diamagnetism. Anas M., Jain A., Gupta M., et al. *Ceramics International*. Vol. 49(6), pg. 9672-9680.

1364. Structural and vibrational properties of GdTaO4under compression: An insight from experiment and first principles simulations. Banerjee S., Garg A.B., Poswal H.K. *Journal of Applied Physics*. Vol. 133(2), ArtNo. 25902.

1365. Structural Changes in Liposomal Vesicles in Association with Sodium Taurodeoxycholate. Kumar D., Suna A., Ray D., et al. *AAPS PharmSciTech*. Vol. 24(4), ArtNo. 95.

1366. Structural characterization of transcription-coupled repair protein UVSSA and its interaction with TFIIH protein. Mistry H., Kumari S., Aswal V.K., et al. *International Journal of Biological Macromolecules*. Vol. 247, ArtNo. 125792.

1367. Structural characterization, defect evolution and luminescence properties of natural CaF2 under 10 MeV electron irradiation. Banerjee R.H., Alexander R., Chaudhary N., et al. *Ceramics International*. Vol. 49(13), pg. 21324-21334.

1368. Structural effects of benzene-centered tripodal diglycolamides on extraction of trivalent f-cations into a room temperature ionic liquid. Ansari S.A., Mohapatra P.K., Boda A., et al. *Journal of Molecular Liquids*. Vol. 382, ArtNo. 121861.

1369. Structural investigation of Ayurveda Lauha (Iron) Bhasma. Tiwari M.K., Singh A., Khooha A., et al. *Journal of Ayurveda and Integrative Medicine*. Vol. 14(2), ArtNo. 100690.

1370. Structural, dielectric, electric and magnetic properties of magnesium substituted lithium nanoferrites. Hashim M., Ravvinder Nayak D., Ahmed A., et al. *Ceramics International*. Vol. 49(19), pg. 31114-31123.

1371. Structural, magnetic, and biocompatibility evaluations of chromium substituted barium hexaferrite (Co2–Y) for hyperthermia application. Suthar M., Khare D., Gangwar A., et al. *Materials Chemistry and Physics*. Vol. 296, ArtNo. 127348.

1372. Structural, spectroscopic, magnetic, and magneto-transport behavior of Ruddlesden-Popper Ca4Mn3-xWxO10 (x = 0, 0.05, 0.1) compounds. Dubey K., Modi A., Pandey D.K., et al. *Journal of Magnetism and Magnetic Materials*. Vol. 587, ArtNo. 171292.

1373. Structurally Heterogeneous Amphiphilic Conetworks of Poly(vinyl imidazole) Derivatives with Potent Antimicrobial Properties and Cytocompatibility. Biswas A., Chandel A.K.S., Anuradha N., et al. *ACS Applied Materials and Interfaces*. Vol. 15(39), pg. 46333-46346.

1374. Structurally optimized MXene-based photocatalytic membrane to achieve self-cleaning properties and enhanced removal for small molecule from wastewater. He Z., Zheng H., Zeng G., et al. *Separation and Purification Technology*. Vol. 324, ArtNo. 124542.

1375. Structure and dynamics of the Li+ ion in water, methanol and acetonitrile solvents: ab initio molecular dynamics simulations. Rana R., Ali S.M., Maity D.K. *Physical Chemistry Chemical Physics*. Vol. 25(45), pg. 31382-31395.

1376. Structure and electrical properties of AM(PO3)4: A = Li, Na and M = Ce and Pr. Saha P., Rao K.S., Deshpande S.K., et al. *Materials Chemistry and Physics*. Vol. 304, ArtNo. 127891.

1377. Structure and stability of Au, Au2 and Au8 cluster on Ni(111) supported h-BN sheet: Role of size and support towards oxygen bond activation. Banerjee S., Nigam S., Majumder C. *Physica E: Low-Dimensional Systems and Nanostructures*. Vol. 147, ArtNo. 115561.

1378. Structure of water in poly(vinyl alcohol)-based ferrogels: effect of carbonyl iron concentration. Lawrence M.B., Rao R. *Journal of Polymer Research*. Vol. 30(2), ArtNo. 94.

1379. Structure, rheology, and 3D printing of salt-induced κ-carrageenan gels. Patel P., Mujmer K., Aswal V.K., et al. *Materials Today Communications*. Vol. 35, ArtNo. 105807.

1380. Structure-based virtual screening of chemical libraries as potential MELK inhibitors and their therapeutic evaluation against breast cancer. Das A., Prajapati A., Karna A., et al. *Chemico-Biological Interactions*. Vol. 376, ArtNo. 110443.

1381. Studies of Transient Photoplasma Evolution in an Electrostatic Field: Single Particle Motion to Its Collective Behavior. Jana B., Dikshit B. *IEEE Transactions on Plasma Science*. Vol. 51(2), pg. 344-351.

1382. Studies on application of indirect mode of ultrasound for feed brine pretreatment as fouling/scaling mitigation on heat exchanger surface. Banakar V.V., Gogate P.R., Raha A., et al. *Chemical Engineering and Processing - Process Intensification*. Vol. 187, ArtNo. 109345.

1383. Studies on diurnal variation of atmospheric tritium concentration at a sampling location near to PHWR site in Semi-Arid Zone, India. Nankar D.P., Patra A.K., Joshi C.P., et al. *Journal of Environmental Radioactivity*. Vol. 261, ArtNo. 107123.

1384. Studies on hydrometallurgical recovery of rare earth elements as mixed fluoride compound from coal fly ash using environmentally friendly organic acid. Karan R., Sreenivas T., Singh D.K. *Separation Science and Technology (Philadelphia)*. Vol. 58(15-16), pg. 2856-2866.

1385. Studies on metabolic regulation of schizosaccharomyces pombe biomass production for glucan yield improvement. Shetty P.R., Batchu U.R., Buddana S.K., et al. *Current Trends in Biotechnology and Pharmacy*. Vol. 17(2), pg. 773-787.

1386. Studies on Reaction Products, Byproducts, and Intermediates in Thermal Steps of the Cu-Cl Thermochemical Cycle for Hydrogen Generation. Singh R.V., Pai M.R., Banerjee A.M., et al. *Energy and Fuels*. Vol. 37(19), pg. 15206-15221.

1387. Studies on synthesis and densification of niobium diboride using carbothermic reduction and hot pressing. Arati D.S., Murthy Tammana S.R.C., Sonber J.K., et al. *International Journal of Refractory Metals and Hard Materials*. Vol. 112, ArtNo. 106119.

1388. Studies on the Rheological Characteristics of Flocculated Calcitic Ore Slurry. Serajuddin M., Kacham A.R., Mukhopadhyay S. *Journal of The Institution of Engineers (India): Series D*. Vol., ArtNo. .

1389. Studies on welding of thin stainless steel sheets with pulsed nanosecond fiber laser in butt joint configuration. Kumar A., Neogy S., Keskar N., et al. *Journal of Laser Applications*. Vol. 35(4), ArtNo. 42013.

1390. Study of an interesting interplay between thiourea and 4,6-dimethylpyrimidine-2-thiol with palladium(II) phosphine substrate. Lokhande S.V., Tyagi A., Butcher R.J., et al. *Polyhedron*. Vol. 230, ArtNo. 116221.

1391. Study of bias-induced degradation mechanism in perovskite CH3NH3PbI3-xClx solar cells by electroluminescence spectroscopy. Gupta D., Veerender P., Sridevi C., et al. *Applied Physics A: Materials Science and Processing*. Vol. 129(2), ArtNo. 127.

1392. Study of fractional-order reaction-advection-diffusion equation using neural network method. Biswas C., Singh A., Chopra M., et al. *Mathematics and Computers in Simulation*. Vol. 208 pg. 15-27.

1393. Study of physico-chemical properties of Cu2NiSnS4 thin films. Kolhe P., Musmade B.B., Koinkar P., et al. *Modern Physics Letters B*. Vol. 37(16), ArtNo. 2340007.

1394. Study of plutonium recovery from acidic feed using polyethersulfone encapsulating TBP, DEHPA, and mixture of TBP and DEHPA beads. Guchhait S.R., Patra K., Yadav K.K., et al. *Separation Science and Technology (Philadelphia)*. Vol. 58(15-16), pg. 2846-2855.

1395. Study of reactive electron beam deposited tantalum penta oxide thin films with spectroscopic ellipsometry and atomic force microscopy. Tokas R.B., Jena S., Prathap C., et al. *Applied Surface Science Advances*. Vol. 18, ArtNo. 100480.

1396. Study of thermal, structural, microstructural, vibrational and elastic properties of MnxMg0.8–xZn0.2Fe2O4 (0.1 ≤ x≤ 0.7) ferrite nanoparticles. Prasad S.A.V., Srinivas C., Jeevan Kumar R., et al. *Ceramics International*. Vol. 49(12), pg. 20419-20428.

1397. Study of thorium-induced micro-structural changes in mice femoral bone using SR-μCT. Agrawal A.K., Yadav R., Singh B., et al. *Toxicology and Environmental Health Sciences*. Vol. 15(4), pg. 399-410.

1398. Study on the influence of vent area on porosity-controlled wood crib compartment fires prior to flashover. Narang A., Kumar R., Dhiman A.K., et al. *Journal of Structural Fire Engineering*.

1399. Study on the integrity of prolonged steam oxidized clad column quenched at various reflood rates. Singh A.R., Puranik B., Gokhale O., et al. *Nuclear Engineering and Design*. Vol. 402, ArtNo. 112109.

1400. Studying the structural organization of non-membranous protein hemoglobin in a lipid environment after reconstitution. Kumari A., Saha D., Bhattacharya J., et al. *International Journal of Biological Macromolecules*. Vol. 243, ArtNo. 125212.

1401. Successive, overlapping transitions and magnetocaloric effect in Te doped Ni-Mn-Sn Heusler alloys. Archana R., Kavita S., Ramakrishna V.V., et al. *Journal of Alloys and Compounds*. Vol. 947, ArtNo. 169434.

1402. Sugar moiety driven adsorption of nucleic acid on graphene quantum dots: Photophysical, thermodynamic and theoretical evidence. Maiti S., Karmakar S., Kundu S., et al. *Journal of Molecular Liquids*. Vol. 371, ArtNo. 121148.

1403. Superior hydrogen storage capacity of Vanadium decorated biphenylene (Bi+V): A DFT study. Mane P., Kaur S.P., Singh M., et al. *International Journal of Hydrogen Energy*. Vol. 48(72), pg. 28076-28090.

1404. Superior Interfacial Contact Yields Efficient Electron Transfer Rate and Enhanced Solar Photocatalytic Hydrogen Generation in M/C3N4 Schottky Junctions. Rawool S.A., Pai M.R., Banerjee A.M., et al. *ACS Applied Materials and Interfaces*. Vol. 15(33), pg. 39926-39945.

1405. Suppression of Transients From Continuous Seismic Records Without Modifying the Amplitude of Ambient Noise. Gupta P., Mukhopadhyay S. *IEEE Sensors Journal*. Vol. 23(24), pg. 30703-30711.

1406. Supramolecular assemblies with macrocyclic hosts: applications in antibacterial activity. Koley S., Gaur M., Barooah N., et al. *Pure and Applied Chemistry*.

1407. Supramolecular assembly of coumarin 7 with sulfobutylether-β-cyclodextrin for biomolecular applications. Gayathry T.C., Gaur M., Mishra L., et al. *Frontiers in Chemistry*. Vol. 11, ArtNo. 1245518.

1408. Supramolecular association of a diguanidine derivative with a porphyrin-cyclodextrin conjugate and its binding to G-Quadruplex DNA. Alexander A., Pillai A.S., Akash B.A., et al. *Journal of Molecular Structure*. Vol. 1280, ArtNo. 135026.

1409. Supramolecular interaction of ofloxacin drug with p-sulfonatocalix[6]arene: Metal-ion responsive fluorescence behavior and enhanced antibacterial activity. Siddharthan A., Kumar V., Barooah N., et al. *Journal of Molecular Liquids*. Vol. 370, ArtNo. 121047.

1410. Surface grafted scintillation sensors for selective detection of low level plutonium alpha activity. Mhatre A., Agarwal C., Parayil R.T., et al. Sensors and Actuators B: Chemical. Vol. 390, ArtNo. 134021.

1411. Surface modification of multiwalled carbon nanotubes network through high energy electron beam and its implications on thermoelectric properties. Chaudhary N., Singh A., Roy M., et al. Materials Science and Engineering: B. Vol. 293, ArtNo. 116464.

1412. Surface modification of thin film composite nanofiltration membrane with graphene oxide by varying amine linkers: Synthesis, characterization, and applications. Vaishnavi P.S.V., Kar S., Adak A.K., et al. Journal of Membrane Science. Vol. 687, ArtNo. 122021.

1413. Surfactant assisted APTES functionalization of graphene oxide intercalated layered double hydroxide (LDH) for uranium adsorption from alkaline leach liquor. Das A., Jana A., Das D., et al. Journal of Cleaner Production. Vol. 390, ArtNo. 136058.

1414. Surfactant Assisted In Situ Synthesis of Nanofibrillated Cellulose/Polymethylsilsesquioxane Aerogel for Tuning Its Thermal Performance. Gupta P., Sathwane M., Chhajed M., et al. Macromolecular Rapid Communications. Vol. 44(2), ArtNo. 2200628.

1415. Susceptibility of Zr-2.5 (wt. %) Nb alloy to undergo nodular corrosion in water and steam environments: Effect of surface, cold work, temperature. Samanta A., Sawarn T.K., Banerjee S., et al. *Progress in Nuclear Energy*. Vol. 163, ArtNo. 104823.

1416. Sustainable approach for the synthesis of chiral β-aminoketones using an encapsulated chiral Zn(ii)-salen complex. Lakhani P., Kane S., Srivastava H., et al. *RSC Sustainability*. Vol. 1(7), pg. 1773-1782.

1417. Swarm Intelligence-based Modeling and Multi-objective Optimization of Welding Defect in Electron Beam Welding. Jaypuria S., Das A.K., Kanigalpula P.K.C., et al. *Arabian Journal for Science and Engineering*. Vol. 48(2), pg. 1807-1827.

1418. Synergistic Catalytic Effects of CeCuO3 @ Vulcan Carbon Composites on the Oxygen Reduction Reaction. Ranjan Mahalik R., Hota I., Bhushan Nayak B., et al. *ChemistrySelect*. Vol. 8(11), ArtNo. e202204124.

1419. Synthesis and 177Lu Labeling of the First Retro Analog of the HER2-Targeting A9 Peptide: A Superior Variant. Sharma A.K., Sharma R., Das A., et al. *Bioconjugate Chemistry*. Vol. 34(9), pg. 1576-1584.

1420. Synthesis and Characterization of Cobalt doped Zinc Ferrite for its Structural and Magnetic Properties. Yadav A.C., Tiwari P.R., Singh G., et al. *Asian Journal of Chemistry*. Vol. 35(10), pg. 2461-2467.

1421. Synthesis and evaluation of phosphonato-triphenylamine fluorophore as a highly sensitive chemosensor for nitroaromatics. Malegaonkar J.N., More K.S., Singh P.K., et al. *Journal of Photochemistry and Photobiology A: Chemistry*. Vol. 445, ArtNo. 115105.

1422. Synthesis and feasibility studies of doping U at Ti site of Y2Ti2O7 as a radioactive waste immobilization matrix. Gumber N., Shafeeq M., Gupta S.K., et al. *Dalton Transactions*. Vol. 52(39), pg. 14170-14181.

1423. Synthesis mechanism and 'orthodoxy' test based field emission analysis of hybrid and pristine graphene nanowalls deposited on thin Kovar wires. Kar R., Sarkar S.G., Mishra L., et al. *Diamond and Related Materials*. Vol. 137, ArtNo. 110134.

1424. Synthesis of amine functionalized SiO2 microspheres loaded polymeric hydrogel and its application for simultaneous eviction of divalent metal ions (Pb2+, Cd2+, Cu2+ and Ni2+). Singh S., Koley S., Modak B., et al. *Materials Today Chemistry*. Vol. 33, ArtNo. 101720.

1425. Synthesis of dual state emissive β-carboline boron complexes. Dutta K., Agrawal R., Wadawale A.P., et al. *New Journal of Chemistry*. Vol. 47(24), pg. 11371-11375.

1426. Synthesis of Galactoacrylamide and Study of Stimuli-Responsive Fluorescent Hierarchical Self-Assembly-Promoted Specific Interactions with Proteins. Ajish J.K., Ajish Kumar K.S. *ChemistrySelect*. Vol. 8(37), ArtNo. e202301497.

1427. Synthesis of Heavy-Atom-Free Triplet Photosensitizers Based on Organoboron Complexes. Koli M., Mula S. *Synlett*. Vol. 35(1), pg. 84-90.

1428. Synthesis of multicolor silver nanostructures for colorimetric sensing of metal ions (Cr3+, Hg2+ and K+) in industrial water and urine samples with different spectral characteristics. Patel M.R., Upadhyay M.D., Ghosh S., et al. *Environmental Research*. Vol. 232, ArtNo. 116318.

1429. Synthesis of PEI functionalized silica microsphere loaded polymeric network for simultaneous removal of Cr (III) & Cr (VI) from aquatic medium. Singh S., Basu H., Pimple M.V., et al. *Materials Today Communications*. Vol. 35, ArtNo. 105706.

1430. Synthesis, biological evaluation and theoretical studies of (E)-1-(4-sulfamoyl-phenylethyl)-3-arylidene-5-aryl-1H-pyrrol-2(3H)-ones as human carbonic anhydrase inhibitors. Ramzan F., Nabi S.A., Lone M.S., et al. *Journal of Enzyme Inhibition and Medicinal Chemistry*. Vol. 38(1), ArtNo. 2189126.

1431. Synthesis, Characterization and in vitro Antifungal Action of Gum Ghatti Capped Copper Oxide Nanoparticles. Kora A.J. *Biointerface Research in Applied Chemistry*. Vol. 13(2), ArtNo. 138.

1432. Synthesis, microstructure and electrochemical properties of Ni-P-based alloy coatings for hydrogen evolution reaction in alkaline media. Gaikwad A.P., Banerjee A.M., Pai M.R., et al. *Materials Research Express*. Vol. 10(8), ArtNo. 86514.

1433. Systematic study of (p, n) and (p, 2n) reactions on 110Cd. Vashi V., Makwana R., Quintana B., et al. *Radiation Physics and Chemistry*. Vol. 208, ArtNo. 110933.

1434. Systematics and mechanisms of α production with weakly and strongly bound projectiles. Parkar V.V., Jha V., Kailas S. *European Physical Journal A*. Vol. 59(4), ArtNo. 88.

1435. Systemic Therapy for Tumor Control in Metastatic Well-Differentiated Gastroenteropancreatic Neuroendocrine Tumors: ASCO Guideline. Del Rivero J., Perez K., Kennedy E.B., et al. *Journal of Clinical Oncology*. Vol. 41(32), pg. 5049-5067.

1436. T9GPred: A Comprehensive Computational Tool for the Prediction of Type 9 Secretion System, Gliding Motility, and the Associated Secreted Proteins. Sahoo A.K., Vivek-Ananth R.P., Chivukula N., et al. *ACS Omega*. Vol. 8(37), pg. 34091-34102.

1437. Ta interfaced CoFeB: Role of CoFeB thickness and thermal annealing in modification of structural and magnetic properties. Vardhan H., Srihari V., Sharma K., et al. *Surfaces and Interfaces*. Vol. 41, ArtNo. 103156.

1438. Tailoring Acid Free-Paper based Analytical Devices (Af-PADs) via radiation assisted modification of cellulose paper. Rawat S., Misra N., Shelkar S.A., et al. *Carbohydrate Polymers*. Vol. 317, ArtNo. 121116.

1439. Tailoring of microwave power density in an ECR ion source using an optimized ridge coupler. Phogat M., Mathew J.V. *Physica Scripta*. Vol. 98(7), ArtNo. 75605.

1440. Tailoring oxygen vacancies in ThO2 for improved light emission and ORR electrocatalysis. Das D., Gupta R., Gupta S.K., et al. *Materials Today Chemistry*. Vol. 32, ArtNo. 101635.

1441. Tamm plasmon polariton in planar structures: A brief overview and applications. Kar C., Jena S., Udupa D.V., et al. *Optics and Laser Technology*. Vol. 159, ArtNo. 108928.

1442. Targeting HER2-receptors with 177Lu-labeled triazole stapled cyclic peptidomimetic. Kumar Sharma A., Satpati D., Sharma R., et al. *Bioorganic Chemistry*. Vol. 135, ArtNo. 106503.

1443. Technetium-99m labeled core shell hyaluronate nanoparticles as tumor responsive, metastatic skeletal lesion targeted combinatorial theranostics. Kaur S., Balakrishnan B., Mallia M.B., et al. *Carbohydrate Polymers*. Vol. 312, ArtNo. 120840.

1444. Techno-economic and 4E comparisons of various thermodynamic power cycles for low-medium grade heat recovery. Srivastava M., Sarkar J., Sarkar A., et al. *Process Safety and Environmental Protection*. Vol. 178 pg. 528-539.

1445. Temperature Dependent Crystal Structure of Nd2CuTiO6: An In Situ Low Temperature Powder Neutron Diffraction Study. Kumar N., Kaushik S.D., Rao K.S., et al. *Crystals*. Vol. 13(3), ArtNo. 503.

1446. Temperature dependent transport characteristics of La0.9Sr0.1MnO3 / SrNb0.002Ti0.998O3 device. Hirpara B., Gadani K., Udeshi B., et al. *Materials Today Communications*. Vol. 35, ArtNo. 106069.

1447. Temperature-dependent anomalous viscosity of aqueous solutions of imidazolium-based ionic liquids. Kaushik D., Hitaishi P., Kumar A., et al. *Soft Matter*. Vol. 19(30), pg. 5674-5683.

1448. Temperature-dependent dielectric measurements and structural properties of barium stannate (BaSnO3). Shrivastava S., Nehra S., Kumar S., et al. *Journal of Alloys and Compounds*. Vol. 957, ArtNo. 170458.

1449. Temperature-driven structural phase transitions in 0.05(Na0.50Bi0.50)TiO3-0.95NaNbO3 solid solution via amplitude mode analysis. Jayakrishnan V.B., Mishra S.K., Sastry P.U. *EPL*. Vol. 143(4), ArtNo. 46003.

1450. Tensile Behavior of Alloy 690 in the Dynamic Strain Aging Regime. Sourabh K., Singh J.B. *Journal of Materials Engineering and Performance*. Vol. 32(7), pg. 2932-2949.

1451. Tensorial stress-plastic strain fields in α - ω Zr mixture, transformation kinetics, and friction in diamond-anvil cell. Levitas V.I., Dhar A., Pandey K.K. *Nature Communications*. Vol. 14(1), ArtNo. 5955.

1452. Terminal Solid Solubility of Hydrogen in an Alpha-Phase Titanium Alloy. Sinha P.K. *Metallurgical and Materials Transactions A: Physical Metallurgy and Materials Science*. Vol. 54(8), pg. 3112-3117.

1453. Ternary flexible ZnO (NWs)/PPy-silver composites film for ppb-level ammonia detection. Benhouhou S., Mekki A., Singh A. *Journal of Materials Science: Materials in Electronics*. Vol. 34(30), ArtNo. 2029.

1454. Testicular Metastasis from Neuroendocrine Tumors: Imaging and Theranostics Through 68Ga-DOTATATE PET/CT and 177Lu-DOTATATE-Based Peptide Receptor Radionuclide Therapy. Parghane R.V., Basu S. *Clinical Nuclear Medicine*. Vol. 48(12), pg. 1051-1052.

1455. The American Brachytherapy Society and Indian Brachytherapy Society consensus statement for the establishment of high-dose-rate brachytherapy programs for gynecological malignancies in low- and middle-income countries. Grover S., Lichter K.E., Likhacheva A., et al. *Brachytherapy*. Vol. 22(6), pg. 716-727.

1456. The atypical thioredoxin 'Alr2205', a newly identified partner of the typical 2-Cys-Peroxiredoxin, safeguards the cyanobacterium Anabaena from oxidative stress. Banerjee M., Waghamare N., Kalwani P., et al. *Biochemical Journal*. Vol. 480(1), pg. 87-104.

1457. The cAMP receptor protein (CRP) enhances the competitive nature of Salmonella Typhimurium. Sawant K., Shashidhar R. *Archives of Microbiology*. Vol. 205(5), ArtNo. 197.

1458. The Development and Validation of Radiopharmaceuticals Targeting Bacterial Infection. Signore A., Ordonez A.A., Arjun C., et al. *Journal of Nuclear Medicine*. Vol. 64(11), pg. 1676-1682.

1459. The elimination of an artifact in the FLURZnrc-derived electron-fluence spectrum close to the Spencer-Attix-Nahum cut-off Δ. Kumar S., Sapra B.K., Nahum A.E. *Physics in Medicine and Biology*. Vol. 68(9), ArtNo. 09NT01.

1460. The inner mitochondrial membrane fission protein MTP18 serves as a mitophagy receptor to prevent apoptosis in oral cancer. Panigrahi D.P., Praharaj P.P., Behera B.P., et al. *Journal of Cell Science*. Vol. 136(13), ArtNo. jcs259986.

1461. The intercellular communications mediating radiation-induced bystander effects and their relevance to environmental, occupational, and therapeutic exposures. Buonanno M., Gonon G., Pandey B.N., et al. *International Journal of Radiation Biology*. Vol. 99(6), pg. 964-982.

1462. The international reference system for beta-particle emitting radionuclides: Validation through the pilot study CCRI(II)-P1.Co-60. Coulon R., Leobino da Silva M.A., Bendall E., et al. *Applied Radiation and Isotopes*. Vol. 200, ArtNo. 110945.

1463. The Journal of Medical Physics Progresses and Achieves an Impact Factor – Time to Change Guards. Pradhan A.S. *Journal of Medical Physics*. Vol. 48(4).

1464. The lifetime risk of developing type II diabetes in an urban community in Mumbai: findings from a ten-year retrospective cohort study. Sharma P., Dilip T.R., Mishra U.S., et al. *BMC Public Health*. Vol. 23(1), ArtNo. 1673.

1465. The N-terminal FleQ domain of the Vibrio cholerae flagellar master regulator FlrA plays pivotal structural roles in stabilizing its active state. Chakraborty S., Agarwal S., Bakshi A., et al. *FEBS Letters*. Vol. 597(17), pg. 2161-2177.

1466. The role of anagostic interactions in the Pd−Superoxo formation in aerobic Pd catalysed C–C coupling reaction: What do DFT computations reveal?. Rasu A., Sundararajan M., Venuvanalingam P. *Computational and Theoretical Chemistry*. Vol. 1228, ArtNo. 114284.

1467. The shape shapes the interfacial liquid-liquid mass transfer: CFD simulations for single spherical and ellipsoidal drops. Sarkar S., Singh K.K., Shenoy K.T. *Chemical Engineering Science*. Vol. 267, ArtNo. 118240.

1468. The total neutron production from the alpha induced reaction on natural zirconium. Vafiya Thaslim T.T., Musthafa M.M., Midhun C.V., et al. *European Physical Journal A*. Vol. 59(7), ArtNo. 167.

1469. Theoretical studies on the mechanism, kinetics, and degradation pathways of auxin mimic herbicides by •OH radical in aqueous media. Upadhyaya H.P. *Structural Chemistry*. Vol. 34(3), pg. 931-943.

1470. Theoretical study on the gas phase hydroxyl radical reaction with tetrahydrothiophene, tetrahydrofuran, thiophene and furan. Upadhyaya H.P. *Chemical Physics Letters*. Vol. 816, ArtNo. 140385.

1471. Thermal catalytic mineralization of ortho-dichlorobenzene at low temperature: an in situ FT-IR and XPS mechanistic investigation. Kumar A., Tyagi D., Varma S., et al. *Materials Advances*.

1472. Thermal Expansion and Elastic Properties of Th–6U–4Zr Alloy. Kumar U., Kaity S., Kumawat N., et al. *Transactions of the Indian Institute of Metals*. Vol. 76(7), pg. 1751-1759.

1473. Thermal neutron as a potential mutagen for induced plant mutation breeding: radiosensitivity response on wheat and rice. Kadam S.T., Vishwakarma G., Kashyap Y., et al. *Genetic Resources and Crop Evolution*. Vol. 70(3), pg. 789-798.

1474. Thermal plasma processing of high temperature insulation wools. Dhamale G.D., Ajith N., Ghorui S. *Waste Management*. Vol. 168 pg. 290-300.

1475. Thermal-Hydraulic Transient Analyses for Primary Coolant System of HFRR Using RELAP5. Veluri V.K., Sengupta S. *Nuclear Technology*. Vol. 209(5), pg. 765-776.

1476. Thermodynamic investigation of ZnMoO4 (s) and Zn3Mo2O9 (s) compounds. Aiswarya P.M., Narang S., Dawar R., et al. *Thermochimica Acta*. Vol. 723, ArtNo. 179486.

1477. Thermodynamic stability and leaching behaviour of Ba and Th charge-coupled substituted monazite solid solution (La1-xBax/2Thx/2)PO4 (x = 0.1, 0.2 and 0.3) and its comparison with Sr and Th substituted monazite. Rawat D., Mishra R.K., Dash S., et al. *Thermochimica Acta*. Vol. 719, ArtNo. 179412.

1478. Thermodynamic Studies on Sr5Nb4O15. Samui P., Bhojane S.M., Singh B.M., et al. *International Journal of Thermodynamics*. Vol. 26(1), pg. 18-24.

1479. Thermoelectric Modules: Key Issues in Architectural Design and Contact Optimization. Basu R. *ChemNanoMat*. Vol. 9(3), ArtNo. e202200551.

1480. Thermoluminescence investigations and kinetic analysis of highly sensitive LiCaAlF6: Eu,Y phosphor for dosimetric applications. Rawat N.S., Dhabekar B., Singh A.K., et al. *Journal of Luminescence*. Vol. 261, ArtNo. 119845.

1481. Thermoresponsive phase behavior and nanoscale self-assembly generation in normal and reverse Pluronics®. Patel D., Vaswani P., Sengupta S., et al. *Colloid and Polymer Science*. Vol. 301(2), pg. 75-92.

1482. Thidiazuron-mediated callogenesis and biosynthesis of anti-cancerous monoterpene indole alkaloid camptothecin in Nothapodytes nimmoniana (J.Graham) Mabb. callus culture. Kadam S.B., Godbole R.C., Pable A.A., et al. *South African Journal of Botany*. Vol. 156 pg. 411-419.

1483. Thioflavin-T -Incorporated Cerium-ATP Coordination Polymer Nanoparticles: A Promising System for Detection of Uranyl Ion (UO22+) in Aqueous Medium. Ghosh M., Swain K.K., Singh P.K. *Langmuir*. Vol. 39(20), pg. 7017-7028.

1484. Thiol-functionalized TiO2 microspheres and Fe(0) nanoparticle-loaded polymeric hydrogel for the selective recovery of Cr(iii) and Cr(vi) from the aquatic medium. Thekke Parayil R., Singh S., Basu R., et al. *Environmental Science: Nano*. Vol. 10(9), pg. 2532-2550.

1485. Thiophene functionalized naphthalene diimide for the sensitive detection of nitroaromatics. Bhusanur D.I., Singh P.K., Bhosale S.V., et al. *Indian Journal of Chemistry (IJC)*. Vol. 62(7), pg. 696-702.

1486. Thiourea Mitigates Potassium Deficiency in Soybean Varieties Through Redox or ABA Dependent Mechanisms. Sahoo S.A., Singh R.D., Kulkarni J., et al. *Journal of Plant Growth Regulation*.

1487. Threshold Photoionization and Density Functional Theory Investigations of Small Lanthanum Monoxide Clusters, LanO (n = 2-10). Bhattacharyya S., Deshpande V.V. *Journal of Physical Chemistry A*. Vol. 127(36), pg. 7460-7469.

1488. Ti-decorated C30 as a high-capacity hydrogen storage material: insights from density functional theory. Nair H.T., Kundu A., Ray P., et al. *Sustainable Energy and Fuels*. Vol. 7(20), pg. 5109-5119.

1489. Ti-decorated nitrogen-rich BeN4 monolayer for reversible hydrogen storage: DFT investigations. Trivedi R., Kaur S., Garg N., et al. *Applied Surface Science*. Vol. 622, ArtNo. 156806.

1490. Time and magnetic field dependent magnetic order in Ca3Co2 O6 revealed by resonant x-ray scattering. Yusuf S.M., Jain A., Bera A.K., et al. *Physical Review B*. Vol. 107(18), ArtNo. 184406.

1491. Topological phonons and low lattice thermal conductivity of Li2CaX (X = Sn and Pb) type Heusler compounds. Sharma V.K., Kanchana V., Gupta M.K., et al. *Materials Today Communications*. Vol. 35, ArtNo. 106289.

1492. Topology driven and soft phonon mode enabled Na-ion diffusion in quaternary chalcogenides, Na3ZnGaX4 (X = S, and Se). Kumar S., Gupta M.K., Mittal R., et al. *Journal of Materials Chemistry A*. Vol. 11(44), pg. 23940-23949.

1493. Total Reflection X-ray Fluorescence Spectrometric Analysis of Ten Lanthanides at the Ultratrace Level Having a High Degree of Overlap in the Emission Lines. Sanyal K., Saha A., Sarkar A., et al. *ACS Omega*. Vol. 8(44), pg. 41402-41410.

1494. Tough, flexible and oil-resistant film from sonicated guar gum and cellulose nanofibers for food packaging. Palanichamy P., Venkatachalam S., Gupta S. *Food Packaging and Shelf Life*. Vol. 40, ArtNo. 101189.

1495. Toward Developing Techniques—Agnostic Machine Learning Classification Models for Forensically Relevant Glass Fragments. Kaspi O., Israelsohn-Azulay O., Yigal Z., et al. *Journal of Chemical Information and Modeling*. Vol. 63(1), pg. 87-100.

1496. Transcription coupled DNA repair protein UVSSA binds to DNA and RNA: Mapping of nucleic acid interaction sites on human UVSSA. Mistry H., Gupta G.D. *Archives of Biochemistry and Biophysics*. Vol. 735, ArtNo. 109515.

1497. Transcriptional Regulation of Small Heat Shock Protein 17 (sHSP-17) by Triticum aestivum HSFA2h Transcription Factor Confers Tolerance in Arabidopsis under Heat Stress. Kumar R.R., Dubey K., Goswami S., et al. *Plants*. Vol. 12(20), ArtNo. 3598.

1498. Transformation of brackish water Reverse Osmosis membranes to nanofiltration & ultrafiltration membranes by NaOCl treatment: Kinetic and characterization studies. Madduri S., Sodaye H.S., Debnath A.K., et al. *Journal of Water Process Engineering*. Vol. 56, ArtNo. 104549.

1499. Transient heat transfer characteristics of submerged heat source under seismic excitation. Chauhan S.P., Chandraker D.K., Kumar N. *International Journal of Thermal Sciences*. Vol. 184, ArtNo. 107964.

1500. Transit time estimation of drying springs in Uttarakhand region using environmental tritium concentration. Chatterjee S., Khati V., Jaryal A.K., et al. *Journal of Environmental Radioactivity*. Vol. 266-267, ArtNo. 107227.

1501. Transition metal atoms anchored 2D holey graphyne for hydrogen evolution reaction: Acumen from DFT simulation. Chodvadiya D., Chakraborty B., Jha P.K. *International Journal of Hydrogen Energy*. Vol. 48(48), pg. 18326-18337.

1502. Transition metal-N2P2 embedded graphene (TM-NPC) as single-atom catalyst for oxygen reduction reaction: a computational study. Kancharlapalli S. *Theoretical Chemistry Accounts*. Vol. 142(8), ArtNo. 77.

1503. Transparency of the γ(n,p)π- reaction in nuclei. Das S. *Physical Review C*. Vol. 107(3), ArtNo. 35201.

1504. Transport selectivities in ion-exchange membranes: Heterogeneity effect and analytical method dependence. Kumar A., Chaudhury S. *Separation Science and Technology (Philadelphia)*. Vol. 58(2), pg. 361-371.

1505. Transverse single-spin asymmetry of charged hadrons at forward and backward rapidity in polarized p+p, p+Al, and p+Au collisions at sNN =200 GeV. Abdulameer N.J., Acharya U., Aidala C., et al. *Physical Review D*. Vol. 108(7), ArtNo. 72016.

1506. Transverse single-spin asymmetry of midrapidity π0 and η mesons in p+Au and p+Al collisions at sNN =200 GeV. Abdulameer N.J., Acharya U., Aidala C., et al. *Physical Review D*. Vol. 107(11), ArtNo. 112004.

1507. Trap engineering through chemical doping for ultralong X-ray persistent luminescence and anti-thermal quenching in Zn2GeO4. Balhara A., Gupta S.K., Abraham M., et al. *Journal of Materials Chemistry C*. Vol. 12(5), pg. 1728-1745.

1508. Trends of surgical-care delivery during the COVID-19 pandemic: A multi-centre study in India (IndSurg Collaboration). Jain S., Mahajan A., Patil P.M., et al. *Journal of postgraduate medicine*. Vol. 69(4), pg. 198-204.

1509. Trichoderma virens exerts herbicidal effect on Arabidopsis thaliana via modulation of amino acid metabolism. Bansal R., Sahoo S.A., Barvkar V.T., et al. *Plant Science*. Vol. 332, ArtNo. 111702.

1510. True coincidence summing correction for a BEGe detector in close geometry measurements. Gupta A., Shareef M., Twisha M., et al. *Applied Radiation and Isotopes*. Vol. 200, ArtNo. 110966.

1511. Tubular Diamond as an Efficient Electron Field Emitter. Karmakar S., Sarkar P.K., Mistari C.D., et al. *ACS Applied Electronic Materials*. Vol. 5(7), pg. 3592-3602.

1512. Tunable magnetoresistance driven by electronic structure in Kagome semimetal Co 1 − x FexSn. Vijay K., Chandra L.S.S., Ali K., et al. *Applied Physics Letters*. Vol. 122(23), ArtNo. 233103.

1513. Tunable upconversion in ZnAl2−xGaxO4:Er,Yb phosphors by modulating the Al/Ga ratio and application in optical thermometry. Parayil R.T., Gupta S.K., Upadhyay M.M., et al. *New Journal of Chemistry*. Vol. 47(44), pg. 20286-20297.

1514. Tunable, efficient, ultrafast broadband nonlinear optical properties of TiO2–loaded complex phosphate glasses. Gangareddy J., Syed H., Chakraborty S., et al. *Materials Research Bulletin*. Vol. 167, ArtNo. 112414.

1515. Tuneable optical properties of Fe2O3 magnetic nanoparticles synthesized from Ferritin. Kumar S., Kumar M., Velaga S., et al. *Journal of Sol-Gel Science and Technology*. Vol. 105(3), pg. 650-661.

1516. Tungsten-based polymer composite, a new lead-free material for efficient shielding of coupled neutron-gamma radiation fields: A FLUKA simulation study. Das A., Ray A., Singh T. *Physica Scripta*. Vol. 98(11), ArtNo. 115302.

1517. Tuning of structure and host dynamics via yttrium doping in Bi2 O3 to enhance oxygen ion diffusion. Goel P., Gupta M.K., Kumar S., et al. *Physical Review Materials*. Vol. 7(9), ArtNo. 95402.

1518. Tunneling nanotubes: The intercellular conduits contributing to cancer pathogenesis and its therapy. Melwani P.K., Pandey B.N. *Biochimica et Biophysica Acta - Reviews on Cancer*. Vol. 1878(6), ArtNo. 189028.

1519. Two-Dimensional Layered Structures of Group-V Elements as Transparent Conductors: Insight from a First-Principles Study. Behera G., Kangsabanik J., Chakraborty B., et al. *Physical Review Applied*. Vol. 19(5), ArtNo. 54068.

1520. Two-dimensional short-range spin-spin correlations in the layered spin- 32 maple leaf lattice antiferromagnet Na2Mn3 O7 with crystal stacking disorder. Saha B., Bera A.K., Yusuf S.M., et al. *Physical Review B*. Vol. 107(6), ArtNo. 64419.

1521. Two-particle azimuthal correlations in γp interactions using pPb collisions at sNN=8.16TeV. Tumasyan A., Adam W., Bergauer T., et al. *Physics Letters, Section B: Nuclear, Elementary Particle and High-Energy Physics*. Vol. 844, ArtNo. 137905.

1522. Two-temperature model for ultrafast melting of Au-based bimetallic films interacting with single-pulse femtosecond laser: Theoretical study of damage threshold. Aeaby C., Ray A. *Physical Review B*. Vol. 107(19), ArtNo. 195402.

1523. Ultra-bright and thermally stable deep red emitting doped yttrium zirconate nanoparticles for tunable white LEDs and indoor plant growth. Parayil R.T., Gupta S.K., Abraham M., et al. *Materials Advances*. Vol. 4(22), pg. 5594-5604.

1524. Ultrafast Dynamics of the 9,10-Bis[(triisopropylsilyl)ethynyl]anthracene Nanoaggregate and Thin Film: Influence of the Molecular Packing and Sample Morphology on Singlet Fission and Excimer Formation. Nandi A., Manna B., Ghosh R. *Journal of Physical Chemistry C*. Vol. 127(26), pg. 12621-12630.

1525. Ultrafast glimpses of the excitation energy-dependent exciton dynamics and charge carrier mobility in Cs2SnI6 nanocrystals. Kaur G., Shukla A., Sinha A., et al. *Nanoscale*. Vol. 15(34), pg. 14081-14092.

1526. Ultrafast Hole Migration at the p-n Heterojunction of One-Dimensional SnS Nanorods and Zero-Dimensional CdS Quantum Dots. Kaur A., Goswami T., Babu K.J., et al. *Journal of Physical Chemistry Letters*. Vol. 14(33), pg. 7483-7489.

1527. Ultrafast isomerization vs bond twisting process – role of a proton. Santra S., Mora A.K., Nath S. *Journal of Photochemistry and Photobiology A: Chemistry*. Vol. 437, ArtNo. 114474.

1528. Ultrasound assisted seed preparation and subsequent application for desupersaturation of calcium sulphate as a measure for scaling control. Banakar V.V., Gogate P.R., Raha A., et al. *Journal of Environmental Chemical Engineering*. Vol. 11(3), ArtNo. 110026.

1529. Unassisted and Efficient Actinide/Lanthanide Separation with Pillar[5]arene-Based Picolinamide Ligands in Ionic Liquids. Cai Y., Ansari S.A., Yuan L., et al. *Industrial and Engineering Chemistry Research*. Vol. 62(12), pg. 5297-5304.

1530. Unbinding of hACE2 and inhibitors from the receptor binding domain of SARS-CoV-2 spike protein. Mishra L., Bandyopadhyay T. *Journal of Biomolecular Structure and Dynamics*. Vol. 41(8), pg. 3245-3264.

1531. Understanding natural radiation induced cationic and anionic defects in natural fluorite single crystals through spectroscopic investigations. Banerjee R.H., Pathak N., Nandi P., et al. *Journal of Luminescence*. Vol. 254, ArtNo. 119540.

1532. Understanding substrate-driven growth mechanism of copper silicide nanoforms and their applications. Sen S., Kanitkar P., Muthe K.P. *Materials Science and Technology (United Kingdom)*. Vol. 39(16), pg. 2341-2352.

1533. Understanding Successful Transfers of Rapid-Composting Technology Using Qualitative Content Analysis for Interpretation. Ponangi T.H., Mukherjee P., Jain K., et al. *Journal of Scientific and Industrial Research*. Vol. 82(9), pg. 956-965.

1534. Understanding the broad-band emission process of 3C 279 through long term spectral analysis. Thekkoth A., Sahayanathan S., Shah Z., et al. *Monthly Notices of the Royal Astronomical Society*. Vol. 526(4), pg. 6364-6380.

1535. Understanding the charge transfer dynamics of the Cu2WS4-CNT-FeOOH ternary composite for photo-electrochemical studies. Dagar P., Ghorai N., Bungla M., et al. *Physical Chemistry Chemical Physics*. Vol. 25(45), pg. 30867-30879.

1536. Understanding the correlation of microscopic structure and macroscopic properties of multi-component glass through atomistic simulations. Sahu P., Ali S.K.M., Shenoy K.T., et al. *Journal of Chemical Sciences*. Vol. 135(2), ArtNo. 31.

1537. Understanding the excited state dynamics and redox behavior of highly luminescent and electrochemically active Eu(iii)-DES complex. Patil S.M., Agrawal R., Gupta R., et al. *Dalton Transactions*. Vol. 52(46), pg. 17349-17359.

1538. Understanding the influence of eccentric pressure tube on the thermal behavior of 37-element based PHWR channel under accident condition. Ajay K., Kumar R., Gupta A., et al. *Annals of Nuclear Energy*. Vol. 181, ArtNo. 109533.

1539. Understanding the influence of graphene-based lubricant/coating during fretting wear of zircaloy. Mishra D., Maurya R., Verma V., et al. *Wear*. Vol. 512-513, ArtNo. 204527.

1540. Understanding the Interaction and Potential of Halophytes and Associated Microbiome for Bio-saline Agriculture. Meena K.K., Bitla U., Sorty A.M., et al. *Journal of Plant Growth Regulation*. Vol. 42(10), pg. 6601-6619.

1541. Understanding the molecular interaction of BSA protein with antibiotic sulfa molecule(s) for novel drug development. Mavani A., Ray D., Aswal V.K., et al. *Journal of Molecular Structure*. Vol. 1287, ArtNo. 135697.

1542. Understanding the self-pinning driven jamming behavior of colloids in drying droplets. Mehta S., Bahadur J., Sen D. *Colloids and Surfaces A: Physicochemical and Engineering Aspects*. Vol. 676, ArtNo. 132284.

1543. Understanding the sorption behavior of tri, tetra and hexavalent f cations on metal–organic framework (MOF), ZIF-67: experimental and theoretical investigation. Mor J., Boda A., Sharma S.K., et al. *Separation Science and Technology (Philadelphia)*. Vol. 58(15-16), pg. 2806-2823.

1544. Understanding the structure-property correlation of tin oxide nanoparticles synthesized through the sol-gel technique. Ali S.I., Dutta D., Das A., et al. *Journal of Luminescence*. Vol. 253, ArtNo. 119465.

1545. Understanding the very high energy γ-ray excess in nearby blazars using leptonic model. Manzoor A., Sahayanathan S., Shah Z., et al. Monthly Notices of the Royal Astronomical Society. Vol. 525(3), pg. 3533-3540.

1546. Unexplored Isomerization Pathways of Azobis(benzo-15-crown-5): Computational Studies on a Butterfly Crown Ether. Sisodiya D.S., Ali S.M., Chattopadhyay A. Journal of Physical Chemistry A. Vol. 127(34), pg. 7080-7093.

1547. Unified correlations for the prediction of the slip velocity, characteristic velocity, flooding throughput and flooding slip velocity in a pulsed disc and doughnut extraction column. Sinha V., Vincent T. Chemical Engineering Communications. Vol. 210(1), pg. 106-118.

1548. Unified view of the hydrogen-bond structure of water in the hydration shell of metal ions (Li+, Mg2+, La3+, Dy3+) as observed in the entire 100–3800 cm−1 regions. Ghosh N., Bandyopadhyay A., Roy S., et al. Journal of Molecular Liquids. Vol. 389, ArtNo. 122927.

1549. Unprecedented confinement time of electron plasmas with a purely toroidal magnetic field in SMARTEX-C. Lachhvani L., Pahari S., Goswami R., et al. Scientific Reports. Vol. 13(1), ArtNo. 19038.

1550. Unraveling the paleo-marine signature in saline thermal waters of Cambay rift basin, Western India: Insights from geochemistry and multi isotopic (B, O and H) analysis. Chatterjee S., Mishra P., Bhushan K.S., et al. Marine Pollution Bulletin. Vol. 192, ArtNo. 115003.

1551. Unravelling redox phenomenon and electrochemical stability of Li1.6Al0.5Ge1.5P2.9Si0.1O12 solid electrolyte against Li metal and silicon anodes for advanced solid-state batteries. Sau S., Panda M.R., Barik G., et al. *Materials Today Energy*. Vol. 38, ArtNo. 101445.

1552. Unravelling the mechanisms of copper precipitation-induced strengthening in austenitic stainless steels: An atomistic approach. Biswal S., Barik R.K., Neogy S., et al. *Materialia*. Vol. 32, ArtNo. 101962.

1553. Unravelling the Potential of Lutetium-177 Labeled Pertuzumab: Targeting HER 2 Receptors for Theranostic Applications. Sharma R., Mukherjee A., Mitra J.B., et al. *International Journal of Radiation Oncology Biology Physics*. Vol. 115(2), pg. 419-425.

1554. Unusual Spin States in Noble Gas Inserted Noble Metal Halocarbenes, FNgCM (Ng = Kr, Xe, Rn; M = Cu, Ag, Au). Kuntar S.P., Chopra P., Ghosh A., et al. *Journal of Physical Chemistry A*. Vol. 127(23), pg. 4979-4995.

1555. Unveiling the potential of P3 phase in enhancing the electrochemical performance of a layered oxide cathode. Vasavan H.N., Badole M., Saxena S., et al. *Materials Today Energy*. Vol. 37, ArtNo. 101380.

1556. Upconverted Nanophosphors for Increasing Efficiency in a Dye-Sensitized Solar Cell. Chouryal Y.N., Sharma R.K., Tomar N., et al. *ACS Applied Energy Materials*. Vol. 6(9), pg. 4934-4941.

1557. Update of the BIPM comparison BIPM.RI(II)-K1.Co-60 of activity measurements of the radionuclide 60Co to include the 2020 result of the PTB (Germany), the 2020 result of the NIST (United States), the 2020 result of the SMU (Slovakia), the 2021 result of th. Coulon R., Michotte C., Courte S., et al. *Metrologia*. Vol. 60(1), ArtNo. 6010.

1558. Uranium in Groundwater: Distribution and Plausible Chemo- Radiological Health Risks Owing to the Long-term Consumption of Groundwater of Panchkula, Haryana, India. Tanwer N., Anand P., Batra N., et al. *Pollution*. Vol. 9(2), pg. 821-838.

1559. Use of modified Madou–Leblond model to predict crack initiation in low alloy steel specimens with different stress states. Kumar S., Samal M.K., Singh P.K., et al. *Engineering Fracture Mechanics*. Vol. 277, ArtNo. 108946.

1560. Utilization of host assisted aggregation-induced emission of ANS dye for ATP sensing. Kanti Mal D., Nilaya Jonnalgadda P., Kant Chittela R., et al. *Journal of Molecular Liquids*. Vol. 376, ArtNo. 121402.

1561. Utilization of γ-radiation in the synthesis of bimetallic Cu-Ni catalysts for selective vapour phase hydrogenation of levulinic acid to γ-valerolactone. Babu G.S., Francis S., Padmakar D., et al. *New Journal of Chemistry*. Vol. 47(13), pg. 6201-6210.

1562. Utilizing deep eutectic solvent for facile, selective and sustainable sequestration of plutonium. Patil S., Paul S., Gupta R., et al. *Separation and Purification Technology*. Vol. 318, ArtNo. 123923.

1563. Utilizing Energy Transfer in Mn2+/Ho3+/Yb3+ Tri-doped ZnAl2O4 Nanophosphors for Tunable Luminescence and Highly Sensitive Visual Cryogenic Thermometry. Balhara A., Gupta S.K., Debnath A.K., et al. *ACS Omega*. Vol. 8(33), pg. 30459-30473.

1564. UV-Visible photo-reactivity of permanently polarized inorganic nanotubes coupled to gold nanoparticles. Patra S., Testard F., Gobeaux F., et al. *Nanoscale*. Vol. 15(8), pg. 4101-4113.

1565. Validation of MCkeff code using ICSBEP results. Shet S., Subbaiah K.V., Prajapati P.M., et al. *Nuclear and Particle Physics Proceedings*. Vol. 336-338 pg. 26-28.

1566. Valorisation of Basa fish (Pangasius bocourti) waste: Oil extraction and encapsulation. Debbarma A., Kumar V., Mishra P.K., et al. *International Journal of Food Science and Technology*. Vol. 58(5), pg. 2764-2771.

1567. Variation of natural radioactivity in sediments of beach placers along the eastern coast of India. Mohanty S., Banerjee D., Sengupta D., et al. *Environmental Earth Sciences*. Vol. 82(7), ArtNo. 184.

1568. Vectorized PoCA algorithm for faster image reconstruction for Muon Tomography. Sehgal R. *Journal of Instrumentation*. Vol. 18(3), ArtNo. P03017.

1569. Vibration Analysis of Single-Link Flexible Manipulator in an Uncertain Environment. Rao P., Roy D., Chakraverty S. *Journal of Vibration Engineering and Technologies*. Vol., ArtNo. .

1570. Vibrational Coupling and Hydrogen-Bond Structure of Water in the Extended Hydration Shell of Metal Ions. Bandyopadhyay A., Saha G., Mondal J.A. *Journal of Physical Chemistry B*. Vol. 127(32), pg. 7174-7180.

1571. Visible light sensitive Au–TiO2 nanocomposites formed by effective attachment of Au with TiO2 nanoparticles using liquid-phase pulsed-laser ablation. Chaturvedi A., Mondal P., Srihari V., et al. *Optical Materials*. Vol. 138, ArtNo. 113732.

1572. Volatile changes associated with fresh-cut jackfruit during storage. Adiani V., Gupta S., Variyar P.S. *Flavour and Fragrance Journal*. Vol. 38(4), pg. 326-335.

1573. What is this image? 2023 Image 3 results: Cardiac tuberculosis presenting as cardiac mass: role of 18F-FDG PET/CT in monitoring response to treatment. Loharkar S., Sonavane S.N., Shah H., et al. *Journal of Nuclear Cardiology*. Vol. 30(6), pg. 2280-2288.

1574. Why is it imperative to use multicomponent geothermometry in medium/low enthalpy thermal waters? Insights from the Gujarat geothermal region, India. Chatterjee S., Mishra P., Keesari T., et al. *Environmental Earth Sciences*. Vol. 82(23), ArtNo. 557.

1575. Withaferin A, a steroidal lactone, selectively protects normal lymphocytes against ionizing radiation induced apoptosis and genotoxicity via activation of ERK/Nrf-2/HO-1 axis. Checker R., Bhilwade H.N., Nandha S.R., et al. *Toxicology and Applied Pharmacology*. Vol. 461, ArtNo. 116389.

1576. Withaferin-A alleviates acute graft versus host disease without compromising graft versus leukemia effect. Kumar Gupta S., Gohil D., Dutta D., et al. *International Immunopharmacology*. Vol. 121, ArtNo. 110437.

1577. WS2 nanosheets decorated multi-layered MXene based chemiresistive sensor for efficient detection and discrimination of NH3 and NO2. Sardana S., Debnath A.K., Aswal D.K., et al. *Sensors and Actuators B: Chemical*. Vol. 394, ArtNo. 134352.

1578. XAFS study of mixed ligand benzimidazole copper complexes having distorted coordination geometry. Hinge V.K., Bairagi M., Yadav N., et al. *Journal of Molecular Structure*. Vol. 1289, ArtNo. 135909.

1579. X-ray absorption near-edge, terahertz and Raman spectroscopies evidence growth-orientation dependent cation order, phase transitions and spin-phonon coupling in half-metallic Ca2FeMoO6 thin films. Yadav E., Prajapati G.L., Rajput P., et al. *New Journal of Physics*. Vol. 25(12), ArtNo. 123044.

1580. Yttrium decorated fullerene C30 as potential hydrogen storage material: Perspectives from DFT simulations. Paul D., Mane P., Sarkar U., et al. *Theoretical Chemistry Accounts*. Vol. 142(10), ArtNo. 94.

1581. ZnGa2−xAlxO4 (x = 0 ≤ 2) spinel for persistent light emission and HER/OER bi-functional catalysis. Parayil R.T., Gupta S.K., Pal M., et al. *RSC Advances*. Vol. 13(44), pg. 31101-31111.

1582. ZnS nano-photocatalysts with elemental type s defects for the visible light harvest and efficient antibiotic, explosive and azo dye pollutants degradation. Juine R.N., Sahu B.K., Das A. *Journal of Environmental Chemical Engineering*. Vol. 11(6), ArtNo. 111175.

1583. β-Bi2O3-Bi2WO6 Nanocomposite Ornated with meso-Tetraphenylporphyrin: Interfacial Electrochemistry and Photoresponsive Detection of Nanomolar Hexavalent Cr. Pal S., Mahamiya V., Ray P., et al. *Inorganic Chemistry*.

1584. β-Silylacrylate as a Multipurpose Reagent in Organic Synthesis. Ghosh S.K. *Helvetica Chimica Acta*. Vol. 106(11), ArtNo. e202300141.

1585. γ-Resistant Microporous CAU-1 MOF for Selective Remediation of Thorium. Gumber N., Pai R.V., Bahadur J., et al. *ACS Omega*. Vol. 8(13), pg. 12268-12282.

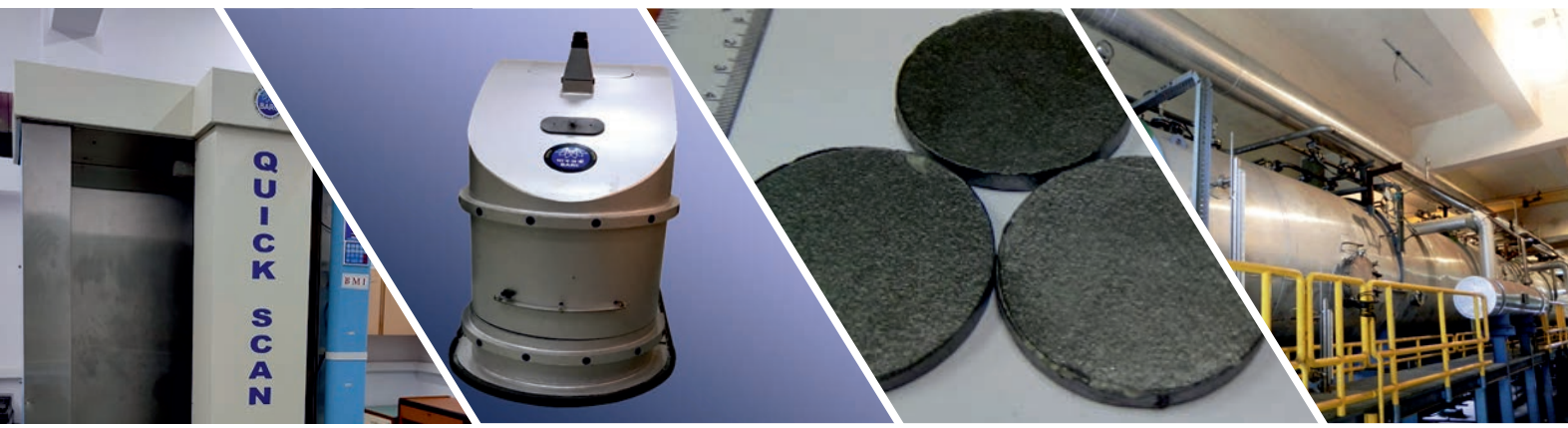
QUICK SCAN